Universitat Autònoma de Barcelona

Regulation of the oocyte pool in mammals

Ana Martínez Marchal

Regulation of the oocyte pool in mammals

Thesis submitted by

Ana Martínez Marchal

To opt for the title of

Doctor in Cell Biology

Doctoral thesis directed by

Dr. Ignasi Roig Navarro

Departament de Biologia Cel·lular, Fisiologia i Immunologia

Institut de Biomedicina i Biotecnologia (IBB)

Universitat Autònoma de Barcelona

Director	PhD candidate
Dr. Ignasi Roig Navarro	Ana Martínez Marchal

Bellaterra (Cerdanyola del Vallès), 2019

This work received financial support from:

- Ministerio de Ciencia e Innovación grant (BFU2010-18965, BFU2013-43965-P and BFU2016-80370-P)
- PIF program fellowship (B16P0048)

A todos los que han formado

parte de esta aventura,

“Magic is just science that we don't understand yet.”

— Arthur C. Clarke

INDEX

ABSTRACT

During mammalian oogenesis, oogonia proliferate forming the so-called cysts. The oogonia enter meiosis progressing through prophase I and the cysts break down concomitantly to massive perinatal oocyte death. During meiotic prophase I, double strand breaks (DSBs) are induced throughout the genome and repaired by homologous recombination to promote the synapsis of the homologous chromosomes. In response to errors in these processes, different response pathways are activated triggering cell cycle arrest or even apoptosis. The DNA damage response (DDR) is activated in response of meiocytes with recombination failure in the recombination checkpoint; while errors in synapsis trigger the synapsis checkpoint. We aimed to characterize the roles of the DDR and synapsis checkpoint in mammalian oogenesis. Contrary to what occurs in spermatocytes, oocytes present high numbers of unrepaired DSBs at pachynema, at the time of the massive oocyte death and cyst breakdown. In order to know if the recombination checkpoint participates in the regulation of the oocyte number in mammals, we analyzed the presence of DSBs, the oocyte number in both perinatal and adult females, the cyst breakdown, the formation of follicles and the reproductive lifespan using control and mutant mice for the effector kinase of the DNA damage response pathway, CHK2. Our data revealed the involvement of CHK2 in the regulation of the oocyte number but only in fetal ovaries prior to birth, raising the question of a possible alternative regulator acting just after birth. Our studies using *in vitro* ovarian cultures using inhibitors, suggest that CHK1 may compensate the loss of CHK2 perinatally *in vivo*. Thus, revealing that the DDR pathway controls the oocyte number in mammals. Furthermore, we found an increased number of oocytes in elder *Chk2* mutant females suggesting that the DDR controls the reproductive lifespan extension in mammals. Finally, we studied the possible involvement of TRIP13 in the synapsis checkpoint. The protein TRIP13 is required for recombination, but it is also needed for the synapsis of sex chromosomes and the sex body formation. Thus, suggesting a possible role in the synapsis checkpoint. We analyzed the oocyte number in females from *Spo11*$^{-/-}$ *Trip13*$^{mod/mod}$ and *Dmc1*$^{-/-}$ *Chk2*$^{-/-}$ *Trip13*$^{mod/mod}$ ovaries in order to infer if TRIP13 is required to implement the synapsis checkpoint in females. Our data revealed a rescue in the number of oocytes in the triple mutant, but not in the double mutant. These results leave open the possibility of a participation of TRIP13 in the synapsis checkpoint, but as an alternative, they could be compatible with a possible role of TRIP13 regulating the DSB repair pathway choice.

ACRONYMS AND ABBREVIATIONS

– Number

% – Percentage

ɣH2AX – Phosphorylated H2AX

ºC – Celsius degrees

µg – microgram

µl – microliter

µm – micrometer

µM – micromolar

A. thaliana – *Arabidopsis thaliana*

AE – Axial element

ANKRD31 – Ankyrin Repeat Domain 31

ATM – Ataxia Telangiectasa Mutated

ATR – Ataxia Telangiectasa and Rad-3 related

ATRIP – ATR Interacting Protein

BAX – Bcl-2-associated X protein

BCL2 – B-cell lymphoma 2

BCLX – Bcl-2-like protein 1

Bp – Base pairs

BRCA1 – Breast cancer type 1 susceptibility protein

BSA – Bovine serum albumin

BSCR – Barrier to sister chromatid recombination

C. elegans – *Caenorhabditis elegans*

c-KIT – Mast/stem cell growth factor receptor Kit

CE – Central element

CHK1 – Checkpoint kinase 1

Chk1i – CHK1 inhibitor

CHK2 – Checkpoint kinase 2

CO – Crossover

CO_2 – Carbon dioxide

Cy3 – Cyanine 3

D. melanogaster – *Drosophila melanogaster*

D-loop – Displacement loop

DAPI – 4',6-diamidino-2-phenylindole

DAPT – N-[N-(3,5-Difluorophenacetyl)-L-alanyl]-S-phenylglycine t-butyl ester

Dazl – Deleted in azoospermia-like

DDR – DNA damage response

DDX4 – DEAD-Box Helicase 4

dHJ – Double Holliday Junction

DMC1 – DNA meiotic recombinase 1

DMSO – Dimethyl sulfoxide

DNA – Desoxyribonucleic acid

dpc – Days *post-coitum*

dpp – Days *post-partum*

DSB – Double strand break

DTT – Dithiothreitol

EDTA – Ethylenediaminetetraacetic acid

EGTA – Egtazic acid

EOA – Early oocyte attrition

EtOH – Ethanol

EXO1 – Exonuclease 1

FBS – Fetal bovine serum

FACS – Fluorescent activated cell sorting

FITC – Fluorescein isothiocyanate

FSC – Forward-scattered light

FSH – Follicle-Stimulating Hormone

g – G-force

GCNA1 – Germ cell nuclear acidic protein 1

H1t – Histone H1t

H2AX – Histone H2AX

H3K9me3 – Trimethylation of the lysine 9 of the Histone 3

HCl – Hydrochloric acid

Hed1 – RED1 suppressor protein 1

HJ – Holliday Junction

Hop1 – Homolog Pairing 1

HORMAD1 – HORMA domain containing 1

HORMAD2 – HORMA domain containing 2

HR – Homologous recombination

HTP-3 – Him-Three Paralog 3

IH –Interhomolog

IHO1 – Interactor of HORMAD1 protein 1

IS – Intersister

IVF – *In vitro* fertilization

KO – Knockout

L1 – LINE-1

L1ORF1 – LINE-1 retrotransposable element ORF1 protein

LE – lateral element

LH – Luteinizing Hormone

LINE-1 – Long interspersed element 1

LOA – Late oocyte attrition

M – Molar

MAD2 – Mitotic arrest deficient 2

Mcmdc2 – Minichromosome maintenance domain containing 2

Mec1 – Mitosis Entry Checkpoint 1

Mek1 – Meiotic Kinase 1

MEI1 – Meiosis inhibitor protein 1

MEI4 – Meiosis-specific protein MEI4

mg – milligram

$MgCl_2$ – Magnesium chloride

ml – milliliter

MLH1 – MutL homolog 1

mM – millimolar

mod – Moderate

MOF – Multi-oocyte follicle

MRE11 – meiotic recombination 11 homolog A

MRN – MRE11, RAD50 and NBS1 complex

mRNA – Messenger RNA

MSCI – Meiotic Sex Chromosome Inactivation

Msh5 – MutS homolog 5

MSUC – Meiotic Silencing of Unsynapsed Chromosomes

NaCl – Sodium chloride

NBS1 – Nijmegen breakage syndrome 1 (nibrin)

NCO – Non-crossover

NHEJ – Non-homologous end joining

NOTCH2 – Neurogenic locus notch homolog protein 2

ORF – Open reading frame

$p31^{COMET}$ – Mad1/Cdc20-bound-Mad2 binding protein

p53 – Cellular tumor antigen p53

p63 – Tumor protein 63

PAR – Pseudoautosomal region

PARP-1 – Poly [ADP-ribose] polymerase 1

PAS – Periodic Acid Schiff

PBS – Phosphate-buffered saline

Pch2 – Pachytene checkpoint protein 2

PCNA – Proliferating cell nuclear antigen

PCR – Polymerase chain reaction

PFA – Paraformaldehyde

PGC – Primordial germ cell

PIC – Proteinase inhibitor cocktail

PTBG – PBS-Tween-BSA-Gelatin

PUMA –p53-upregulated modulator of apoptosis

RAD51 – Radiation sensitive protein 51

RAD54 – Radiation sensitive protein 54

Rec8 – Meiotic recombination protein REC8

REC114 – Meiotic recombination protein REC114

Red1 – Reductional division protein 1

REV7 (MAD2L2) – Mitotic arrest deficient 2-like protein 2

RPA – Replication protein A

Rpm – Revolutions per minute

RNA – Ribonucleic acid

RNF212 – Ring finger protein 212

S – Seckel

S. cerevisiae – *Saccharomyces cerevisiae*

S. pombe – *Saccharomyces pombe*

SC – Synaptonemal complex

SCF – Stem cell factor

SDS – Sodium dodecyl sulfate

SDSA – Synthesis dependent strand annealing

SEM – Standard error of the mean

SETDB1 – SET domain bifurcated histone lysine methyltransferase 1

SHLD1 – Shieldin complex subunit 1

SHLD2 – Shieldin complex subunit 2

SHLD3 – Shieldin complex subunit 3

SPO11 – Sporulation protein 11

SSC – Side-scattered light

ssDNA – Single-stranded DNA

STAT3 – Signal transducer and activator of transcription 3

SWS1 – SWIM domain containing Srs2 interacting protein 1

SWSAP1 – SWIM-type zinc finger 7 associated protein 1

SYCE1 – Synaptonemal complex central element protein 1

SYCE2 – Synaptonemal complex central element protein 2

SYCE3 – Synaptonemal complex central element protein 3

SYCP1 – Synaptonemal complex protein 1

SYCP2 – Synaptonemal complex protein 2

SYCP3 – Synaptonemal complex protein 3

TAp63 – Main isoform of the protein p63

Tel1 – Telomere maintenance protein 1

TEX12 – Testis-expressed protein 12

TF – Transverse filament

TOPOVIBL – Type 2 DNA topoisomerase 6 subunit B-like

TRIP13 – Thyroid hormone receptor interactor 13

TUNEL – Terminal deoxynucleotidyl transferase dUTP nick end labeling

WT – Wild type

Zip1 – Synaptonemal complex protein ZIP1

INTRODUCTION

Chapter 1

1.1. Oogenesis

The success of the sexual reproduction is given by the capacity of the two haploid gametes to merge and form a new individual. Gametogenesis, the formation of gametes, ensures the ploidy reduction by meiotic division with one round of DNA replication followed by two successive rounds of cell division, in order to avoid duplicating the genome in each generation. The mammalian gametogenesis presents a high sexual dimorphism, with several differences in timing, cell morphology and functions between males and females (Fig. 1.1).

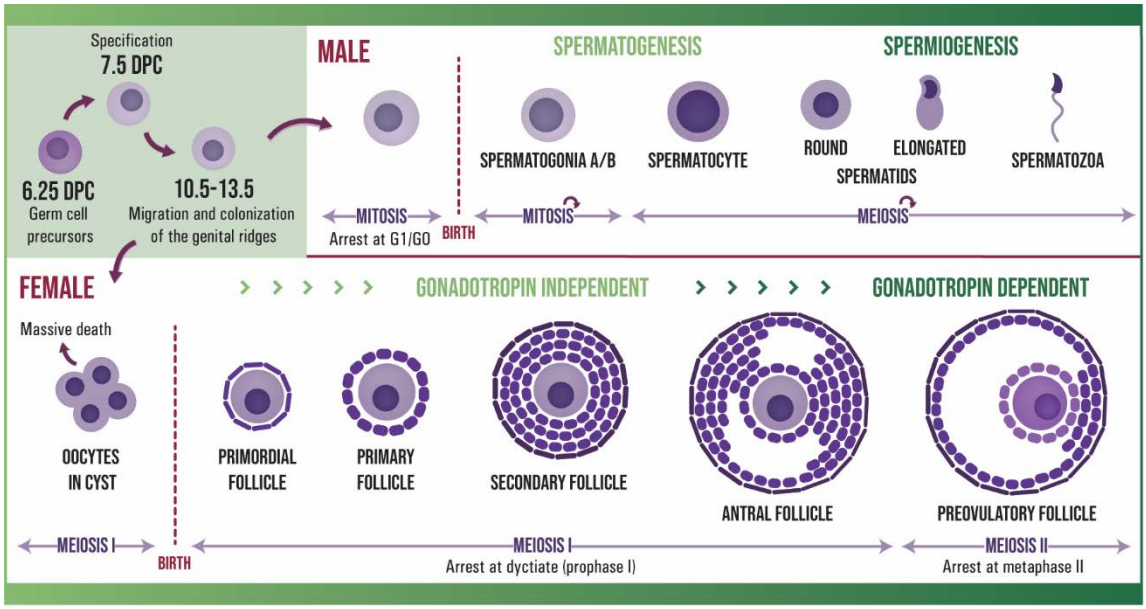

Figure 1.1 Mammalian gametogenesis present a high dimorphism. Representative diagram of the mice germ cell differentiation in males and females. Gametogenesis begins in both sexes in the fetal period, with the specification of the PGC, their proliferation by mitosis and migration to the genital ridges, where sex differentiation occurs. At this point, male germ cells (top panel) suffer a mitotic arrest and will resume their proliferation after birth. Spermatogonia enter meiosis differentiating to spermatocytes that start the transformation into spermatozoa. Spermatogenesis is maintained and repeated during the whole lifespan of the male. Oppositely, oogenesis in females (bottom panel) is a one-time process. All the oogonia enter meiosis during the fetal period becoming oocytes and arresting at dyctiate. Around birth, there is a massive death of oocytes, allowing the surviving ones to be surrounded by a layer of somatic cells and to form primordial follicles. These will resume their growth, progressing through the different follicle types and finally resuming meiosis just to arrest at metaphase II. Only when the oocyte is fertilized, meiosis II will conclude.

Both males and females share the early steps of mammalian gametogenesis. In mouse, at around 6.25 days of embryo development (6.25 dpc) growth factor signals from the extra-embryonic ectoderm and the visceral endoderm delimit the region of formation of the primordial germ cells (PGC) precursors. At this time, these cells repress the somatic programs and induce pluripotency-related genes. At 7.5 dpc, around 40 PGCs are detectable in the proximal epiblast, and those proliferate and migrate from the extraembryonic tissues, the base of the allantois, through the elongating hindgut towards the future site of the

primitive gonads, the genital ridges, which are finally colonized around 10.5-12.5 dpc. Once there, the PGCs become less motile and keep proliferating until 13.5 dpc, when around 25,000 PGCs reside in the gonads. The first evidence of sex differentiation is observed at 13.5 dpc, when the sex-specific signaling environment produces a change in the transcriptional profile of the germ cells. During this time there is an epigenetic reprogramming, with a genome-wide demethylation triggering transcription of germ-cell specific genes. At this point, the oogonia in the developing ovary enter prophase I of meiosis becoming oocytes, while the spermatogonia in developing testis arrest their mitotic cycle, only resuming mitosis and entering meiosis after birth, around 5 dpp (reviewed in Spiller et al., 2017; Bowles and Koopman 2013, 2007).

1.1.1. Cyst formation

During the oogenesis, just after the PGCs arrive to the genital ridges at 10.5-12.5 dpc (Molyneaux et al., 2001) they become oogonia and proliferate (Fig. 1.2). These oogonia divide synchronously by mitosis, but with an incomplete cytokinesis, resulting in an aggrupation of cells coming from the same progenitor joined by the cytoplasm and interconnected by cellular bridges (Fig. 1.2) (McLaren, 1984; Pepling and Spradling, 1998; Tam and Snow, 1981). These groups of cells, called cysts, will be partially fragmented into smaller groups prior to meiosis, allowing cells from different progenitors to mix and aggregate with each other (Lei and Spradling, 2013; Mork et al., 2012).

This syncytial interconnected structure is also found in some species of insects and lower vertebrates (review in Matova and Cooley, 2001) and its function has been widely discussed. In Drosophila oogenesis, the cysts are produced by four rounds of synchronous mitosis with incomplete cytokinesis. These divisions result always in groups of 16 cystocytes that end up losing the synchrony producing a polarization of the cysts in a way that only one of the cells, the future oocyte, receives and accumulates oocyte-specific factors from the other 15 cystocytes, called nurse cells. The factors accumulated include organelles, gene transcripts and proteins (de Cuevas et al., 1997).

A possible nurse function of the cysts in mammals has been questioned, but in more recent works it has been found that some mouse oocytes within cysts present and accumulate additional organelles like centrioles, Golgi, mitochondria and cytoplasmic components that most likely has been transported from the interconnected sister cells of the same cyst (Lei and Spradling, 2016; Pepling et al., 2007). This highly conserved process shows the importance of a correct cyst formation for the proper outcome of the remaining oocytes.

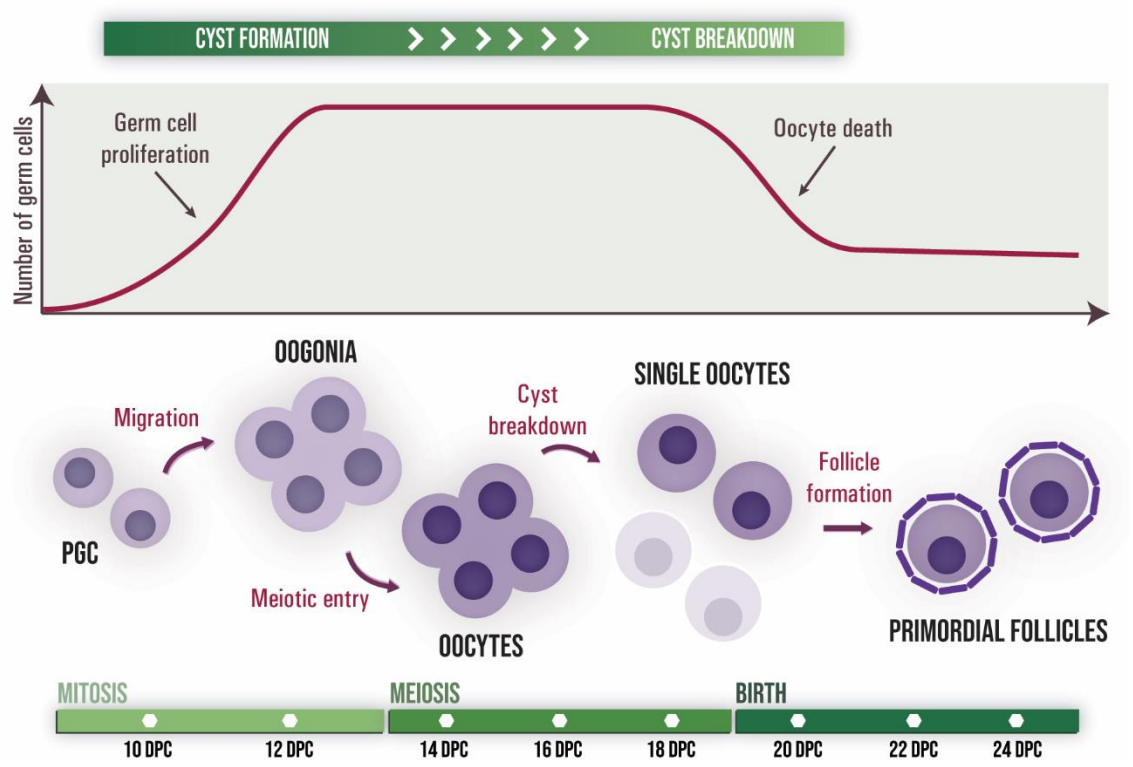

Figure 1.2 Fetal and postnatal oogenesis in mouse. The timeline shows all the perinatal events of the oogenesis in mouse. It begins with the migration and proliferation of the PGCs to the genital ridges, where they differentiate to oogonia forming cyst and later entering meiosis becoming oocytes. Around birth, many oocytes die concurrently with a cyst breakdown that will resulting in single oocytes that can be surrounded by a layer of pre-granulosa cells and form primordial follicles. Those will represent the pool of gametes available for the female.

1.1.2. Meiotic entry

The oogonia in cysts enter meiosis at 13.5 dpc in an asynchronic wave, going from the anterior to the posterior part of the ovary (Bullejos and Koopman, 2004; Menke et al., 2003; Monk and McLaren, 1981), becoming oocytes (Fig. 1.2) and upregulating germ-cell specific genes like *Ddx4*, *Dmc1 Gcna1*, *Dazl* and *Sycp3* (Cooke et al., 1996; Di Carlo et al., 2000; Fujiwara et al., 1994; Maatouk et al., 2006). Those oocytes progress through prophase I and arrest at the end of the diplotene stage, at a specific stage called dictyate (Borum, 1961).

1.1.3. Cyst breakdown and oocyte death

Around birth, there is a massive death of two-thirds of the oocytes, accompanied by the cyst breakdown (Fig. 1.2). The close succession and the fast progression of these two events suggest that these are two regulated developmental related processes. The function and the mechanisms controlling this oocyte death are still not clear. It has been postulated that the oocyte death is fundamental for the physical separation of the cysts, the individualization of the oocytes and the posterior encasement of the survivor oocytes in pre-granulosa cells forming primordial follicles (Jefferson et al., 2006; Pepling and Spradling,

2001). One possible explanation for this excess production of germ cells is that the cyst formation and oocyte death are means to select the best oocytes. In mammals, this process could be analogous to the one seen in Drosophila, in which the cysts provide a mechanism to only develop the germ cells of higher quality, helped by the other surrounding nurse cells that end up dying in favor of the surviving oocytes (de Cuevas et al., 1997).

Regarding the mechanisms of this perinatal programmed cell death, it has been attributed to apoptotic mechanisms, probably mediated by the Bcl-2 family of proteins (De Felici et al., 1999; Ratts et al., 1995; Rucker et al., 2000), even though there are several contradictions and discrepancies about this topic. For instance, the lack of the anti-apoptotic BCL2 or BCLX results in a lower oocyte survival (De Felici et al., 1999; Kolp et al., 2014; Rucker et al., 2000), while the lack of the pro-apoptotic BAX has the opposite effect with a higher oocyte survival (Greenfeld et al., 2007; Perez et al., 1999). These data show the impact of the apoptosis pathway in the perinatal ovaries. Surprisingly, though, when analyzing the apoptotic rates on normal ovaries, the number of oocytes stained by TUNEL or marked with PARP-1, two apoptotic markers, are pretty low, not corresponding to the high loss of oocytes (Jefferson et al., 2006; Pepling and Spradling, 2001). Furthermore, in some studies, this apoptosis and oocyte loss has been found to be continuous through all prophase I meiotic stages (Ghafari et al., 2007; McClellan et al., 2003); while in other ones it has been found to be concentrated in a short time window (Lobascio et al., 2007; Pepling and Spradling, 2001), corresponding mostly with oocytes at pachynema, which would be consistent with a developmental meiotic programmed death. The biological reasons of this massive death still remain unknown, but some possible explanations have been postulated (Ghafari et al., 2007); it has been proposed that the oocytes dying are the ones that accumulate mutations in mitochondrial DNA (Krakauer and Mira, 1999); that the death is a way to avoid the mitotic and/or meiotic errors during germ cell development (Speed, 1988); or that is a process, like in Drosophila, to favor some oocytes to the detriment of others (Pepling and Spradling, 2001). The fact that meiotic errors like the lack of recombination (Di Giacomo et al., 2005) or synapsis (Cloutier et al., 2015) trigger a higher oocyte death could reinforce the hypothesis that there is a selection in order to get the best quality oocytes.

1.1.4. Follicle formation

Once the cysts breakdown and the oocytes individualize, somatic pre-granulosa cells of the ovary surround single oocytes to form primordial follicles (Fig. 1.2) (Hirshfield, 1991). These follicles will represent the total pool of viable gametes produced by the female long before are needed. In mouse, follicle formation begins after birth, just after the oocytes reached diplonema. It is not a synchronic process, instead, the oocytes in the medulla, the inner part of the ovary, are the first to form follicles in a wave that extends towards the cortex, the outer part of the ovary (Byskov et al., 1997; Nandedkar et al., 2007; Pepling et al., 2010).

Normally, the follicles formed consist in only one oocyte surrounded by several pre-granulosa cells, but sometimes some multi-oocyte follicles (MOFs), containing two or more

oocytes per follicle, can be observed (Kent, 1960). These abnormal structures are thought to be residues of former cysts that did not completely breakdown and were enclosed to form a follicle. This relation was established due to the observation of high numbers of MOFs in ovaries lacking certain signaling molecules, among others, the Notch pathway proteins, that have defects in the cyst breakdown (Bray, 2006; Hahn, 2005; Trombly et al., 2009; Xu and Gridley, 2013). This pathway is composed by a family of receptors and ligands present in both somatic granulosa cells and oocytes, showing the importance of the interaction between these two cell types in the ovary (Bray, 2006; Hahn, 2005; Trombly et al., 2009; Xu and Gridley, 2013).

1.1.5. Follicular recruitment and resumption of meiosis

Just after the formation of the primordial follicles around birth, there is a first wave of follicular development. The follicles in the medulla of the ovary grow and become primary, secondary, and antral follicles, but die later due to the lack of gonadotropins. This process is repeated until sexual maturity (Fig. 1.3) (McGee and Hsueh, 2000). It's then that a cohort of follicles are activated and recruited cyclically (Fig. 1.3), every two weeks in mice, forming primary follicles, with the flat layer of granulosa cells becoming a cubic layer. At this point, the diameter of the oocyte barely changes since it's more a commitment phase to the following growing stages (Salha et al., 1998). The primary follicle keeps growing and develops two or more layers of granulosa cells, becoming a secondary follicle. In this stage, the follicle enters its growth phase, increasing the size of the oocyte with a high proliferation of the granulosa cells. At this point, ovarian stromal cells form another external layer, the theca cells, which provide structural and vascular support to the follicle (Tajima et al., 2007). Furthermore, during this growth, there is an increase in RNA and protein synthesis. The oocyte cytoplasm organization changes, increasing the amount of organelles like mitochondria and ribosomes; and redistributing the existing ones, like the loss of the centriole or the enlargement of the Golgi and it's movement to the periphery (Picton et al., 1998).

Up to this stage, all the steps of follicle development are gonadotropin independent, driven by locally secreted factors. But beginning at the pre-antral stage, the follicles express FSH and LH receptors that allows them to respond to gonadotropins (Fig. 1.3) (Sánchez and Smitz, 2012). The secondary follicles form a fluid-filled cavity, the antrum, and become antral follicles. This fluid is an important source of regulatory substances, derived from blood or secretions of the follicular cells, like gonadotropins, steroids or growth factors (van den Hurk and Zhao, 2005). Moreover, the granulosa cells differentiate into two population: the cumulus cells, closest to the oocyte; and the mural cells, proximal to the basal lamina (Li and Albertini, 2013; Sánchez and Smitz, 2012). At this moment, and after a transient increase in FSH, only a few follicles are rescued from apoptotic atresia, reaching the preovulatory stage (Fig. 1.3) (Hirshfield, 1991; Hsueh et al., 1994) and becoming competent to undergo germinal vesicle breakdown and resume meiosis (Picton et al., 1998). This competence is related to the nuclear and cytoplasmic maturity of the oocytes, which

accumulates transcripts, regulatory factors, reorganize the chromatin and the microtubule configuration, in order to be fertilized, prevent polyspermy and develop into a healthy embryo (Chesnel and Eppig, 1995; Gosden, 2002; Wickramasinghe et al., 1991).

The mature preovulatory antral follicles are ready to be ovulated in reaction to an increase in LH (Fig. 1.3). The apical follicle wall ruptures and the oocyte with its cumulus cells is released, finally resuming meiosis and arresting at metaphase II, awaiting for fertilization to finish meiosis (Russell and Robker, 2007). After the first and second meiotic divisions, the segregated chromosomes are packed into a separate cellular structure, the first and second polar bodies, that will be later discarded. These divisions result in the formation of only one single fertilizable gamete. Once the oocyte is released, the granulosa and theca cells undergo transformation to form the corpus luteum that supports gestation (Stocco et al., 2007).

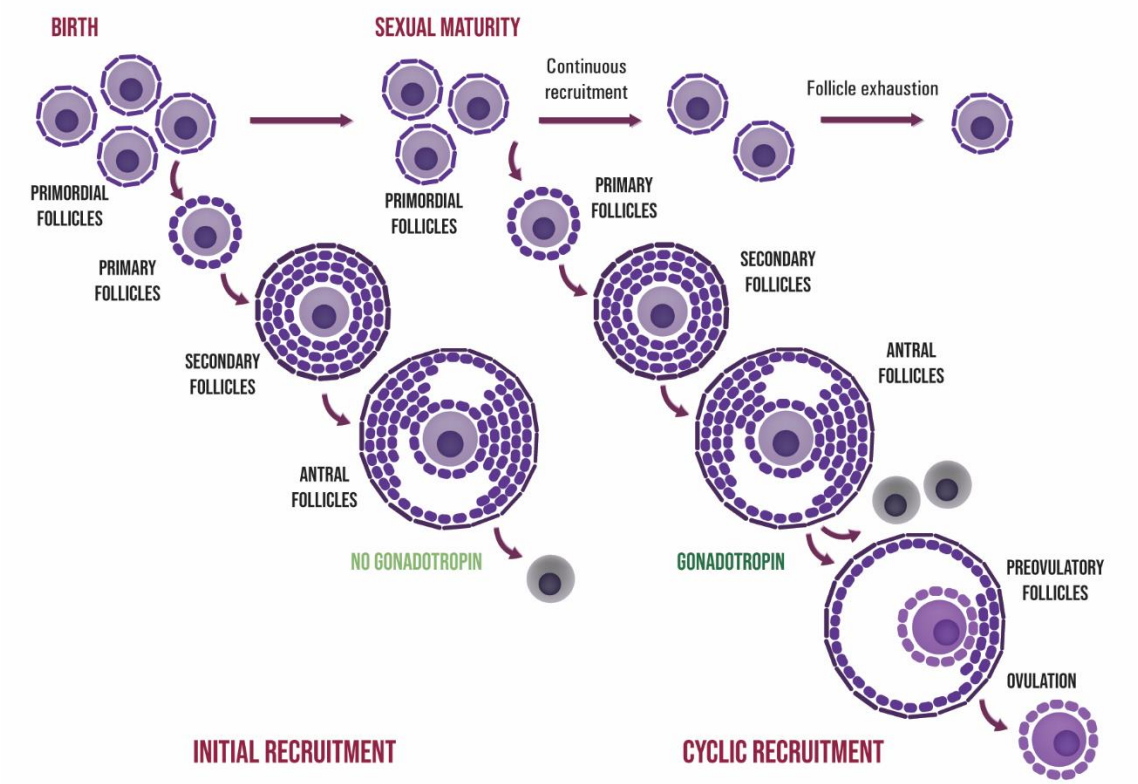

Figure 1.3 Folliculogenesis. Just after birth, a cohort of primordial follicles start the initial recruitment with the first wave of follicular development. Those primordial follicles develop into primary, secondary and antral follicles but die at this stage due to the lack of gonadotropins. Long after, at sexual maturity, the recruited follicles can complete folliculogenesis thanks to the presence of gonadotropins and become preovulatory follicles, which are ready to resume meiosis and ovulate.

1.2. Meiosis

The ability to form haploid gametes is provided by a specialized cell division, meiosis, that consist in one single DNA replication round followed by two segregation rounds (meiosis I and meiosis II) (Kleckner, 1996). Thus, the chromosome complement is reduced to half in order to allow the posterior restoration of the diploidy at fertilization.

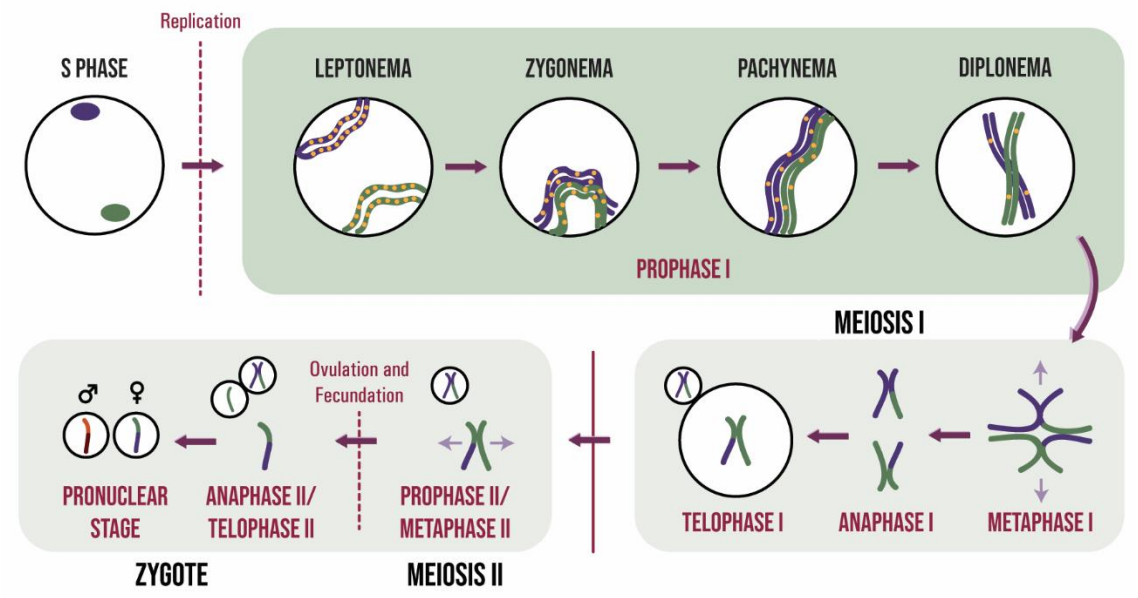

Figure 1.4 Mammalian female meiotic division. Meiosis consist in a single replication round followed by two consecutive segregation rounds. Meiosis I starts with prophase I, which can be subdivided in four stages: at leptonema multiple DSBs are induced throughout all the genome (marked in yellow); at zygonema the homologous chromosomes start to pair and repair their DSBs by HR; at pachynema homologues are full synapsed and at diplonema they desynapse and form the COs. Following the prophase I, there is a reductional division facilitated by the presence of COs. At metaphase I and anaphase I the homologous chromosomes orientate and separate resulting in two cells. In females, one chromosome stays in the oocyte and the other forms the first polar body. Later there is a second equal segregation, the meiosis II, in which there is a separation of the sister chromatids forming the fertilizable oocyte and the second polar body. In females, meiosis is only completed after fertilization of the oocyte.

After a long premeiotic S phase, the oogonia and spermatogonia enter meiosis, initiating the first meiotic prophase (prophase I) and progressing through all the stages: leptonema, zygonema, pachynema and diplonema. These stages are determined based on the events related to the movement, configuration and interaction of the homologous chromosomes; and they are mediated by the formation of a proteinaceous structure along those chromosomes, the synaptonemal complex (SC) (Fig. 1.4) (Handel and Schimenti, 2010). At leptotene stage the protein SPO11 catalyzes DNA double-strand breaks (DSBs) throughout all the genome (Keeney et al., 1997). These DSBs are repaired mostly during zygonema by homologous recombination (HR) using the homologous chromosome as a template. Thus, the homologous chromosomes pair and synapse, reaching full synapsis at

pachynema, and desynapsing later at diplonema, with at least one crossover (CO) per chromosome. COs are the sites where the genetic material is reciprocally exchanged between the homologues, yielding genetic diversity due to the transmission of new combinations of linked alleles to the offspring. COs also provide a physical connection between the homologous chromosomes (called chiasmata) allowing them to correctly orientate at metaphase I and segregate at anaphase I. This first meiotic division (meiosis I) is reductional, resulting in the segregation of the homologous chromosomes. Following this, the second meiotic division (meiosis II) is an equal segregation that separates sister chromatids (Fig. 1.4). As shown, meiosis, and especially the prophase I, is a complex process that it is highly controlled by several signaling mechanisms in order to produce balanced gametes that will ensure a healthy progeny.

1.2.1. Meiotic recombination

A very particular characteristic of the meiotic division that distinguishes it from mitosis is the intentional induction of DSBs all over the genome during the first meiotic prophase. The topoisomerase-like SPO11 is an evolutionary conserved protein responsible of catalyzing programmed DSBs at leptotene stage (Fig. 1.5), together with other proteins like TOPOVIBL, REC114, IHO1, ANKRD31 MEI1 and MEI4 (Baudat et al., 2013; Boekhout et al., 2019; Keeney et al., 1997; Papanikos et al., 2019; Robert et al., 2016; Stanzione et al., 2016). SPO11 remains covalently linked to the 5' end of every broken DNA strand until MRE11 releases it by endonucleolytic cleavage and then the ends are resected first 3' to 5' by MRE11 exonuclease activity and 5' to 3' by exonuclease EXO1 to expose the 3' single-stranded DNA (ssDNA) tails (Lam and Keeney, 2014). The ssDNA is coated by the protein RPA, promoting the loading of the strand exchange proteins RAD51 and the meiosis specific DMC1, which bind to the ssDNA ends forming nucleoprotein filaments that promote homology search and catalyze the strand invasion into the homologous chromosome DNA (Fig. 1.5) (Lam and Keeney, 2014). Other factors that also promote the loading of these proteins include TRIP13, ATR and the Shu complex SWS1-SWSAP1 (Abreu et al., 2018; Pacheco et al., 2018; Roig et al., 2010; Widger et al., 2018). Based on the RAD51/DMC1 foci counts at leptonema, it has been suggested that around 200-400 DSBs per cell are created in spermatocytes and oocytes (Baudat and de Massy, 2007). The strand invasion begins at zygonema, when the DMC1/RAD51-coated ssDNA insert into the template DNA of the homologue leading to the formation of a displacement loop (D-loop) allowing the extension by synthesis of the invading end and forming a cross-shaped structure called Holliday junction (HJ) (Fig. 1.5). At this point, if the other resected end is incorporated forming a second Holliday junction, the D-loop is stabilized and forms a stable double Holliday junction (dHJ), which will be mostly resolved as a COs. However, if the resected end is displaced, the D-loop is not stabilized and the DSB is repaired by synthesis-dependent strand annealing (SDSA), with no reciprocal exchange of the DNA, resolving as a non-crossover (NCO) (Fig. 1.5). Opposite to the COs, that consist of a reciprocal exchange of genetic material, the NCOs involve only a unidirectional transfer of genetic information, called gene conversion. In mice,

only approximately a 10% of the DSBs formed initially at leptonema end up repairing as COs at mid pachynema (Cole et al., 2012; Guillon and De Massy, 2002).

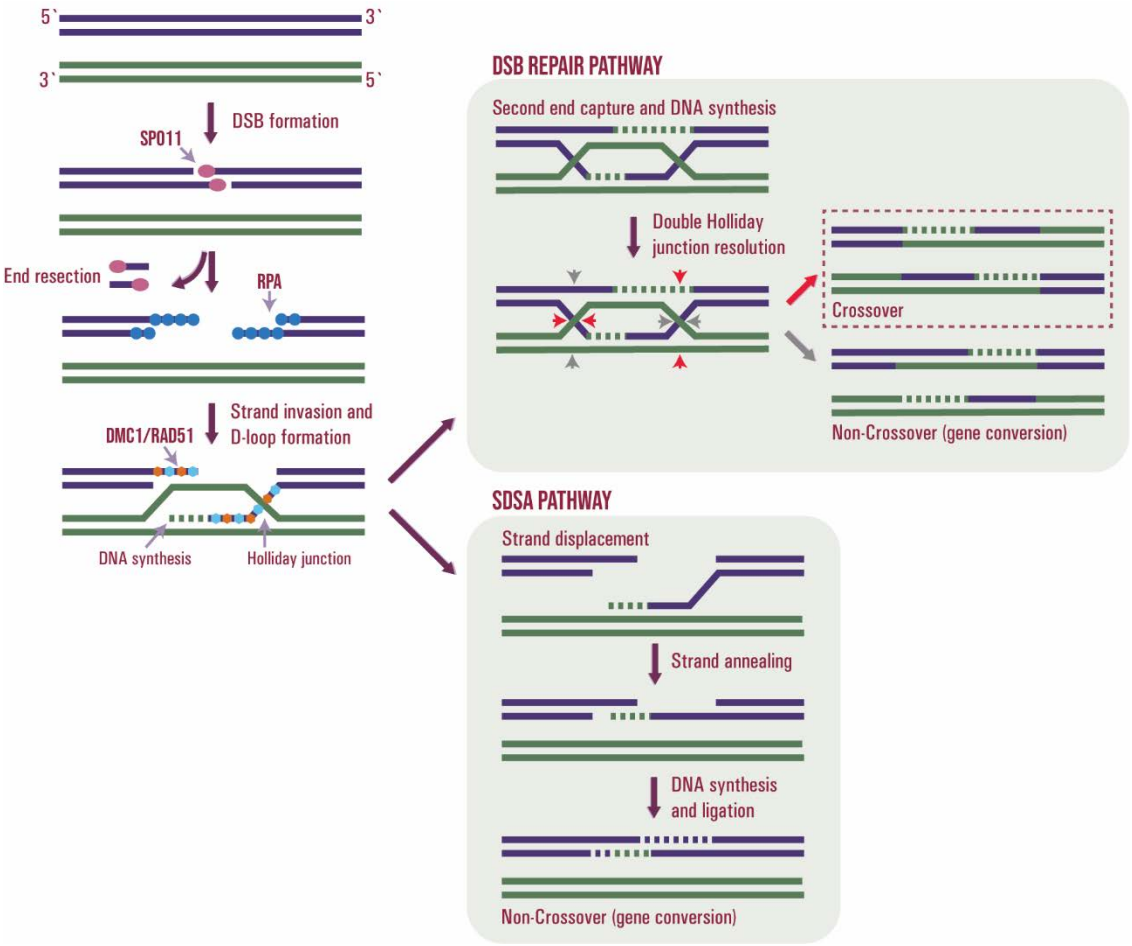

Figure 1.5 Mammalian meiotic recombination. Recombination starts with the formation of DSBs throughout the genome by SPO11 (pink circle), that remains covalently linked to the 5' end until it is released by MRE11. The ends are later resected exposing the 3' ssDNA tails, detected by RPA that attracts the strand exchange proteins DMC1 and RAD51. Those two promote the homology search and catalyze the strand invasion into the homologous chromosome, generating the D-loop. Once the D-loop is formed and extended there is two possible pathways: the capture of the second end forming a dHJ, that can be resolved preferentially as a CO; and the synthesis dependent strand annealing, which displaces the strand, annealing it and ligating it to form NCOs.

1.2.2. Homologous chromosome synapsis

The synapsis of the homologous chromosomes begins at zygonema and it is linked to the approach and access of the DNA strand of one chromosome to its template in the homologue. Thus, in mammals, the meiotic recombination is a prerequisite for synapsis (MacQueen and Hochwagen, 2011). The physical union between homologous chromosomes is stabilized by the formation of the synaptonemal complex (SC), a proteinaceous structure that maintains the chromosomes together during prophase I (Fig. 1.6). It also acts as an anchor site for several proteins that are indispensable during prophase I, including

recombination, cell cycle and checkpoint proteins. Like in other processes involved in meiosis, the architecture of the SC is evolutionarily conserved among several organisms (Bogdanov et al., 2007). Cytologically, the different stages of prophase I are established by the levels of synapsis indicated by the assembly of the different elements of the SC (Fraune et al., 2012; Morelli and Cohen, 2005; Page and Hawley, 2003; Yang and Wang, 2009).

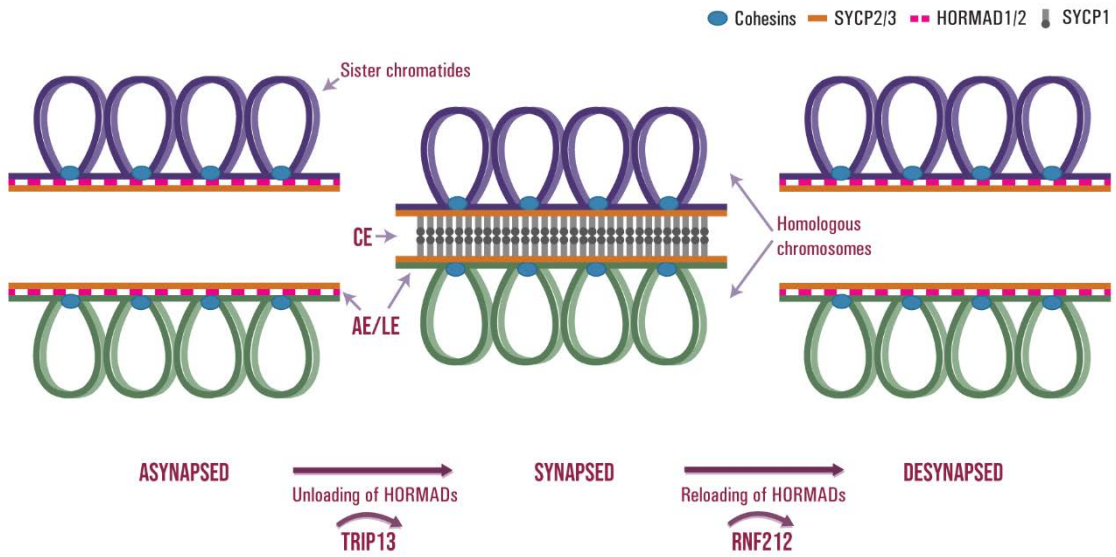

Figure 1.6 Synaptonemal complex assembly. At leptonema the AE composed by SYCP2, SYCP3, HORMAD1, HORMAD2 and cohesin complexes attach to the DNA loops. Once the DSBs are created and start to repair at zygonema, the axis of the homologous chromosomes come closer and synapse as the transverse filament protein SYCP1 assembles to the axial element (AE) forming the central element (CE). As the chromosomes synapse, HORMAD1/2 are removed from the axes by TRIP13 and reloaded at diplonema in a RNF212-dependent manner as the chromosomes desynapse.

At leptotene stage the axial element (AE), composed by SC proteins SYCP2, SYCP3 and cohesin complexes, attach to the DNA loops of each pair of sister chromatids (Fig. 1.6) (Revenkova and Jessberger, 2006). As homologous chromosomes align and pair at zygonema, synapsis begins when the transverse filament (TF) protein SYCP1 assembles progressively in a zipper-like structure, associating with lateral element (LE) proteins SYCP2 and SYCP3 via the C-terminal end. It also associates with the SYCP1 assembled in the LE of the homolog via the N-terminal end forming the central element (CE) (Fig. 1.6) (Liu et al., 1996; Meuwissen et al., 1992; Schmekel et al., 1996), together with other proteins like SYCE1, SYCE2, SYCE3 or TEX12 (Costa et al., 2005; Hamer et al., 2006; Schramm et al., 2011). At pachynema, the SC is completely formed, hence, the homologous chromosomes are fully synapsed forming bivalents, with the exception of the XY chromosomes in males, which only synapse by a small homologous region, the pseudoautosomal region (PAR). Finishing the prophase I, at diplonema, the central element disassembles promoting the desynapsis of the homologues, that now remain attached by the chiasmata.

Other proteins found in the chromosomal axes are the meiosis specific HORMA-domain proteins. In yeast, the HORMA-domain protein Hop1 is required for DSB formation, SC formation, prophase checkpoint and for promoting the interhomolog (IH) bias, the inhibition of the DSB repair from the sister chromatid in favor of the homologous chromosome (Bailis et al., 2000; Carballo et al., 2008; Hollingsworth and Byers, 1989; Schwacha and Kleckner, 1994; Woltering et al., 2000). In mammals, HORMA-domain proteins HORMAD1 and HORMAD2 accumulate on unsynapsed chromosomes, colocalizing with SYCP3 in both males and females. As the chromosomes synapse during prophase I, HORMADs are depleted from the axes by TRIP13 and are reloaded in females at diplonema in a RNF212-dependent manner (Fig. 1.6) (Fukuda et al., 2010; Qiao et al., 2018; Wojtasz et al., 2009a). Similar to yeast, in mice, these HORMAD proteins participate in the SC formation, chromosome segregation, prophase checkpoint and in DSB repair promoting the IH bias (Carofiglio et al., 2018; Daniel et al., 2011; Kogo et al., 2012b, 2012a; Shin et al., 2013, 2010; Wojtasz et al., 2012).

1.2.3. Sexual dimorphisms during meiotic prophase I

The events occurring at prophase I present a sexual dimorphism, with differences between males and females (reviewed in Morelli and Cohen, 2005). The SC length is twice as long in females compared to males, and this difference determines an increase in the recombination rate in human and mouse females (Tease and Hultén, 2004). Additionally, the COs are located more distally in males than in females (Hassold et al., 2000). Other difference is found in the dynamics of the SC, which is retained in males at the centromeres through anaphase II (Moens and Spyropoulos, 1995), while in females all the SC proteins have disappeared by the dictyate arrest (Hodges et al., 2001; Kolas et al., 2005). There are also timing differences in the SC formation and chromosome distribution in relation to the DSB formation and resolution of the recombination events. In human oocytes the clustering of telomeres, the bouquet, last longer, up to early pachytene stage, while in males is restricted to leptonema and zygonema. Also the γH2AX patches, signaling unrepaired DSBs, are more abundant in oocytes at pachynema than in spermatocytes at the same stage, indicating a slower progression of DSB repair in females (Roig et al., 2004). Besides these structural and functional differences, there is also a marked sexual dimorphism regarding the phenotypes caused by mutations in proteins involved in the recombination and synapsis (see below).

1.3. Meiotic checkpoint mechanisms

As described above, in mammals both meiotic recombination and homologous chromosome synapsis are coupled together during prophase I in order to succeed and prepare the spermatocytes and oocytes to the following meiotic divisions. Since the failure of one process mostly disturbs the other and produce infertility or an increase in aneuploidies, it is very important that both events develop correctly. This fact highlights the

importance of having particular and specific surveillance mechanisms monitoring these processes.

In order to achieve the successful formation of haploid gametes, all the processes of meiosis have to be regulated and coordinated with one another. The checkpoint mechanisms, as first described, are signaling pathways detecting cell cycle events that create dependent relationships between metabolically independent processes (Hartwell and Weinert, 1989; MacQueen and Hochwagen, 2011; Subramanian and Hochwagen, 2014; Zhou and Elledge, 2000). Therefore, these checkpoint mechanisms are not responding only to abnormal events, instead, are always activated during a normal mitotic and meiotic division. For example, the creation of DSBs in the genome is, in most cell types, an abnormal event, but not in meiocytes, in which these DSBs are needed for the success of the division. These mechanisms are necessary to determine the correct timing and to avoid deleterious interactions between processes, and they are responsible to delay the cell cycle progression and activate the repair or death responses when something goes awry.

1.3.1. The DNA damage response

When the DSBs are induced at leptotene stage, the DNA damage response (DDR) is activated. The DDR has been long studied in somatic cells in mammals. It starts detecting the presence of the unprocessed ends of the DSBs through the sensor proteins of the MRN complex (MRE11/RAD50/NBS1) (Oh and Symington, 2018; Stracker and Petrini, 2011). This complex capture the DNA ends leading to the autophosphorylation of the kinase ATM (ataxia-telangiectasa mutated), the primary transducer of DSB-induced signaling (Paull, 2015; Stracker et al., 2013). ATM then spreads the signal phosphorylating several downstream targets involved in DNA repair, cell cycle progression and apoptosis, including the histone H2AX (Stracker et al., 2013), the effector kinases CHK1 and CHK2 (Bartek and Lukas, 2003; Chaturvedi et al., 1999; Matsuoka et al., 2000; Stracker et al., 2009), and the tumor suppressor p53, among others (Banin et al., 1998; Canman et al., 1998; Khanna et al., 1998). When p53 is phosphorylated, it arrests the cell cycle until the DNA is repaired, and if the damage persists, it induces the expression of pro-apoptotic genes to activate a programmed cell death (Barlow et al., 1997; Vogelstein, 2000; Oren, 1994; Roos and Kaina, 2006; Taylor and Stark, 2001). Once the DSB has been resected and processed, RPA bounds to the ssDNA ends allowing the recruitment of the other primary transducer, ATR (ataxia-telangiectasia and Rad-3 related protein), through its activator ATR-interacting protein (ATRIP). Once active, ATR, as ATM, phosphorylates a large number of substrates to activate the DNA-damage response (Cimprich and Cortez, 2008; Maréchal and Zou, 2013).

The knowledge about the DDR in oocytes and spermatocytes is inferior, but the creation of mutants lacking some of the proteins involved in this response to the meiotic DSBs has allowed the study of this pathway (see some examples in 1.3.3.1). The MRN complex sense the meiotic DSBs (Cherry et al., 2007; Pacheco et al., 2015; Stracker and Petrini, 2011), leading to the activation of ATM/ATR. It has been found that there is

overlapping in the ATM-CHK2 and ATR-CHK1 axis in somatic cells (Cuadrado et al., 2006; Kastan and Lim, 2000; Stracker et al., 2013; Wang et al., 2006). In meisosi, CHK2 can be activated by both ATM and ATR and signal to both p53 and TAp63, regulating the oocyte and spermatocyte population (Bolcun-Filas et al., 2014; Marcet-Ortega et al., 2017; Pacheco et al., 2015). Moreover, the phosphorylation of the histone H2AX, signals the DSB sites at early prophase I, but later it marks the asynapsed regions of the homologous chromosomes (Mahadevaiah et al., 2001).

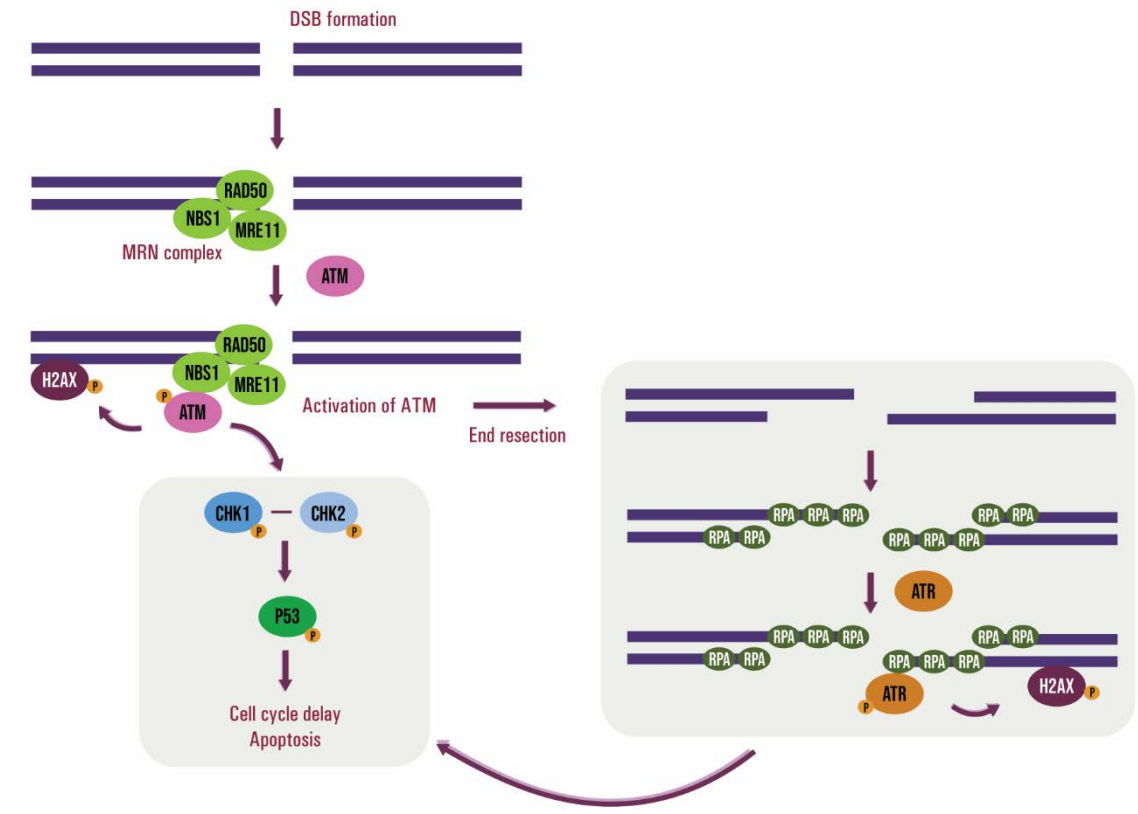

Figure 1.7 The DNA damage response (DDR). The signaling pathway of the DDR starts with the detection of the DSBs by the MRN complex, which recruits and activates ATM. At this point, ATM phosphorylates H2AX that extends the signal, and CHK1 and CHK2 that will phosphorylate p53 producing a delay in the cell cycle. If the DSBs are not repaired this delay will result in apoptosis. DSBs are resected, leaving the ssDNA tail that are detected by RPA, which is the primary activator of the ATR kinase, that like ATM, can phosphorylate H2AX, CHK1 and CHK2.

1.3.2. Choice of the DSB repair mechanism

A key aspect in the regulation of the recombination is the choice of repair mechanism. In meiosis, the HR is fundamental to promote the pairing and posterior segregation of the homologous chromosomes. Hence, the other possible available repair mechanism, the non-homologous end joining (NHEJ), which ligate the broken DNA ends without an homologous template, has to be diminished or repressed during early meiotic prophase. Additionally,

the choice of repair template is also very important for the meiocytes. The HR has to occur between homologous chromosomes, and not between sister chromatids (Goedecke et al., 1999; Lao and Hunter, 2010). The presence of the interhomolog (IH) bias or barrier to sister chromatid recombination (BSCR), the preferably use of the homologue instead of the sister chromatid, has been well studied in other organisms like *S. cerevisiae*, in which this preference is regulated by recombination proteins (Rad51, Dmc1) associated with the synaptonemal complex proteins (Hop1, Red1, Hed1, Rec8) and DDR proteins (Mec1/Tel1). For example, activation of Tel1 and Mec1 (ATM and ATR orthologues respectively) phosphorylate the AE HORMA-domain protein Hop1 activating the DNA-damage effector kinase Mek1 (CHK2 paralogue). Once active, Mek1 autophosphorylates and promotes IH recombination by phosphorylating several proteins, like Hop1 and Rad54. Without this Hop1 phosphorylation, the DSBs are repaired via a Dmc1-independent intersister (IS) repair pathway, leading to spore lethality (Callender and Hollingsworth, 2010; Carballo et al., 2008; Niu et al., 2005, 2007, 2009; Schwacha and Kleckner, 1997; Wu et al., 2010).

In mammals, the study of this IH bias is harder, for example, because of the absence of 2D gels experimental settings, but some works about this topic have seen the light. Importantly, the mentioned key proteins participating in this IH bias have mammalian orthologs: ATM, ATR, DMC1, RAD51, RAD54, CHK2 and HORMAD1/2. Studies in female mice lacking SYCP3 or SYCP2 support a model by which the rescue of IH recombination-deficient oocytes is attributable to altered recombination partner choice. In a way, the SC AE facilitate IH recombination and inhibit IS recombination. The model is that the nucleoprotein filaments of RAD51/DMC1 at the resected ends are oriented to the AE proteins, inhibiting the IS recombination and favoring the IH one (Li et al., 2011). The proteins HORMAD1 and HORMAD2, the mammalian orthologues of Hop1, are depleted from the axes by TRIP13 as homologues synapse and later re-associate as they desynapse at diplonema (Fukuda et al., 2010; Wojtasz et al., 2009a). It has been postulated that, like their orthologues, HORMAD1 and HORMAD2 participate in the IH bias by impeding IS repair. Recent lines of research indicate this participation. In absence of HORMAD2 in females, there is a reduction of the unrepaired DSBs detected as RAD51 foci at pachynema and diplonema, difference that gets more evident irradiating mutant ovaries (Rinaldi et al., 2017a). This pattern is the same for *Hormad1*$^{-/-}$ males and females, with a decrease in the ɣH2AX signal, and a reduction in DMC1 and RAD51 foci in spermatocytes and oocytes (Fukuda et al., 2010; Shin et al., 2010). 8 hours after irradiating *Hormad1*$^{-/-}$ ovaries to produce exogenous DSBs, there is a reduction in the ɣH2AX signal at zygonema, and a reduction of RAD51 foci, but not of DMC1 (Shin et al., 2013). All these data are consistent with the interpretation that *Hormad1* or *Hormad2* deficiency promotes the IS recombination repair in a *Dmc1*-independent pathway. The exogenous induction of DSBs in *Spo11*$^{-/-}$ mice are processed by HR resulting in a higher synapsis of the homologues, but they are unable to correctly complete HR resulting in the presence of persistent repair intermediates. In irradiated *Spo11*$^{-/-}$ *Hormad1*$^{-/-}$ mouse, though, the spermatocytes presented a reduction of RAD51 and DMC1 foci, hence, a reduction of repair intermediates (Carofiglio et al., 2018). These data also support the presence of the IH bias in mammals.

In *S. cerevisiae*, the phosphorylation of the AE protein Hop1 by Mec1/Tel1 is required for the recruitment of the effector kinase Mek1 to the AE (Carballo et al., 2008). As Mek1 is excluded by Pch2 (TRIP13 in mammals) from the synapsed axes, both IS and IH recombination can occur (Subramanian et al., 2016). Hence, it has been proposed that the same happens at the removal of HORMADs at pachytene stage in mammals (Rinaldi et al., 2017a). On that matter, studies with mouse spermatocytes after irradiation showed that there are two types of response to the DNA damage, one from leptotene to early pachytene, where the DSBs are preferentially repaired by HR; and a second one, from mid pachytene to diplotene stages, mediated initially by NHEJ and later by an HR pathway involving RAD51 but not DMC1 (Enguita-Marruedo et al., 2019). This shift in the repair pathway might be important for the resolution of DSBs that could not be repaired during the early prophase I. In that same direction, the presence of the protein RNF212 impedes DSB repair in perinatal oocytes and promotes or stabilizes the reloading of HORMADs into the chromosome axes at diplonema, probably impeding the repair of the residual DSBs by IS recombination (Qiao et al., 2018). This would represent a quality control mechanism regulating the unrepaired damage maintained through diplonema, impeding the repair of DSBs in abnormal oocytes with recombination or synapsis errors, and triggering apoptosis.

1.3.3. The pachytene checkpoint

The terminal response (arrest and apoptosis) to chromosomal damage activated by the lack of recombination or the incorrect synapsis of homologous chromosomes during meiotic prophase is known as the pachytene checkpoint. In mammals, this response has been separated in two different mechanisms: the recombination checkpoint, activated by the presence of recombination intermediates; and the synapsis checkpoint, presumably activated by the presence of asynapsis. Nonetheless, there are discrepancies regarding the separation and function of these checkpoints in different species and even between males and females (MacQueen and Hochwagen, 2011; Rinaldi et al., 2017a; Roeder and Bailis, 2000; Subramanian and Hochwagen, 2014).

1.3.3.1. **The recombination checkpoint**

The activation of the signaling cascade of ATM and ATR as a response to the presence of persistent recombination intermediates at pachynema, produces a delay in the meiotic progression allowing the cell to repair the DSBs or die by apoptosis (Hochwagen and Amon, 2006; Longhese et al., 2009). The mechanism of activation of this checkpoint differs between species. In *D. melanogaster* and *S. cerevisiae* it requires the CHK2 homologues, Mnk and Mek1 respectively, while CHK1 is dispensable (Hochwagen and Amon, 2006; MacQueen and Hochwagen, 2011; Wu et al., 2010). Oppositely, in *C. elegans*, CHK-1 is necessary for the cell cycle arrest while CHK-2 has other meiotic functions (Gartner et al., 2000; MacQueen and Villeneuve, 2001). Moreover, the effects of the ATM/ATR activation

are also different. In the plant *A. thaliana*, the presence of unrepaired DSBs doesn't trigger a delay of meiotic progression (Couteau et al., 1999); and in *S. pombe*, a specie that does not form an SC, the meiotic recombination-deficient mutants don't present a meiotic arrest and only the most severe repair defects trigger a delay (Shimada et al., 2002).

In mouse, the responses of the recombination checkpoint activation are very different comparing males and females. This can be studied through the use of mutant mice lacking key proteins involved in recombination or in the DDR.

In males, the single mutants for *Dmc1*$^{-/-}$, *Trip13*$^{mod/mod}$ and *Msh5*$^{-/-}$ are all infertile due to the apoptosis of the spermatocytes at pachytene stage, showed histologically as an arrest at epithelial stage IV. Due to this reduction of cells in the tubules, mutant testis present a reduction in size and weight. Due to the lack of an essential protein involved in the recombination process, all these mutants are deficient for meiotic recombination and accumulate recombination intermediates. This deficiency, in *Dmc1*$^{-/-}$ and *Msh5*$^{-/-}$ also leads to an impaired synapsis (Barchi et al., 2005; Barlow et al., 1996, 1998; Li and Schimenti, 2007; Pacheco et al., 2015; Pittman et al., 1998; Roig et al., 2010; Vries et al., 1999; Xu et al., 1996; Yoshida et al., 1998). This death is consequence of the activation of the recombination-dependent arrest, and importantly, it was discovered that this apoptosis was triggered prior the incorporation of the testis specific histone H1t, at early pachynema (Barchi et al., 2005; Pacheco et al., 2015). When the lacking protein is involved in late recombination events, for example in CO formation, like MLH1, the arrest is produced later. *Mlh1*$^{-/-}$ mice are also infertile, but since the DSBs are repaired, the pachytene checkpoint is not activated and the arrest is produced later, at epithelial stage XII corresponding with cells at metaphase I due to the activation of the spindle assembly checkpoint (Eaker et al., 2002).

The study of the role of certain proteins in meiosis involved in recombination, like CHK1, ATR, MRE11 and NBS1, it's been challenging since their absence is embryonic lethal due to its role in somatic cells (Brown and Baltimore, 2000; Roig et al., 2010; Stracker and Petrini, 2011; Takai et al., 2000). In this case, alternative mouse models were created. For example, mice bearing hypomorphic mutations like *Nbs1*$^{\Delta B/\Delta B}$ and *Mre11*$^{atld/atld}$, which attenuate ATM activation and/or diminish phosphorylation of subsets of ATM targets; are all viable. The males are subfertile with spermatocytes carrying some synaptic defects and accumulation of early recombination markers at pachynema, but advancing past this stage, as shown by the presence of H1t-positive spermatocytes (Cherry et al., 2007; Pacheco et al., 2015; Stracker and Petrini, 2011). For the study of CHK1, a germline-specific KO mouse model was created recently, in which testes were smaller due to the lack of spermatogonia produced between 3 and 5 dpp (Abe et al., 2018). Regarding ATR, two murine models have been created. The first one is a humanized mouse model of ATR Seckel syndrome, *Atr*$^{S/S}$, an hypomorphic mutant with a reduction of the levels of ATR in most tissues (Murga et al., 2009). Those mutants present smaller testis, maybe attributable to the dwarfism of the mice, since males present apparently no gross meiotic defects and are able to produce mature spermatozoa (Pacheco et al., 2018). In the second mouse model, a conditional deletion of *Atr* was performed in testes, which were smaller without a reduction in the body

size. The mutant males present a spermatocyte arrest at mid pachynema at epithelial stage IV (Widger et al., 2018).

Thanks to the study of these mouse models, and the creation of mice combining different mutations creating double and triple mice mutants, it has been found that in males, the recombination-dependent arrest depends on the MRN complex, ATM, CHK2, p53 and TAp63. These double and triple mutants are needed to unravel the checkpoint functions of proteins like p53 and CHK2, since their absence alone does not cause disruptions in the meiotic processes. Introducing a second mutation with defective recombination, like in *Trip13*$^{mod/mod}$ *Chk2*$^{-/-}$, *Trip13*$^{mod/mod}$ *p53*$^{-/-}$ and *Trip13*$^{mod/mod}$ *Tap63*$^{-/-}$, it was found that the recombination defective spermatocytes that normally die in the recombination arrest checkpoint (detected by the lack of H1t), were skipping this checkpoint progressing further in meiosis (incorporating H1t), only to die later by sex body defects in a synapsis checkpoint. (Marcet-Ortega et al., 2017; Pacheco et al., 2015). This observation supports the presence of two genetically distinct elimination pathways.

In female mice, the timing and mechanisms of this recombination checkpoint are more diffuse (Di Giacomo et al., 2005; Rinaldi et al., 2017a). Different recombination mutants have different ovarian phenotypes, for example, mutant mice lacking recombination proteins that allows the initiation of recombination but are defective for their repair or synapsis, like *Dmc1*$^{-/-}$, *Msh5*$^{-/-}$, *Trip13*$^{mod/mod}$ and *Mcmdc2*$^{-/-}$ have ovaries containing between 50 and 60% of the oocytes of a wild type at birth, but few days later the oocyte pool is completely depleted (Di Giacomo et al., 2005; Finsterbusch et al., 2016; Li and Schimenti, 2007; McNairn et al., 2017). Contrarily, females lacking MLH1, a protein found in COs at late pachynema, are able to repair their DSBs, hence, despite being infertile, present a little amount of oocytes from all the follicle types at adult age (Baker et al., 1996; Edelmann et al., 1996). These data reveal that the checkpoint in females, as seen in males, acts differently depending on the timing of the error, with the females carrying an early recombination protein mutation having a more severe phenotype that those with a late recombination protein defect, that seems to have a weaker regulation due to the ability of those cells to repair their DSBs without triggering the recombination checkpoint.

The oocyte elimination reported in the early recombination mutants is dependent on DSB formation, since the elimination of the DSBs by suppression of SPO11 in these mutants produces a rescue of the number of oocytes found in the ovaries. The double mutants *Spo11*$^{-/-}$ *Dmc1*$^{-/-}$, *Spo11*$^{-/-}$ *Msh5*$^{-/-}$ and *Spo11*$^{-/-}$ *Trip13*$^{mod/mod}$ still contain some oocytes by 3 weeks of age, mostly primary to antral follicles without primordial follicles. This phenotype is the same as the *Spo11*$^{-/-}$ single mutants, showing that the abolition of DSBs cancels the effects of the lack of recombination proteins and demonstrating the epistasis of the *Spo11* mutation with the recombination mutations (Di Giacomo et al., 2005; Li and Schimenti, 2007). Nonetheless, these double mutants are infertile and have a significant loss of oocytes, compared to WT ovaries, presumably by the activation of the synapsis checkpoint (see below).

Regarding the proteins triggering and regulating this checkpoint in females, similar to male mice, flies and budding yeast, the oocyte death described in recombination mutants is mediated by CHK2. If CHK2 acts as a recombination checkpoint protein, in its absence there should be a rescue of oocytes of the recombination-defective mutants. Indeed, 3 weeks old *Dmc1*$^{-/-}$ *Chk2*$^{-/-}$ ovaries have a partial rescue of the ovarian reserve with primary to antral follicles but without primordial ones, leading to a total depletion of oocytes by 2 months (Bolcun-Filas et al., 2014), resembling the phenotype of the Spo11$^{-/-}$ ovaries and suggesting that the absence of CHK2 allows the surpass of the recombination checkpoint, but not the synapsis checkpoint. Interestingly, in *Trip13*$^{mod/mod}$ *Chk2*$^{-/-}$ double mutant ovaries, there was an almost complete rescue of the number of oocytes at 3 weeks, and unlike the previous mutants, the ovaries contain all the follicle types from primordial to antral. Since TRIP13 is required for DSB repair, it is expected to find an increase of DSBs in this mutant, and indeed, all dictyate oocytes present abundant γH2AX staining, marker of DSBs (Bolcun-Filas et al., 2014). Despite this high number of DSBs, the females are fertile and are able to produce multiple litters, smaller than the controls but with no visible abnormalities up to one year, suggesting that all those DSBs are eventually repaired (Bolcun-Filas et al., 2014). It also suggests that TRIP13 is dispensable for the proper synapsis of the homologous chromosomes since these oocytes are not eliminated in a synapsis checkpoint.

Chk2$^{-/-}$ *Atm*$^{-/-}$ double mutants present an oocyte rescue similar to the *Dmc1*$^{-/-}$ *Chk2*$^{-/-}$ females, indicating that ATM is not the only protein activating CHK2 (Bolcun-Filas et al., 2014). Adding this to the fact that CHK2 can be activated by ATR in somatic cells (Wang et al., 2006), is indicating that probably ATR signals to CHK2 in the oocytes. CHK2, in turn, signals to p53 and TAp63 that act in a partially redundant way eliminating oocytes with unrepaired DSBs (Bolcun-Filas et al., 2014; Suh et al., 2006). This signaling pathway is similar in males, with CHK2 signaling to p53 and TAp63, but differently than females, they act in a non-redundant manner activating the recombination dependent-arrest (Marcet-Ortega et al., 2017).

1.3.3.2. **The synapsis checkpoint**

The relation between recombination and synapsis changes depending the species. For example, in *C. elegans* and Drosophila, unlike mice, the DSB formation, chromosome pairing and synapsis can occur independently of each other. Homologous chromosomes pair and synapse and then initiate meiotic recombination (Dernburg et al., 1998; McKim et al., 1998). In those species, the DSB-independent signals activate checkpoint proteins regulating chromosome dynamics. An example of this is found in *C. elegans*, with the chk-2 mutants displaying failure in recombination initiation, chromosome telomere clustering in the nuclear envelope, chromosome pairing and SC assembly. Similar to the HORMA-domain-containing protein HTP-3, implicated in promoting DSB initiation, homolog pairing and synapsis initiation. This signal pathway, being DSB-independent, requires CHK2 but not ATM/ATR (Goodyer et al., 2008; MacQueen and Villeneuve, 2001).

The synapsis checkpoint is activated by defects in the formation or assembly of the SC axis that creates asynapsis sites. This asynapsis triggers the recruitment of several proteins in order to delay meiotic progression independently of the DSB formation. Due to the independence of recombination and synapsis, the study is extensive in *C. elegans* and Drosophila. In the first, the activation of the checkpoint requires CHK-1, and both require PCH-2 (Bhalla and Dernburg, 2005; Joyce and McKim, 2009). In *S. cerevisiae*, Pch2 is needed for checkpoint activation in response to cells with incomplete synapsis, including Zip1 mutants, which lack the TF of the SC (Mitra and Roeder, 2007; San-Segundo and Roeder, 1999; Wu and Burgess, 2006). In mammals, as mentioned before, the Pch2 homolog, TRIP13 regulates the distribution of HORMADs in the axes of the homologous chromosomes (Wojtasz et al., 2009a) and it is required for recombination and correct chromosomal structure during meiosis (Roig et al., 2010). Up to date, the synapsis checkpoint function for TRIP13 has not been found in mammals, possibly due to its main role in recombination, even though it is required for synapsis of the XY chromosomes and for a correct sex body formation (Pacheco et al., 2015; Roig et al., 2010)

The responses in males and females are different, basically due to the formation of the sex body in males. The X and Y chromosomes in males only share a little region of homology, the PAR. As a consequence, at pachynema, synapsis in the sex chromosomes is only achieved at this region, leaving the rest of the XY chromosomes asynapsed. This asynapsis triggers the formation of the sex body, a structure that silence the sex chromosomes allowing the meiotic progression through the pachytene checkpoint (McKee and Handel, 1993). This silencing, known as Meiotic Sex Chromosome Inactivation (MSCI) is a specialization of the general mechanism of Meiotic Silencing of Unsynapsed chromosomes (MSUC). The MSCI is required for the spermatocytes to survive, since the expression of certain X- and Y-linked genes at pacynema has been found to be lethal for spermatocytes (Baarends et al., 2005; Pacheco et al., 2015; Royo et al., 2010; Turner, 2007; Turner et al., 2005).

The persistence of asynapsed regions at late zygonema, including the XY in males, triggers the phosphorylation of axial proteins like HORMAD1 and HORMAD2, which attract BRCA1 (Daniel et al., 2011; Fukuda et al., 2012; Turner et al., 2004; Wojtasz et al., 2012). This protein acts as a sensor and recruits ATR that maintains the signaling continuously recruiting more BRCA1. Furthermore, ATR phosphorylates H2AX (ɣH2AX) spreading the signal, inducing post-translational modifications and gene silencing (Fernandez-Capetillo et al., 2003; Royo et al., 2013; Turner et al., 2004).

In male mice, the synapsis checkpoint arrests and eliminates the spermatocytes with a defective sex body. As explained before, mutant spermatocytes with recombination defects arrest at early pachynema before the incorporation of H1t (Marcet-Ortega et al., 2017; Pacheco et al., 2015). Differently, the spermatocytes that only show defects in the sex body formation suffer an arrest at late pachynema, after the incorporation of H1t. For example, the *Spo11*$^{-/-}$ males are unable to create DSBs, skipping the recombination checkpoint, but still die due to an aberrant sex body formation (Barchi et al., 2005).

Similar to the mechanism in males, recombination defective female mutants present a total depletion of oocytes few days after birth, while *Spo11*$^{-/-}$ ovaries are able to skip the recombination checkpoint and maintain a little amount of oocytes for few weeks after birth (Di Giacomo et al., 2005). This difference in the severity and timing of oocyte elimination shows that there is, also in females, two different independent responses, the recombination checkpoint mediated by CHK2, and the synapsis checkpoint, mediated by HORMAD1/2. Both *Hormad1*$^{-/-}$ and *Hormad2*$^{-/-}$ young and adult ovaries are indistinguishable from the WT ones, containing a normal pool of oocytes with all the follicle types, even though *Hormad1*$^{-/-}$ females are infertile (Kogo et al., 2012a, 2012b; Shin et al., 2010). The deletion of either HORMAD1 or HORMAD2 in *Spo11*$^{-/-}$ females produces a total rescue of the oocyte pool, resulting in ovaries containing the numbers of oocytes of a WT and all the follicle types, but those are nonfertile (Daniel et al., 2011; Kogo et al., 2012a). These data sugests that HORMAD1 and HORMAD2 are components of the synapsis checkpoint. Furthermore, the study with XO females showed the presence of an oocyte elimination mechanism at diplonema triggered by the presence of asynapsed chromosomes (Cloutier et al., 2015). They showed how this elimination, similar to what happens in males, is linked to the presence of γH2AX on the asynapsed regions. The accumulation of this protein is not the cause of death, instead, is the MSUC mechanism that is responsible of the oocyte death silencing genes necessary for the viability of the oocyte (Cloutier et al., 2015).

1.3.3.3. **The relation between the recombination and synapsis checkpoints**

As described earlier, in mammals, recombination drives homologous synapsis, hence the line that separates the recombination checkpoint and the synapsis checkpoint is sometimes diffuse.

The sex body, besides accumulating the proteins mentioned before (HORMAD1/2, ATR, γH2AX, among others), also accumulates DSB repair proteins. In fact, most of the MSUC machinery is implicated in DSB repair. The X, but not the Y chromosome, and unsynapsed axes, accumulates both RAD51 and DMC1 during mid and late pachynema (Kauppi et al., 2011; Moens et al., 2002, 1997). 60% of *Spo11*$^{-/-}$ spermatocytes present an incomplete MSUC activation in the form of a pseudo sex body, not on the X and Y chromosomes, but only in a section of the unsynapsed chromatin in the autosomes, even though all the asynapsed axes are coated with HORMAD1/2 (Barchi et al., 2005; Carofiglio et al., 2013; Fukuda et al., 2010; Wojtasz et al., 2009a). If present, this pseudo sex body have some characteristics of a regular sex body, like the recruitment and phosphorylation of several proteins, even though at lower levels, and the consequent silencing of the genes of that region (Bellani et al., 2005; Mahadevaiah et al., 2008). Interestingly, this pseudo sex body contains RAD51, DMC1 and RPA, demonstrating that the proteins involved in processing the DSBs are also involved in triggering the MSUC mechanism, even in the absence of DSBs (Carofiglio et al., 2013). Recently, the histone H3-lysine-9 methyltransferase SETDB1 has been found to be the link between the DDR and the silencing in males. Silencing depends

on the DDR network, proven by the fact that the H3K9me3 enrichment on the sex body, signal of silencing, is directed by DDR factors. In absence of SETDB1, the X chromosome accumulates DDR proteins, but not H3K9me3, showing that this protein is the responsible of the enrichment and XY silencing, with its recruitment being dependent of H2AX (Hirota et al., 2018).

In wild type females, the pseudo sex body is observed in 20% of the oocytes, marked with γH2AX and BRCA1 and, as in males, coated with RAD51, DMC1 and RPA (Carofiglio et al., 2013; Kouznetsova et al., 2009). In SPO11-deficient females the pseudo sex bodies were also coated with recombination repair proteins. Moreover, these female mutants present a *de novo* accumulation of RAD51 foci along the axes at pachynema, which are independent of SPO11-driven DSB formation (Carofiglio et al., 2013). These data indicated that the SPO11-independent DNA damage foci contribute to the MSUC response in females.

As mentioned before, CHK2 deletion is able to partially rescue the ovaries of recombination mutants like *Dmc1*$^{-/-}$ and *Trip13*$^{mod/mod}$, showing its role in the recombination checkpoint (Bolcun-Filas et al., 2014). Strikingly, a recent paper shows the ablation of CHK2 in *Spo11*$^{-/-}$ adult ovaries also produces a partial rescue of oocytes, reaching approximately half of the oocytes of a *Chk2*$^{-/-}$ ovary (Rinaldi et al., 2017a). The fact that the proteins needed for the homologous recombination are also involved in triggering the synapsis checkpoint, and that the deletion of a protein regulating the recombination checkpoint is rescuing oocytes without SPO11-induced DSBs, is pointing out that the pachytene checkpoint is very complex and possibly is overlapping signaling pathways affecting to both the recombination and the synapsis processes.

One possible explanation about this overlapping proposed in Rinaldi et al., 2017a was that the pachytene checkpoint consists in a single checkpoint responding to canonical DNA damage and that the asynapsis does not trigger a distinct synapsis checkpoint, but triggers the oocyte death by inhibiting HR repair (Rinaldi et al., 2017a).

1.4. Regulation of the oocyte population

As we just saw, the most probable fate of an oocyte is death, with the majority of the oocytes dying early in the perinatal death, and the rest dying later during follicular recruitment until the exhaustion of the pool, the so called menopaused in women. Hence, the quality of the surviving oocytes must be adequate to success in the possible future fertilization.

The perinatal massive oocyte death is an extensively reported process conserved in several species, from *C. elegans* and *D. melanogaster* to mouse and humans (Hassold and Hunt, 2001; Hunter, 2017; Matova and Cooley, 2001). Despite this evolutionary conservation, the cause, reasons and mechanisms of this process are unknown. Some theories about the reasons and mechanisms of oocyte elimination has been considered. For

example, it has been proposed that the oocytes die “by neglect” or “self-sacrifice” (Hartshorne et al., 2009; Tilly, 2001). In the death “by neglect”, the cells die because they receive insufficient growth factors from the environment. There are some examples of this death in the gametogenic failure of mutants lacking germ-cell survival factors, such as SCF or interleukin-1αβ (Mintz and Rusell, 1957; Morita et al., 2001). In the death “by defect” the meiotic checkpoints would eliminate the oocytes with recombination or synapsis problems, selecting and keeping the better oocytes. Lastly, in the death “by self-sacrifice”, as observed in Drosophila, one oocyte receives the cytoplasm, organelles and factors from the accompanying oocytes that become nurse cells supporting the proper growth and survival of the future oocyte (de Cuevas et al., 1997).

To this day, mouse perinatal oocyte death can be classified in two major stages, the early oocyte attrition and the late oocyte attrition (Hunter, 2017). The first one occurs at embryonic development, just before the birth of the female, and is correlated with the activation of the retrotransposon LINE-1 (L1) (Malki et al., 2014). This element is the only autonomous retroelement that remains active in the human genome (Cordaux and Batzer, 2009) and can act both promoting and silencing gene transcription. Its expression it’s related to the DDR and the downstream pathway leading to cell cycle arrest and apoptosis (Belgnaoui et al., 2006; Gasior et al., 2006; Wallace et al., 2008). More recently it has been found that L1ORF1, the translated protein, is detected in the nucleus of fetal oocytes during prophase I, at different levels among different oocytes, apparently in a stochastic pattern; and the oocytes with higher levels of L1ORF1 are the ones targeted for death (Malki et al., 2014). The late oocyte attrition occurs after birth, while the oocytes are progressing through prophase I and arresting at dictyate. Therefore, this death appears to be responding to the errors detected by meiotic checkpoints, both recombination and synapsis errors (see 1.3.3).

Even though this insightful data in mammals is providing a lot of knowledge about the process of oocyte creation and death, there is still a lot of unanswered questions about this topic and about the importance of the establishment of an errorless oocyte pool that will ensure the correct development of a new individual.

OBJECTIVES

Chapter 2

Oogenesis is a complex process that includes the differentiation from the PGC to oogonia, the cyst formation, the entry to meiosis and the oocyte development. Once the meiosis has started, several DSBs are deliberately introduced in the genome, which are repaired by homologous recombination to allow the synapsis of the homologous chromosomes. At the time of this repair, there is a massive oocyte death, necessary to stablish the final pool of primordial follicles. After that, the follicles can be recruited to grow and finally become preovulatory follicles with a fertilizable oocyte.

The mechanisms regulating the meiotic processes of recombination and synapsis, and the ones regulating the cyst breakdown, oocyte death and follicle formation remain still mostly unknown in females. In our work, we aim to stablish a relation between these processes, and for that, we used the *Chk2* mouse mutant model. The protein kinase CHK2 is known to participate in the recombination-dependent checkpoint eliminating oocytes with DNA damage, like the ones of the *Trip13* or *Dmc1* mutants (Bolcun-Filas et al., 2014). Moreover, we also used the *Trip13* mutant to assess its possible participation in the synapsis checkpoint, since its orthologue in budding yeast, Pch2, has this function (Mitra and Roeder, 2007; San-Segundo and Roeder, 1999; Wu and Burgess, 2006) and TRIP13 is required for MSUC (Pacheco et al., 2015; Roig et al., 2010).

In order to achieve our purposes, we stablished the following objectives:

I. Study the role of CHK2 in the recombination checkpoint regulating the oocyte pool

   a. **Asses if the prophase I oocytes lacking CHK2 present a higher number of DSBs.**

   b. **Analyze if CHK2 is responsible of the recombination-dependent perinatal oocyte death.**

   c. **Study if the cyst breakdown and follicle formation processes are regulated by CHK2.**

   d. **Analyze if CHK2 regulates the oocyte death in adult follicles**.

II. Study the role of TRIP13 in the synapsis checkpoint.

   a. **Analyze if TRIP13 is responsible for the elimination of oocytes with synaptic errors.**

MATERIALS AND METHODS

Chapter 3

3.1. Mice and biological samples

3.1.1. Animals and genotyping

Chk2, Spo11, Dmc1 and Trip13 mutant mice were generated previously and described elsewhere (Takai et al., 2002; Baudat et al., 2000; Pittman et al., 1998; Roig et al., 2010). The lines were maintained in a C57Bl/6-129/Sv mixed background. All experiments were performed using at least two animals and compared with control littermates or with animals of closely related parents.

Spo11 simple mutants and *Spo11 Trip13* double mutants were obtained mating heterozygous mice due to the sterility of these animals (Baudat et al., 2000; Li and Schimenti, 2007). *Dmc1 Chk2 Trip13* triple mutants were obtained from $Dmc1^{+/-}$ $Chk2^{-/-}$ $Trip13^{+/-}$ males mated with $Dmc1^{+/-}$ $Chk2^{-/-}$ $Trip13^{-/-}$ females since Dmc1 mutants are sterile (Pittman et al., 1998) and *Chk2* rescues the sterile phenotype of *Trip13* only in the females (Pacheco et al., 2015; Bolcun-Filas et al., 2014).

In the experiments using $Chk2^{-/-}$ animals, the controls used were both $Chk2^{+/+}$ and $Chk2^{+/-}$ animals, and they will be referred in the text as wild type (WT).

All the animals used for experimental procedures were sacrificed using CO_2 or decapitation euthanize methods approved by the Ethics Committee for Animal Experimentation of the Universitat Autònoma de Barcelona and the Catalan Government.

3.1.2. Biological samples

Ovarian samples were obtained from females at different ages depending on the experimental procedure. The presence of a vaginal plug was used to determine the age of the unborn fetuses. Females were caged overnight with males and if the vaginal plug was found next morning, the female was isolated and defined as 1 dpc. For nuclei spreads and histological procedures, the samples were obtained from embryos from 16 to 20 dpc. Females were sacrificed and the fetuses were removed, rinsed in PBS and dissected under a stereo microscope (Nikon SMZ-1). For histological procedures, ovarian samples were obtained from newborn mice from 1 to 4 dpp (20 to 23 dpc), young mice at 30 dpp and 40 dpp, and elder mice at 400 dpp. The pups were born at 20 dpc, and this day was defined as 1 dpp.

3.2. Molecular biology techniques

3.2.1. Genomic DNA extraction from mouse tails

With the purpose to determine the mice genotype, a piece of the tail was cut and digested to isolate and amplify the genomic DNA.

Protocol

- Obtain the last 0.5 cm of the mouse tail and place it in a 1.5 ml tube.
- Add 500 µl of lysis buffer (0.1 M Tris-HCl pH= 8.5, 0.2 M NaCl, 0.2% SDS, 5 mM EDTA, 0.4 mg/ml proteinase K [Roche Diagnostics] in Milli-Q water)
- Incubate the tubes overnight at 56ºC and 350 rpm in the thermomixer.
- Centrifuge the tubes for 15 minutes at 13200 rpm and transfer the supernatant into a new tube containing 0.5 ml of isopropanol. Shake vigorously until DNA precipitates.
- Centrifuge the tubes for 3 minutes at 13200 rpm and discard the supernatant.
- Add 0.5 ml of ice-cold 70% ethanol to the pellet and shake for washing it.
- Centrifuge the tubes for 3 minutes at 13200 rpm and discard the supernatant. Let the tubes open at room temperature for the pellet to air dry.
- Dissolve the pellet in 100 µl of Milli-Q water and place the tubes in the thermomixer at 60ºC for 10 minutes.
- Store the extracted DNA at -20ºC until use.

3.2.2. Genotyping

In order to genotype the mice, the genomic DNA was amplified using the Polymerase Chain Reaction (PCR). The primers used were previously designed for each gene to distinguish the wild type and mutant alleles based on the amplified products.

Table 3.1 *Chk2* Primers

Primer name	Sequence	Allele specificity	Amplified product
WT1F	5′ – GTGTGCGCCACCACTATCCTG – 3′	+/-	
WT2R	5′ – CCCTTGGCCATGTTTCATCTG – 3′	+	450 bp
NeoMutR	5′ – TCCTCGTGCTTTACGGTATC – 3′	-	625 bp

Table 3.2 *Spo11* Primers

Primer name	Sequence	Allele specificity	Amplified product
SP16R	5′ – ATGTTAGTCGGCACAGCAGTAG – 3′	+/-	
SP1F	5′ – CTACCTAGATTCTGGTCTAAGC – 3′	+	1024 bp
PRSF2	5′ – CTGAGCCCAGAAAGCGAAGGAA – 3′	-	600 bp

Table 3.3 *Dmc1* Primers

Primer name	Sequence	Allele specificity	Amplified product
oIMR9133F	5′ – AAAGGGACTGCTGAGGCATA – 3′	+/-	
oIMR9132R	5′ – CCGGCCAGATTACATTTCTT – 3′	+	233 bp
oIMR5332R	5′ – GCCAGAGGCCACTTGTGTAG – 3′	-	147 bp

Table 3.4 *Trip13 moderate* Primers

Primer name	Sequence	Allele specificity	Amplified product
neOct15R	5′ – TTCAGAACCGTGTTCCTTCC – 3′	+/-	
neOct15F	5′ – TCCATTGCTTTGTGCCATTA – 3′	+	290 bp
RRB047F	5′ – CCACGCTCACCGGCTCCAGA – 3′	-	855 bp

Protocol

- Prepare the PCR Mix following manufacturer Canvax Horse-Power Taq DNA Polymerase recombinant kit and add it to a 0.2 ml PCR tube.

Table 3.5 Components of the PCR mix reaction

Component	Volume
10x PCR Buffer	2 µl
$MgCl_2$ 25 mM	1.36 µl
dNTPs 8 mM	2 µl
Forward primer 10 µM	1 µl
Reverse primer 10 µM	1 µl
Mutant primer 10 µM	1 µl
Template DNA	1 µl
Horse-Power Taq DNA polymerase (5U/µl)	0.4 µl
Milli-Q water	Up to 20 µl

- Place PCR tubes in the thermal cycler and perform the PCR amplification using the following cycling conditions.

Table 3.6 *Chk2* PCR conditions

Step	Temperature	Volume	
Predenaturation	95 °C	3 minutes	
Denaturation	95 °C	45 seconds	x 35 cycles
Annealing	60 °C	45 seconds	
Extension	72 °C	5 seconds	
Final extension	72 °C	7 minutes	

Table 3.7 *Spo11* PCR conditions

Step	Temperature	Volume	
Predenaturation	94 °C	2 minutes	
Denaturation	94 °C	20 seconds	x 34 cycles
Annealing	61.5 °C	30 seconds	
Extension	72 °C	35 seconds + 1 second/cycle	
Final extension	72 °C	3 minutes	

Table 3.8 *Dmc1* PCR conditions

Step	Temperature	Volume	
Predenaturation	94 ºC	3 minutes	
Denaturation	94 ºC	20 seconds	x 33 cycles
Annealing	60 ºC -0.5ºC/cycle	30 seconds	
Extension	72 ºC	20 seconds	
Final extension	72 ºC	7 minutes	

Table 3.9 *Trip13 moderate* PCR conditions

Step	Temperature	Volume	
Predenaturation	94 ºC	3 minutes	
Denaturation	94 ºC	45 seconds	x 34 cycles
Annealing	61 ºC	1 minute	
Extension	72 ºC	2 minutes	
Final extension	72 ºC	5 minutes	

- Run the amplification products by electrophoresis in a 1% agarose gel with 0.0085% of SYBR safe (Thermo Fisher Scientific), using the appropriate molecular weight marker to determine the size of the products.
- Scan the gel with Gel Doc XR+ system (Bio-Rad) to determine the size of the amplified bands.

3.3. Histology techniques

3.3.1. Fixation, embedding and sectioning

Ovaries from embryos at 16-18 dpc, newborn mice at 1-4 dpp and adults at 30, 40 and 400 dpp were collected and processed in order to section, stain and study the histological structure of the samples. For the histological analysis with immunodetection, perinatal ovaries were fixed with 4% paraformaldehyde, embedded in paraffin and sectioned. For the histological analysis with PAS-Hematoxylin staining the adult ovaries were fixed with *Bouin's solution*, embedded in paraffin and sectioned.

Protocol

Fixation

- Remove the ovaries from a mouse and immerse them in a tube with 1 ml of fixative solution and fix it overnight at 4ºC. The solutions used were 4% PFA (4% paraformaldehyde in PBS, pH=7.4) and *Bouin's solution* (70% saturated picric acid solution, 25% formaldehyde, 5% glacial acetic acid).

Processing

- Wash the tissue in cold PBS two times for 30 minutes.
- Submerge the sample in cold 50% ethanol for 30 minutes.
- Submerge the sample in cold 70% ethanol for 30 minutes. At this step, the tissue can be stored up to 4 months.
- Submerge the sample in 85% ethanol for 30 minutes at room temperature.
- Submerge the sample in 96% ethanol for 30 minutes at room temperature. For the perinatal ovaries add 0.1% of eosin to slightly stain them.
- Submerge the sample two times in 100% ethanol for 30 minutes at room temperature.
- Submerge the sample 3 times in Histo-Clear II (National Diagnostics) for 30 minutes at room temperature.
- Place the tissue in a cassette and immerse it in a pre-embedding solution with 1:1 Histo-clear II/Paraffin for 45 minutes at 56ºC.
- Immerse the cassette in paraffin for 2 hours at 56ºC.
- Immerse the cassette in a second paraffin bath overnight at 56ºC.

Embedding in Paraffin Blocks

- Introduce the metal mold and the cassette in the 60ºC melted paraffin bath from the embedding center.
- Open the cassette, transfer the ovaries to the mold and place it in the cold plate.
- Place a cassette on top of the mold and add hot paraffin to cover the tissue.
- Transfer the mold to the cold block and let the paraffin solidify.
- Store the block at least overnight at 4ºC until sectioning.

Sectioning

- Attach the block into the microtome (Reichert-Jung) with the proper orientation.
- Cut the sections at a thickness of 7 µm and transfer them to the surface of a warm water bath to smooth the tissue out.
- Pick the sections up onto poly-L-lysine-coated slides. Place the tissue in the slides in a non-consecutive way, every two sections for the perinatal ovaries, and every five sections for the young and adult ovaries.
- Let them dry overnight at 37ºC and store them at room temperature.

3.3.2. PAS-Hematoxylin staining

The Periodic Acid Schiff staining is a method used to detect the structures rich in mucopolysaccharide and glycogen, typically found in connective tissue and basal laminae. Hematoxylin stains acid compounds, such DNA into dark blue. This staining was used to analyze the structure and morphology of young and adult ovarian histological sections.

Protocol

Deparaffinization and rehydration

- Deparaffinize the slides with 3 washes of xylene for 5 minutes.
- Rehydrate the tissue with a gradient of ethanol washes:
  - 100% ethanol twice for 3 minutes.
  - 96% ethanol twice for 2 minutes
  - 70% ethanol for 2 minutes
  - Distilled water for 2 minutes

Staining

- Oxidize the tissue in a 1% Periodic Acid Schiff in distilled water for 10 minutes at room temperature.
- Wash two times in distilled water for 3 minutes.
- Incubate the slides in Schiff's reagent for 10 minutes at room temperature and in darkness. Note that Schiff reagent must be stored at 4º in darkness. Red colored solution indicates a deteriorate Schiff reagent.
- Wash two times in sulphurous water (10% Potassium metabisulfite, 0.1 M HCl in Milli-Q water) for 3 minutes.
- Wash in distilled water for 2 minutes.
- Stain with Mayer's Hematoxylin (Merck) for 1 minute at room temperature.
- Rinse with running tap water to eliminate the excess for 1 minute.

Dehydration and mounting

- Dehydrate the tissue with a gradient of ethanol washes:
  - 70% ethanol for 2 minutes
  - 96% ethanol twice for 2 minutes
  - 100% ethanol twice for 3 minutes.
  - Submerge 3 times in xylene for 5 minutes.
- Place a drop of DPX mounting medium (Merck) on each section and add a coverslip.
- Let the slide completely air dry.
- Analyze with a bright field microscope.

3.3.3. Immunofluorescence staining on ovarian sections

To easily identify, count and classify the oocytes in the sectioned ovaries from the perinatal mice, an immunofluorescence was performed using an antibody against DDX4 protein, a germ cell marker. The indirect immunofluorescence consists on the detection of a target molecule with a primary antibody and a secondary antibody chemically conjugated with a fluorochrome directed to the primary antibody.

Protocol

- Deparaffinize the slides with 3 washes of xylene for 5 minutes.
- Rehydrate the tissue with a gradient of ethanol washes:
  - 100% ethanol twice for 3 minutes.
  - 96% ethanol twice for 2 minutes
  - 70% ethanol for 2 minutes
  - Distilled water for 2 minutes

Antigen retrieval

- Pre-heat a water bath with a coplin jar containing Sodium Citrate buffer (10 mM Sodium Citrate, 0.05% Tween 20 in Milli-Q water, pH 6.0) to 95-100ºC.
- Immerse the slides in the buffer and incubate for 20 minutes.
- Remove the coplin jar from the water bath and let the slides in the buffer to cool down for 20 minutes at room temperature.

Immunofluorescence

- Block the slides with blocking solution (0.2% BSA, 0.2% gelatin, 0.05% Tween-20 in PBS) for 15 minutes at room temperature.
- Add 5 µl per section of primary antibody rabbit DDX4 (Abcam) in blocking solution (1:100) and cover with parafilm.
- Incubate the slides at 4ºC in a humid chamber overnight.
- Wash the slides 4 times for 3 minutes in the blocking solution.
- Add 5 µl per section of anti-rabbit Cy3 conjugated secondary antibody (Jackson Immunoresearch) in blocking solution (1:100) and cover with parafilm.
- Incubate the slides at 37ºC in a humid chamber for 1 hour.
- Wash the slides 4 times for 3 minutes in the blocking solution.
- Drain the slides and add 20 µl of 8 µg/ml DAPI (Sigma-Aldrich) in Vectashield mounting medium (Vector Labs) and cover with a coverslip.
- Analyze with an epifluorescence microscope or store at -20ºC (or 4ºC for short periods of time).

3.3.4. Oocyte counts

All the oocytes were counted manually under the microscope (Zeiss Axipohot) with the 63x objective. In the perinatal ovaries the oocytes were counted under the fluorescence microscope and classified in oocytes in cyst (connected by the cytoplasm), single oocytes, oocytes in follicles (with one layer of flat granulosa cells) and multi-oocyte follicles (this last only in the cultured ovaries, connected by the cytoplasm but surrounded by one layer of flat granulosa cells). Only the oocytes with DDX4 antibody signal and with visible nucleus in DAPI were taken into account. In the young and adult ovaries the oocytes were counted under the bright field microscope and classified in multi-oocyte follicles (with two or more oocytes inside the same follicle), primordial follicles (with one layer of flat granulosa cells), primary follicles (with one layer of cuboid granulosa cells), secondary follicles (with two or more layers of granulosa cells) and antral follicles (with the antrum) and atresic follicles (big oocytes with one layer or without granulosa cells). Only the oocytes with a visible nucleus were counted.

3.4. Cytology techniques

3.4.1. Oocyte nuclei spreads from perinatal ovaries

The first meiotic prophase in mouse starts during fetal development and goes until the first postnatal days. Hence, to study the events occurring during prophase I in the nucleus of the oocyte, chromosome spreads from fetal and perinatal mice were performed.

Protocol

- In a 24-well plate, dispense 500 µl of M2 medium (Sigma-Aldrich) in the first row.
- Remove the ovaries from the female fetuses or pups under a stereo microscope (Nikon SMZ-1) and place the two ovaries from each female into one well from row 1 containing M2 medium. Repeat this for all the females.
- Add 25 µl of 50 mg/ml Collagenase (Sigma-Aldrich) to the wells from the second row and transfer the ovaries.
- Incubate the ovaries in the collagenase for 20 minutes at 37ºC
- Transfer the ovaries to the third row containing 500 µl of hypotonic buffer (30 mM Tris-HCl pH=8.2, 50 mM Sucrose, 17 mM Sodium Citrate, 5 mM EDTA, 0.5 mM DTT [Roche Diagnostics], 1x PIC [Roche Diagnostics] in Milli-Q water) and incubate them for 30 minutes at room temperature.
- Add 60 µl of 100 mM sucrose pH=8.2 in the fourth-row wells and transfer the ovaries.
- Pipette up and down the ovaries in the sucrose under the stereo microscope ensuring that the tissue is disaggregated and the oocytes are suspended.
- Distribute 10 µl of the cell suspension on the slides (6 slides per female).

- Add 40 µl of fixative solution (1% PFA, 5 mM Sodium Borate, 0.15% Triton X-100, 3 mM DTT, 1x PIC in Milli-Q water, pH= 9.2) and let the slides fixing for 2 hours in a humid chamber.
- Open the chamber and let the slides air dry.
- Wash the slides 4 times in 0.4% Photoflo (Kodak) solution for 2 minutes. The different genotypes must be washed separately.
- Let the slides air dry and perform the immunofluorescence or store at -80ªC until use.

3.4.2. Immunofluorescence on surface spreads

Oocyte nuclei spreads were stained for immunofluorescence to visualize the proteins of interest.

Protocol

- Block the slides with blocking solution (0.2% BSA, 0.2% gelatin, 0.05% Tween-20 in PBS) for 15 minutes at room temperature under agitation.
- Prepare the primary antibodies dilution (Table 3.10) in PTBG and add 100 µl to each slide covering it with parafilm.
- Incubate the slides at 4ºC in a humid chamber overnight.
- Wash 4 times for 3 minutes in the blocking solution.
- Prepare the secondary antibodies dilution (Table 3.11) in PTBG and add 100 µl to each slide covering it with parafilm.
- Incubate the slides at 37ºC in a humid chamber for 1 hour.
- Wash 4 times for 3 minutes in the blocking solution.
- Drain the slides and add 20 µl of 8 µg/ml DAPI (Sigma-Aldrich) in Vectashield mounting medium (Vector Labs) and cover with a coverslip.
- Analyze with an epifluorescence microscope or store at -20ºC (or 4ºC for short periods of time).

Table 3.10 List of primary antibodies used for immunofluorescence

Antigen	Host	Supplier	Dilution
SYCP3	Rabbit	Abcam	1:200
γH2AX (Ser 139)	Mouse	Millipore	1:200

Table 3.11 List of secondary antibodies used for immunofluorescence

Target	Antigen	Host	Supplier	Dilution
Rabbit	FITC	Goat	Jackson Immunoresearch	1:200
Mouse	Cy3	Goat	Jackson Immunoresearch	1:200

3.4.3. Cell Sorting

Flow cytometry based on forward and side scattering

The flow cytometry allows to differentiate the cell populations that are present in the perinatal ovaries, the germ cells and the somatic cells. This technique uses the forward and side scattering of light, together with the propidium iodide to discern between live and dead cells, and between oocytes and somatic cells (Wojtasz et al., 2009b). Propidium iodide fluorochrome staining penetrates through the damaged plasma membranes allowing to discern between dead and live cells.

Protocol

Enzymatic ovarian dissociation

- In a 24-well plate, dispense 500 µl of M2 medium (Sigma-Aldrich) in the first row.
- Remove the ovaries from the females under a stereo microscope (Nikon SMZ-1) and place the two ovaries from each female into one well from row 1 containing M2 medium. Repeat this for all the females.
- Add 25 µl of 50 mg/ml Collagenase (Sigma-Aldrich) to the wells from the second row and transfer the ovaries.
- Incubate the ovaries in the collagenase for 20 minutes at 37ºC
- Transfer the ovaries to the third row containing 50 µl of trypsin (0.25% in M2 medium) and incubate them for 5 minutes at 37ºC.
- Add 500 µl of M2 medium with 10% FBS to stop the trypsin and pipette up and down to disaggregate the tissue and resuspend the oocytes.

Cell suspension preparation

- Transfer the cell suspension to a 1.5 ml tube and centrifuge for 5 minutes at 510g. Discard supernatant.
- Add 500 µl of PBS supplemented with 0.02% EGTA and 10 µg/ml polyvinyl alcohol, pH 7.4.
- Keep the samples in ice until acquisition.

Cytometer acquisition and analysis

- Stain with 1 µg/ml of propidium iodide and mix gently.
- Transfer the samples to cytometer tubes and acquire the cells in the FACSCanto cytometer (BD Biosciences) equipped with a 488-nm solid state blue laser and a 635-nm He-Ne laser.

Flow cytometry based on fluorescence sorting

The fluorescent activated cell sorting (FACS) of fixed cells is used to differentiate the cell populations, but in this case through the use of an immunofluorescent staining with DDX4. This antibody marks the germ cells allowing to differentiate them from the rest of the cells from the perinatal ovaries (White et al., 2012).

Protocol

Enzymatic ovaries dissociation

- In a 24-well plate, dispense 500 µl of M2 medium (Sigma-Aldrich) in the first row.
- Remove the ovaries from the females under a stereo microscope (Nikon SMZ-1) and place the two ovaries from each female into one well from row 1 containing M2 medium. Repeat this for all the females.
- Add 25 µl of 50 mg/ml collagenase (Sigma-Aldrich) to the wells from the second row and transfer the ovaries.
- Incubate the ovaries in the collagenase for 20 minutes at 37ºC
- Transfer the ovaries to the third row containing 500 µl of PBS and incubate for 30 minutes at room temperature
- Pipette up and down to disaggregate the tissue and resuspend the oocytes.

Immunofluorescence

- Transfer the cell suspension to a 1.5 ml tube and centrifuge at 300g for 5 minutes. Discard supernatant.
- Wash with 1 ml of PBS with 2% of fetal bovine serum (FBS), centrifuge at 300g for 5 minutes. Discard supernatant
- Fix the cells with 500 µl of 4% Paraformaldehyde (pH 7.4). Resuspend to dissolve the pellet.
- Incubate with the PFA 10 minutes at room temperature, centrifuge at 400g for 5 minutes.
- Wash with 1 ml of PBS with 2% of FBS, centrifuge at 400g for 5 minutes. Discard supernatant.
- (Preheat sodium citrate solution at 55ºC and add it to the cells, resuspending them).
- (Incubate the samples at 55ºC or 75ºC for 45 minutes, centrifuge at 400g for 5 minutes at room temperature. Discard supernatant).
- Wash with 1 ml of PBS with 2% of FCS and 0.1% of saponin, centrifuge at 400g for 5 minutes. Discard supernatant
- Add the primary antibody rabbit DDX4 previously conjugated using a FITC Fast Conjugation Kit (Abcam), resuspended in 100 µl of PBS with 2% of FCS and 0.3% of saponin.
- Incubate for 45 minutes at 37ºC in the darkness.

- Wash with 1 ml of PBS with 2% of FCS and 0.1% of saponin, centrifuge at 400g for 5 minutes. Discard supernatant
- Add 500 µl of PBS and resuspend.

Cytometer acquisition

Transfer the samples to cytometer tubes and acquire the cells in the FACSCanto cytometer (BD Biosciences) equipped with a 488-nm solid state blue laser and a 635-nm He-Ne laser.

3.5. Organ culture

3.5.1. Perinatal ovary culture

New techniques in organ cultured allow to study the progression of folliculogenesis *in vitro* by culturing perinatal mouse ovaries (Morgan et al., 2015). Using this protocol, it was possible to culture ovaries from newborn females to study the folliculogenesis and follow the perinatal massive oocyte death. Modifying this culture method with the addition of drugs in the media allowed us to inhibit the function of some proteins and see how this suppression affects to the whole process. Specifically, we inhibited the Notch signaling (Xu and Gridley, 2013; Trombly et al., 2009) and the DDR effector kinase CHK1 (Chen et al., 2012) for the previously reported roles in folliculogenesis and meiosis in females.

Protocol

Preparation of dissection and culture media

- Working in sterile conditions in a laminar flow hood, dissolve 3mg/ml BSA (Sigma-Aldrich) in the dissection media Leibowitz L15 (Sigma-Aldrich) medium and filter sterilize through a 0.2 µm pore, 25 mm diameter filter (Merck). Repeat the process for the culture media α-Minimum Essential Medium (Thermofisher Scientific).
- In the experiments with pharmacological drugs, add the correspondent inhibitor or DMSO (Sigma Aldrich) as control vehicle to the culture media (Table 12).
- Add 1 ml of the prepared culture media into each well of a 24-well plate. Place one previously UV sterilized polycarbonate membrane (Whatman) on top of the medium in each well.
- Let the plate equilibrate in the incubator at least for 1 hour at 37ºC and 5% CO_2.

Table 3.12 List of drugs used in culture

Drug	Inhibition	Supplier	Concentration
DAPT	γ-Secretase (Notch pathway)	Sigma-Aldrich	20 µM
LY2603618	CHK1	Selleckchem	1, 5 and 10 µM
DMSO	Control vehicle	Sigma-Aldrich	0.05%

Ovary dissection and culture

- Remove the ovaries from newborn females at 1 dpp and place them in the petri dish with previously warmed dissection media.
- Under the stereo microscope use the forceps to trim away the bursal sac from the ovaries and any excess material like the fallopian tube and the uterus.
- Transfer the ovaries to a well of the 24 well plate and place them on top of the membrane. When an inhibitor is added, culture one ovary from the same mice with inhibitor and the other one with DMSO. Place two ovaries per well.
- Incubate at 37ºC, 5% CO_2. Note that the culture media must be changed every two days, replacing carefully 0.5 ml of the old media with fresh media without touching the membranes or moving the ovaries.
- At the end of the culture, harvest the ovaries and fix them in 4% Paraformaldehyde for histological analysis by immunofluorescence.

3.6. Microscopy, image processing and data analysis

3.6.1. Microscopy and image acquisition

PAS-Hematoxylin stained section from ovaries were observed on a brightfield microscope Zeiss Axioskop and images were captured with a ProgRes Jenoptik camera. The software used to capture the images was ProgRes Capture Pro 2.7.7

For fluorescent samples, a Zeiss Axiophot microscope connected to a fluorescence bulb was used; and images were captured with a Point Gray Research, Inc. camera with the ACO XY Software (A.COLOMA Open microscopy).

The same microscope setup of the fluorescent samples was used for the acquisition of composite panoramic images from both PAS-Hematoxylin and fluorescent samples.

3.6.2. Image and data analysis

All the images were processed with Adobe Photoshop CC to overlay the different fluorescent channels.

The software Image Composite Editor (https://www.microsoft.com/en-us/research/product/computational-photography-applications/image-composite-editor/) was used to stitch the composite panoramic images.

The results from the flow cytometry were visualized and analyzed with the software BD FACSDiva 4.0.

Data analysis and statistical inference were performed using the GraphPad Prism 5 software. (https://www.graphpad.com/scientific-software/prism/).

RESULTS

Chapter 4

4.1. Study of the role of the mammalian recombination checkpoint in the oocyte pool and follicle formation

Unraveling the proteins and mechanisms participating in the pachytene checkpoint controlling meiotic recombination is fundamental to understand oocyte death and follicle formation. Since in females the oocyte pool is established perinatally, the regulation of this processes will determine the quality of the oocytes available for the reproductive life of the female. In this work, we used cytological and histological techniques in a murine *Chk2* mutant model to identify if the recombination checkpoint regulates the oocyte number in mammalian females.

Specifically, knowing that CHK2 is a component of the recombination checkpoint, we hypothesize that this protein regulates the perinatal elimination of the oocytes with a higher number of unrepaired DSBs. Additionally, due to the close succession and relation of these events, we think that it can also have a role in the regulation of the oocyte cyst breakdown and follicle formation processes.

4.1.1. Analysis of oocyte elimination with a high number of unrepaired DSBs by the recombination checkpoint

The DDR effector kinase CHK2 is a component of the meiotic DNA damage-dependent checkpoint (also known as the recombination checkpoint) that takes place during the pachytene stage of the first meiotic division (Bolcun-Filas et al., 2014; Pacheco et al., 2015). CHK2 is dispensable for fertility and embryo viability (Takai et al., 2002). With this information we wanted to evaluate if, according to our hypothesis, the ovaries lacking CHK2 have oocytes with a higher number of unrepaired DSBs.

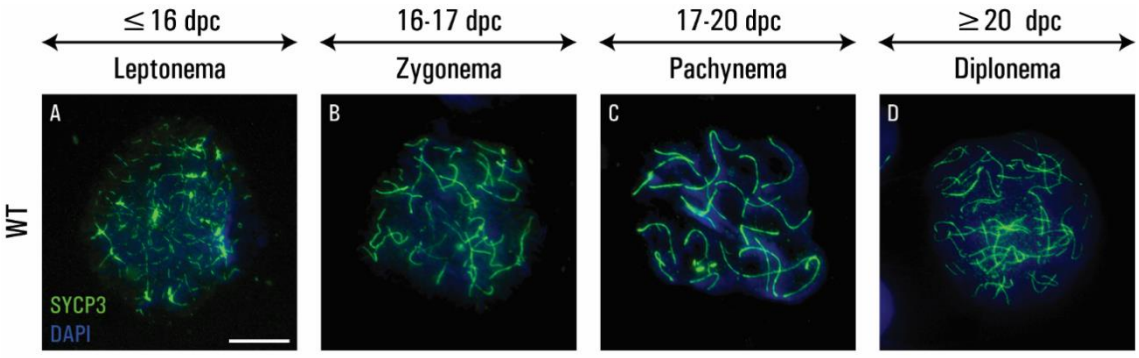

Figure 4.1 Progression of meiotic prophase I in wild type (WT) oocytes A-D) Representative images of all the different stages of prophase I during perinatal development. The oocytes are immunostained against SYCP3 (green) and with DAPI as a DNA counterstain (blue). Scale bar represent 10 µm and applies to all images.

Since the mammalian female prophase I is a one-time process that begins in the fetal period and finishes few days after birth, first we wanted to determine the optimal time of analysis in our murine model and ensure the presence of oocytes at pachynema and diplonema. For that, we performed an immunofluorescence against SYCP3, the synaptonemal complex protein, in wild type (WT) oocyte spreads at different times. Beginning at 16 days *post coitum* (dpc), we only found oocytes at leptonema (Fig. 4.1A) and zygonema (Fig. 4.1B); at 17 dpc most meiocytes were at zygonema and pachynema (Fig. 4.1C); at 18 dpc we mostly found oocytes at pachytene stage; and finally, at 20 dpc (1 day *post partum*, dpp) we found oocytes at pachynema and diplonema (Fig. 4.1D).

Thus, we analyzed and compared oocyte spreads at 18 and 20 dpc from WT and *Chk2*$^{-/-}$ females. We performed an immunofluorescence against SYCP3 and γH2AX, a marker of DNA damage (Mahadevaiah et al., 2001; Rogakou et al., 1998; Roig et al., 2004), and counted the resultant patches comparing the numbers of unrepaired DSBs at pachynema and diplonema between both genotypes. We hypothesized that if CHK2 participates in the recombination checkpoint as an effector kinase, in its absence there should be an increase of oocytes with high number of unrepaired DSBs at pachytene stage and onwards. Indeed, at 18 dpc we found a 12% increase in the number of unrepaired DSBs in *Chk2*$^{-/-}$ early pachytene oocytes compared to WT ($p=0.0083$ t-test, Fig. 4.2, Table 4.1). At 20 dpc, the number of unrepaired DSBs in late pachytene stage oocytes had significantly reduced by half compared to the early pachytene ones ($p<0.0001$ t-test, Fig. 4.2, Table 4.1). But it was still significantly higher in the *Chk2*$^{-/-}$oocytes, with a 32% increase in the number of unrepaired DSBs, compared to WT ($p<0.0001$ t-test, Fig. 4.2, Table 4.1). Furthermore, analyzing the 20 dpc diplotene oocytes, the number of DSBs kept decreasing from late pachynema ($p<0.0001$ t-test, Fig. 4.2, Table 4.1), but the *Chk2*$^{-/-}$ early diplotene oocytes still had a higher number of unrepaired DSBs compared to the WT ($p=0.0355$ t-test, Fig. 4.2, Table 4.1), even though the difference was smaller than in pachytene oocytes. Finally, the number of unrepaired DSBs in late diplotene oocytes was equal in both *Chk2*$^{-/-}$ and WT oocytes ($p=0.6856$ t-test Fig. 4.2, Table 4.1).

These data confirms the role of CHK2 in the recombination checkpoint even in an unperturbed meiosis, since in its absence there is an increase in the number of unrepaired DSBs at pachynema and early diplonema. The fact that the range of γH2AX patches remains the same between both genotypes at the same stage, suggests that there is not an initial increase in the quantity of DSBs before the checkpoint in absence of CHK2. Instead, we postulate that CHK2 promotes the death of WT oocytes with a high number of unrepaired DSBs. Moreover, the fact that the *Chk2*$^{-/-}$ oocytes are able to level the number of unrepaired DSBs to WT numbers by the end of the prophase I, opens two possibilities. First, that a CHK2-independent DNA damage checkpoint is activated and extends its action further until diplonema. Or alternatively, that in the absence of CHK2, the checkpoint is not active, but the oocytes are able to repair the extra DNA damage to WT levels during diplonema.

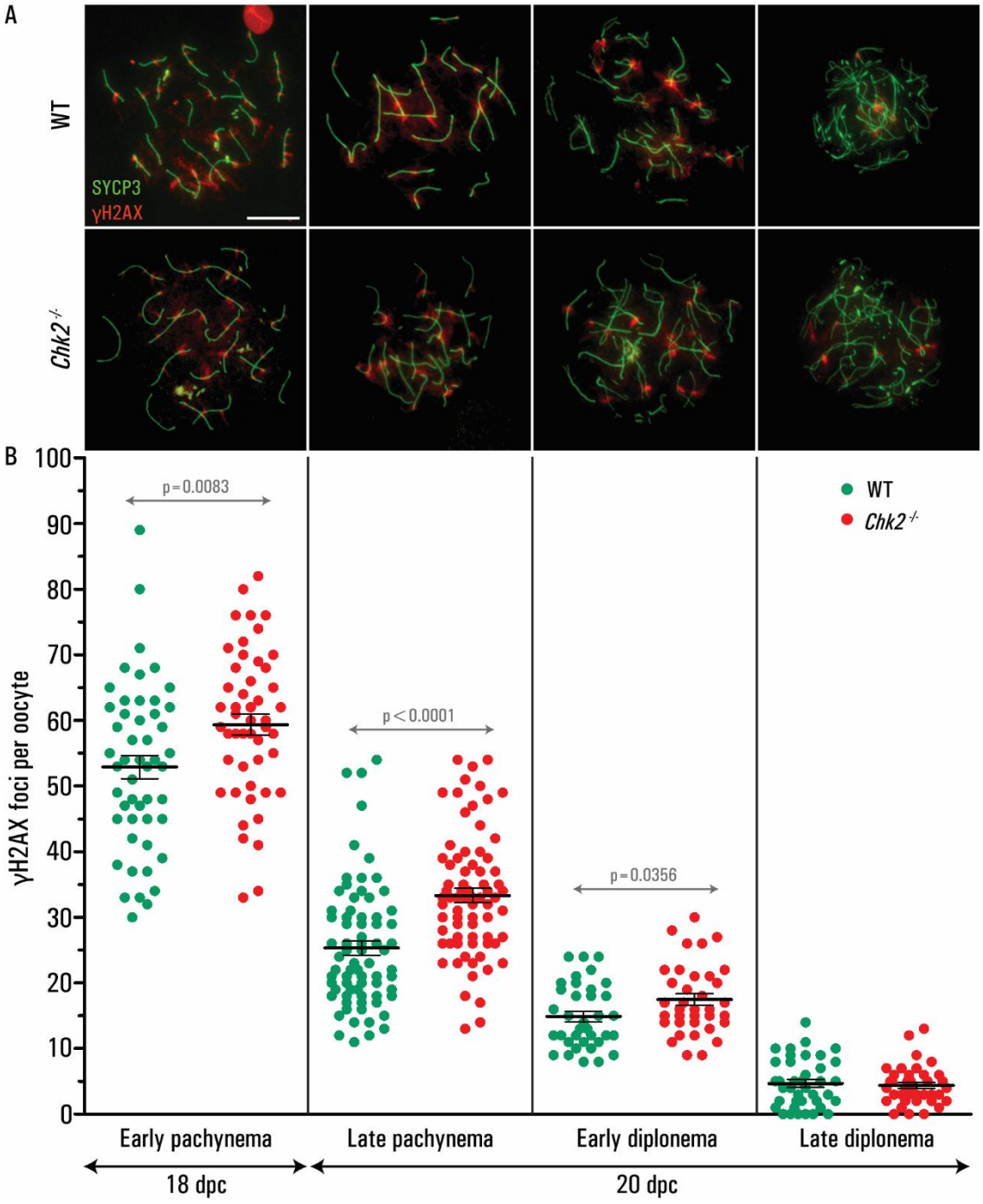

Figure 4.2 *Chk2*$^{-/-}$ oocytes present a higher number of unrepaired DSBs at pachynema and early diplonema. A) Representative images of WT and *Chk2*$^{-/-}$ oocytes at pachynema and diplonema. The cells are immunostained against SYCP3 (green) and γH2AX (red). Scale bar represent 10 μm and applies to all images. **B)** Quantification of the number of γH2AX patches found in WT and *Chk2*$^{-/-}$ oocytes at pachynema and diplonema. The horizontal lines represent the means ± standard error of the mean (SEM). There is a significant increase in the number of unrepaired DSBs at pachynema and early diplonema, but not at late diplonema in the *Chk2*$^{-/-}$ oocytes compared to the WT ones.

Table 4.1 Number of γH2AX patches per oocyte at pachynema and diplonema from WT and *Chk2*$^{-/-}$ ovaries. The numbers express the average ± SEM. N indicates the number of oocytes counted. * represents the statistical difference between the two genotypes.

Stage	WT	*Chk2*$^{-/-}$
Early pachynema	52.9 ± 1.8* (N=50)	59.3 ± 1.6* (N=50)
Late pachynema	25.3 ± 1.1* (N=75)	33.3 ± 1.1* (N=75)
Early diplonema	14.9 ± 0.8* (N=36)	17.5 ± 0.9* (N=36)
Late diplonema	4.7 ± 0.6 (N=39)	4.4 ± 0.5 (N=39)

4.1.2. Quantification of the number of oocytes in perinatal ovaries

According to our hypothesis, we confirmed the role of CHK2 in the recombination checkpoint regulating the oocytes with a high number of unrepaired DSBs, so our next step was to evaluate the changes in the oocyte pool consequently to the perinatal death and check if there is actually an increase in the total number of oocytes in absence of CHK2.

The massive perinatal oocyte death has been for years noticed and reported, even though the mechanisms controlling it are not well known (reviewed in Hartshorne et al., 2009; Hunter, 2018; Pepling, 2012; Tilly, 2001), and it has been reported to be susceptible to time changes depending on the different mouse strains (Pepling et al., 2010). Since our objective was to test if the mechanisms regulating the recombination checkpoint control the oocyte pool, we quantified the number of oocytes present in WT and *Chk2*$^{-/-}$ ovaries at different developmental times.

The processing and manual counting of fetal and newborn oocytes could be difficult and time consuming, so we wanted first to use cytometry to quantify the oocytes. We attempted to set up a cytometry technique based on the separation of the different ovarian cell populations by its side- and forward-scattering properties. Theoretically, this technique can be used to differentiate the oocytes from ovarian somatic cell population in fetal and newborn mice analyzing an alive cell suspension (Wojtasz et al., 2009d) (Fig. 4.3A). We could not distinguish between the oocyte and the somatic cell population using 2 dpp ovaries. Since Wojtasz et., al optimized the technique for fetal ovaries, we next analyzed 18 dpc WT and *Chk2*$^{-/-}$ ovaries, but like with the newborn ones, we were not able to separate the two expected populations (Fig. 4.3B).

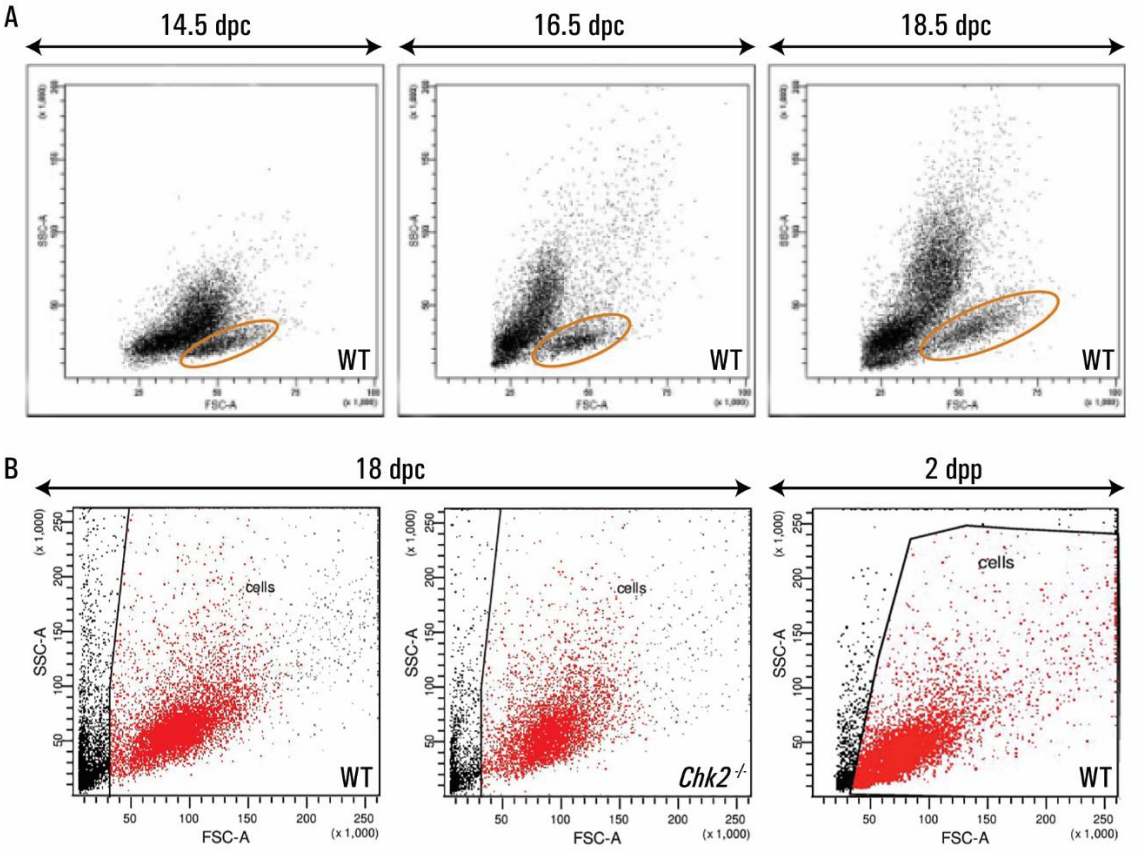

Figure 4.3 Cytometry separation of perinatal cells from mouse ovaries. A) Citometry plots of live cell suspensions of 14.5 dpc, 16.5 dpc and 18.5 dpc WT females gonads. Germ cell population are marked by the orange circle. Extracted from Wojtasz et al. 2009b. **B)** Representative images of cytometry plots using alive cells from 18 dpc and 2 dpp WT and *Chk2*$^{-/-}$ ovaries. Cells are classified on the X axis according to the forward-scattered light, which corresponds to the size of the cell; and on the Y axis according to the side-scattered light, which corresponds to the internal complexity of the cell. The cells (in red) were gated and included in the analysis, while the debris (in black) was discarded.

Since we were not able to identify oocytes with the first technique, we tried with another one. In this case, we disaggregated the ovaries, fix the cells and perform an immunofluorescence against the germ cell protein DDX4 in order to detect the fluorescent cells, the oocytes (White et al., 2012). After the first experiments we noticed how the several washes and steps in the processing reduced drastically the number of obtained cells making the analysis impossible. For this reason we decided to reduce the washes and conjugate the primary antibody with the fluorochrome in order to reduce the manipulation and enable a better analysis without losing a lot of cells. Furthermore, and to optimize the levels of fluorescence, we introduced an antigen retrieval step, performed at 55 or 75ºC . In 2 and 3 dpp *Chk2*$^{-/-}$ ovaries, we obtained a disseminated cell population, with some FITC positive cells, especially in the samples with antigen retrieval, but in any case none of this fluorescent cells were part of a unique cell population nor formed a distinguished isolated population (Fig. 4.4).

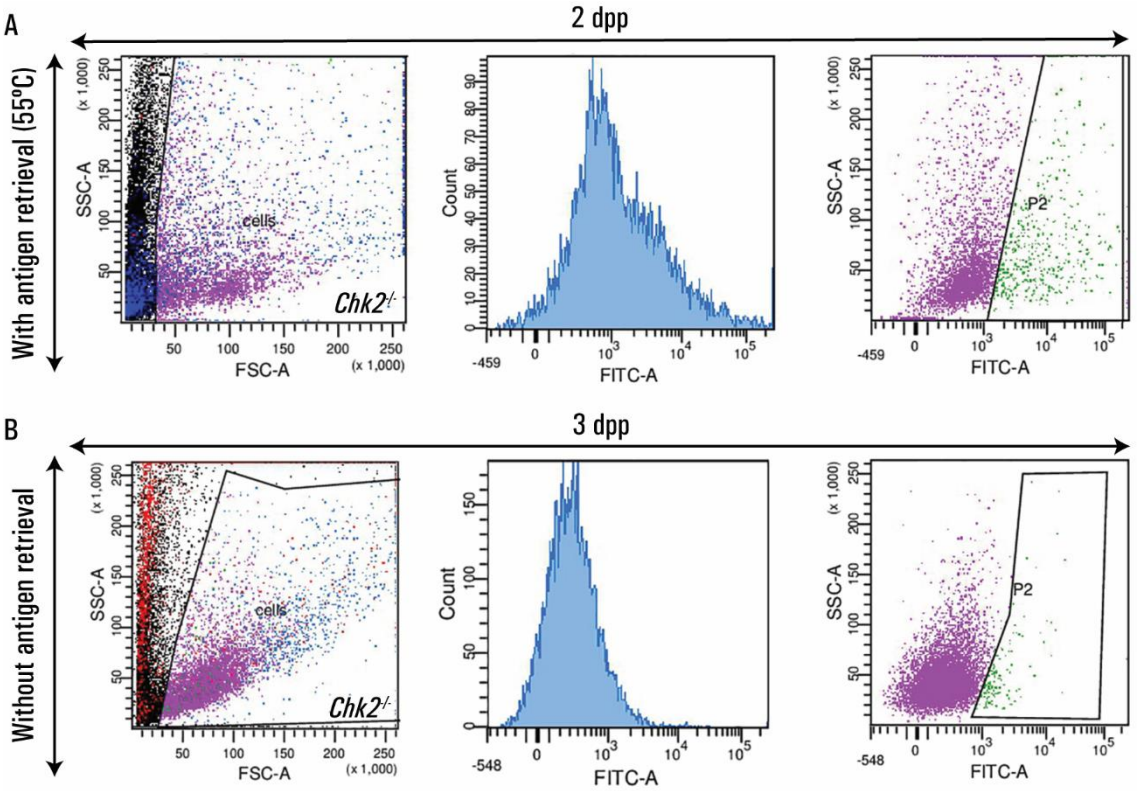

Figure 4.4 Cytometry separation of post-natal immunostained cells from mouse ovaries. A-B) Representative images of cytometry plots using immunostained fixed cells from 2 (A) and 3 dpp (B) *Chk2*$^{-/-}$ ovaries. Some of the cells were treated with an antigen retrieval protocol at 55ºC (A). Cells were classified on the X axis according to the forward-scattered light (FSC-A) (left plots); or according to the presence of FITC fluorescence (FITC-A) (middle and right plots). On the Y axis, according to the side-scattered light (SSC-A) (left and right plots); or according to count of fluorescence (middle plots). The cells were gated and included in the analysis, while the debris (in black) was discarded. The gate "P2" (right plots) in green includes the fluorescent cells. Pink color marks the single cells. Notice how there is no clear population in the fluorescent gate.

After being unable to identify the oocytes by cytometry, we decided to use classical histology techniques to quantify the number of oocytes in sections of WT and *Chk2*$^{-/-}$ ovaries at different times from 16 dpc to 23 dpc (4 dpp). Sections were immunostained against the germ cell marker DDX4. First we wanted to determine the timing of the perinatal oocyte death on WT samples. At 16 dpc WT ovaries had an average of 8832 oocytes (Fig 4.5, Table 4.2), but two days later, at 18 dpc, the number of oocytes had dramatically decreased to 4207 (p=0.0012 t-test, Fig. 4.5, Table 4.2). This pool of oocytes remained stable for the following post-natal days, from 20 to 23 dpc (1 to 4 dpp) (Fig 4.5, Table 4.2). This data suggest that in our mouse colony, the massive oocyte death mostly occurs within 2 days, from 16 dpc to 18 dpc.

With CHK2 acting as an effector kinase of the recombination checkpoint, in its absence we expected a lack of oocyte death, hence, an increase in the number of oocytes compared

to the WT. At 16 dpc *Chk2*$^{-/-}$ ovaries had an average of 7407 oocytes (Fig 4.5, Table 4.2), and two days later, at 18 dpc, the mutants had 9344 oocytes, a 20.7% increase respect to the numbers at 16 dpc (p=0.0034 t-test, Fig. 4.5, Table 4.2). At 20 dpc, the pool significantly decreased a 32% (6354 oocytes, p=0.0010 t-test, Fig. 4.5, Table 4.2), and at 21 dpc, the Chk2$^{-/-}$ oocyte number decreased to 4290 oocytes (p=0.0124 t-test, Fig. 4.5, Table 4.2). Finally, the mutant oocyte pool remained unchanged from 22 to 23 dpc (3 to 4 dpp).

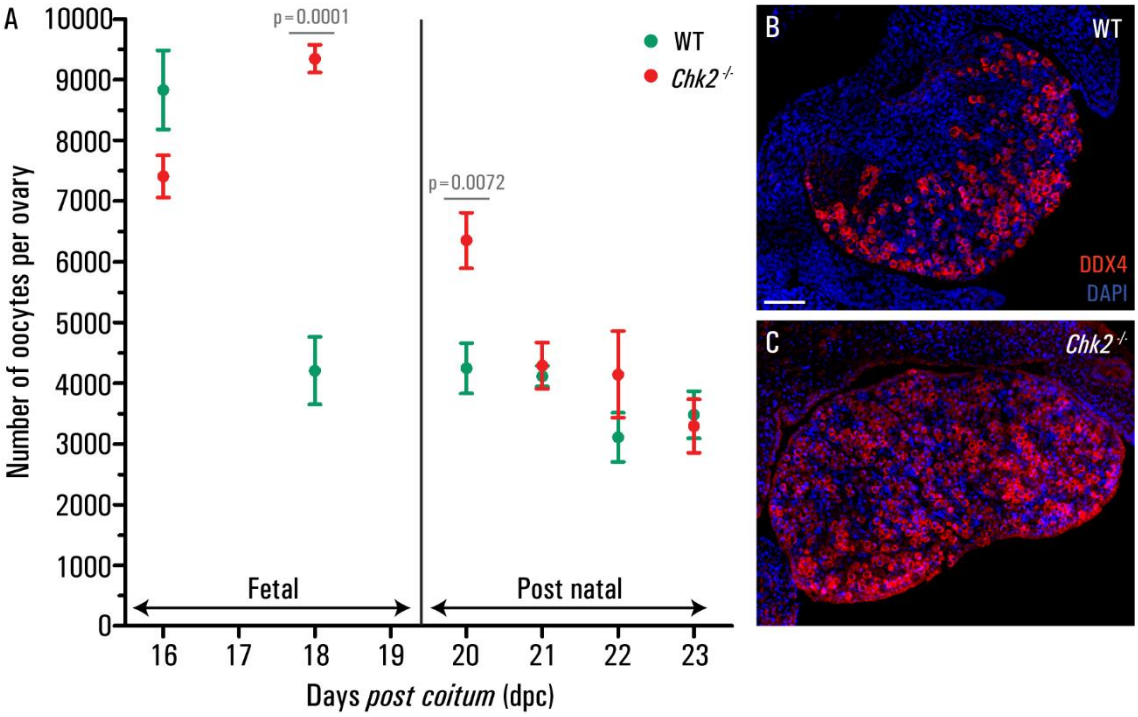

Figure 4.5 CHK2 regulates the number of oocytes in fetal ovaries. A) Number of oocytes in fetal and postnatal WT and *Chk2*$^{-/-}$ ovaries. The round symbols represent the mean and the lines the SEM. There is a massive fetal oocyte death in the WT around 17 dpc but it is delayed in the mutants. **B-C)** Representative images of 18 dpc WT (B) and Chk2$^{-/-}$ (C) histological sections of ovaries immunostained against DDX4 (red) and the DNA counterstained with DAPI (blue). Notice how in the WT ovary there are more empty spaces and the density of oocytes is lower. Scale bar represent 40 µm and applies to both images.

Interestingly, comparing the data from both genotypes we found that there was, indeed, an increase in the number of oocytes in absence of CHK2, but only in the fetal ovaries. At 16 dpc both genotypes had the same oocytes (p=0.1181 t-test, Fig. 4.5, Table 4.2), but this changed at 18 dpc, moment when the mutants had twice as many oocytes compared to the WT ovaries (p=0.0001 t-test, Fig. 4.5, Table 4.2). At 20 dpc the difference with the WT was still significant, with the mutants having a 33.2% more of oocytes (p=0.0072 t-test, Fig. 4.5, Table 4.2). From 21 to 23 there was no differences between both groups (Fig. 4.5, Table 4.2). With this information we know that the perinatal death in the *Chk2*$^{-/-}$ females is delayed, so CHK2 is responsible of this death but only in fetal ovaries. Once the female is born there should be another mechanism leveling the oocytes to WT numbers, compensating the absence of CHK2.

Table 4.2 Oocyte number on the different perinatal days from WT and *Chk2*$^{-/-}$ ovaries. The numbers express the average ± SEM. N indicates the number of ovaries counted. * represents the statistical difference between the two genotypes.

Stage	WT	*Chk2*$^{-/-}$
16 dpc	8832 ± 652.4 (N=5)	7407 ± 345.9 (N=4)
18 dpc	4207 ± 556.6* (N=4)	9344 ± 228.3* (N=4)
20 dpc (1 dpp)	4246 ± 416.8* (N=8)	6354 ± 457.2* (N=5)
21 dpc (2 dpp)	4117 ± 169.1 (N=6)	4290 ± 382.9 (N=4)
22 dpc (3 dpp)	3108 ± 405.4 (N=6)	4145 ± 710.7 (N=4)
23 dpc (4 dpp)	3480 ± 384.9 (N=8)	3297 ± 440.1 (N=4)

4.1.2.1. Analysis of the oocyte elimination mediated by CHK2 in absence of SPO11

Classically the pachytene checkpoint in females was reported to be driven by different DNA damage-dependent and -independent mechanisms. Therefore, the lack of proteins needed to complete recombination, such as DMC1 or ATM, would trigger the DNA damage-dependent response, eliminating all of the oocytes at birth. In the other hand, the lack of SPO11, the protein responsible of DSB formation, would trigger the DNA damage-independent response (Di Giacomo et al., 2005). Knowing the existence of these two mechanisms, we wanted to test if the action of CHK2 was exclusive of the recombination checkpoint, hence of the DNA damage-dependent mechanism.

For that reason we analyzed the number of oocytes in 20 dpc (1 dpp) *Spo11*$^{-/-}$ *Chk2*$^{-/-}$ ovaries and compared them to same age *Spo11*$^{-/-}$. We expected the same oocyte number in both genotypes, since the absence SPO11 should not activate the DDR. We found a very low number of oocytes at birth in Spo11$^{-/-}$, as reported before (Baudat et al., 2000b; Di Giacomo et al., 2005). The mutant ovaries had 1600 oocytes, less than 40% of the number of a normal WT ovary (p=0.0015 t-test, Fig. 4.6, Table 4.3). This has been explained previously by the activation of the DNA damage-independent or synapsis checkpoint (Di Giacomo et al., 2005). Surprisingly, we found a rescue of the total number of oocytes in the *Spo11*$^{-/-}$ *Chk2*$^{-/-}$ ovaries with 3287 oocytes, twice the number of the *Spo11*$^{-/-}$ ones (p=0.0118 t-test, Fig. 4.6, Table 4.3). Moreover, the double mutants presented the same number of oocytes than the WT ovaries, but less than the *Chk2*$^{-/-}$ ones (p=0.0022 t-test, Fig. 4.6, Table 4.3). Our results open two possible explanations: that CHK2 participates in the recombination-independent checkpoint, or that the *Spo11*$^{-/-}$ oocytes die due to the activation of the recombination CHK2-dependent checkpoint. A recent work revealed results supporting this second explanation (Rinaldi et al., 2017a). Both *Spo11*$^{-/-}$ oocytes and spermatocytes present

markers of unrepaired DSBs at prophase I (Carofiglio et al., 2013), supporting the activation of a CHK2-dependent DNA damage response.

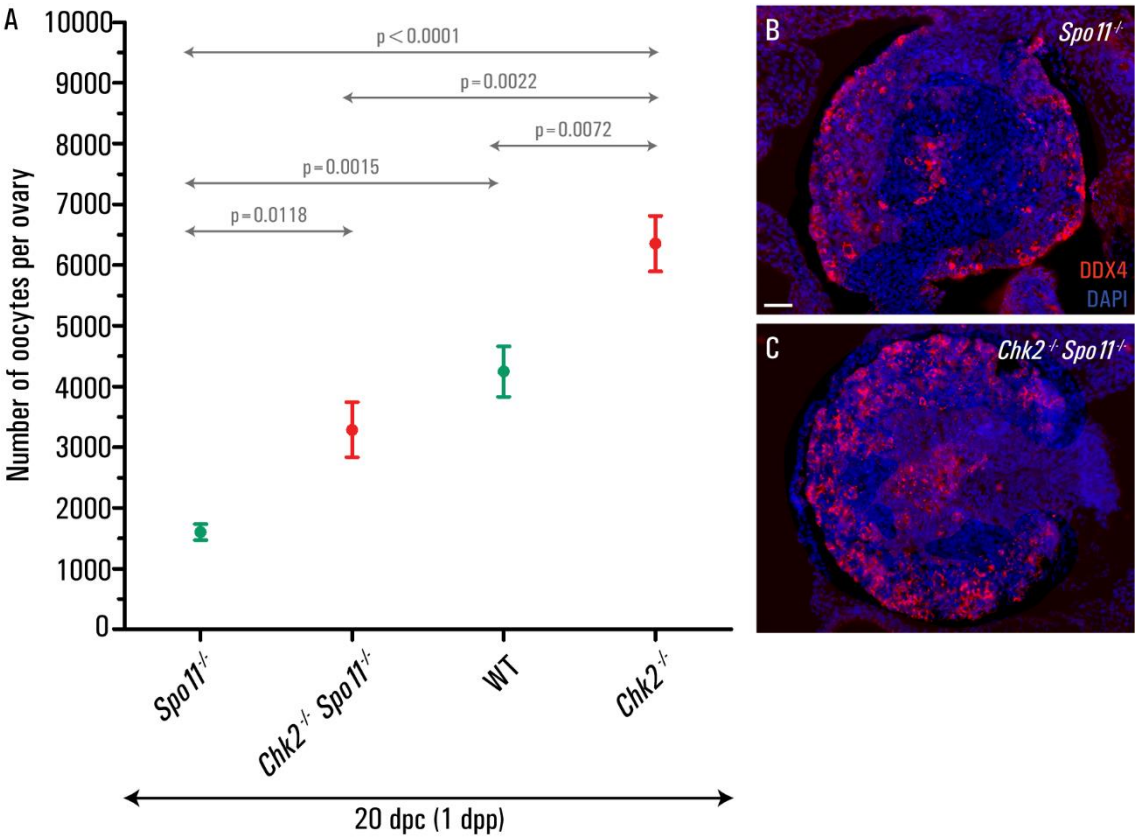

Figure 4.6 CHK2 rescues the number of oocytes in a SPO11 background. A) Number of oocytes in 20 dpc *Spo11*$^{-/-}$, *Chk2*$^{-/-}$ *Spo11*$^{-/-}$, WT and *Chk2*$^{-/-}$ ovaries. The round symbols represent the mean and the lines the SEM. **B-C)** Representative images of 20 dpc *Spo11*$^{-/-}$ (B) and *Chk2*$^{-/-}$ *Spo11*$^{-/-}$ (C) histological sections of ovaries immunostained against DDX4 (red). The DNA is counterstained with DAPI (blue). Scale bar represents 40 µm and applies to both images. The data of WT and *Chk2*$^{-/-}$ was extracted from Figure 4.5.

Table 4.3 Oocyte number at 20 dpc from the ovaries of indicated genotype. The numbers express the average ± SEM. N indicates the number of ovaries counted. The data of WT and *Chk2*$^{-/-}$ was extracted from Table 4.2.

Genotype	20 dpc (1 dpp)
Spo11$^{-/-}$	1600 ± 132.2 (N=4)
Spo11$^{-/-}$ *Chk2*$^{-/-}$	3287 ± 453.7 (N=4)
WT	4246 ± 416.8 (N=8)
Chk2$^{-/-}$	6354 ± 457.2 (N=5)

4.1.3. Study of the cyst breakdown and follicle formation in perinatal ovaries

In mouse, like in other mammalian and insect species, germ cells form cysts to share organelles and cytoplasm and act as nursing cells for the oocytes that are finally going to survive and become primordial follicles (Lei and Spradling, 2016; Pepling et al., 2007; Pepling and Spradling, 2001). In this context, in mammals, it is assumed that the oocyte loss is required for the cyst to breakdown and to individualize the oocytes. This led us to hypothesize that the recombination checkpoint could promote the cyst breakdown and the subsequent follicle formation.

In order to determine if this was true, we classified the counted perinatal oocytes in the three sub-types present in the ovary: oocytes in cyst, sharing cytoplasm (Fig 4.7A); single individualized oocytes (Fig 4.7B); and oocytes in follicle, surrounded by one layer of flat granulosa cells (Fig. 4.7C). First, we determined the dynamics and timing of cyst breakdown and follicle formation in WT ovaries. At 16 dpc we found 3844 oocytes in cyst, a 43.6% of the total, with the other 4987 being single oocytes (Fig. 4.7, Table 4.4). At 18 dpc, we found the first primordial follicles in a very low proportion, a 1.1% of the total (Fig. 4.7, Table 4.4); but two days later this numbers significantly increased to 7.8% ($p=0.0025$ for the numbers; $p=0.0017$ for the percentages, t-test, Fig. 4.7, Table 4.4). Due to the decrease in the total number of oocytes at 18 dpc produced by the oocyte death, the number of cysts and single oocytes significantly decreases respect the numbers at 16 dpc ($p=0.0013$ for the cysts, and $p=0.0024$ for the single oocytes, t-test, Fig. 4.7, Table 4.4). At 21 dpc, the number and percentage of cysts is reduced by half compared to the previous day ($p=0.0087$ for the numbers; $p=0.0042$ for the percentages, t-test, Fig. 4.7, Table 4.4), and it keeps decreasing at 22 dpc, compared to the previous day ($p=0.0002$ for the numbers; $p=0.0005$ for the percentages, t-test, Fig. 4.7, Table 4.4). In an inverted pattern, there is a two-fold increase in the number and percentage of follicles from 20 to 21 dpc ($p=0.0023$ for the numbers; $p=0.0028$ for the percentages, t-test, Fig. 4.7, Table 4.4), a two-fold increase in the number of follicles and a three-fold increase in the percentage of follicles, from 21 to 22 dpc ($p=0.0085$ for the numbers; $p<0.0001$ for the percentages, t-test, Fig. 4.7, Table 4.4). These data confirms the previously reported progression of cyst breakdown and follicle formation in the perinatal days (Lei and Spradling, 2013; Pepling, 2012, 2006; Pepling and Spradling, 2001; Tingen et al., 2009).

Interestingly, in *Chk2*$^{-/-}$ females, the proportion of all oocyte types at all days remained the same as the WT. The only difference that we found was in the follicles at 18 dpc, *Chk2*$^{-/-}$ had 5 times less percentage of follicles than the WTs ($p=0.0250$ t-test, Fig. 4.7, Table 4.4). We justify this difference in the follicles as a technical issue distinguishing the low number of follicles in a mutant ovary containing the double the amount of oocytes than the WT. Analyzing the numbers, we see an increase in the cysts and single oocytes at 18 dpc ($p=0.0011$ for the cysts, and $p<0.0001$ for the single oocytes, t-test, Fig. 4.7, Table 4.4), and an increase in the single oocytes at 20 dpc, compared to the controls ($p=0.0099$ t-test, Fig. 4.7, Table 4.4). With these results, we propose that CHK2 is dispensable for the timing of cyst breakdown and follicle formation. Furthermore, the fact that at 16 dpc we only found

less than half of the oocytes in cyst when the CHK2-dependent death has not happened yet, indicates that there might be a previous cyst breakdown process activated by other mechanisms.

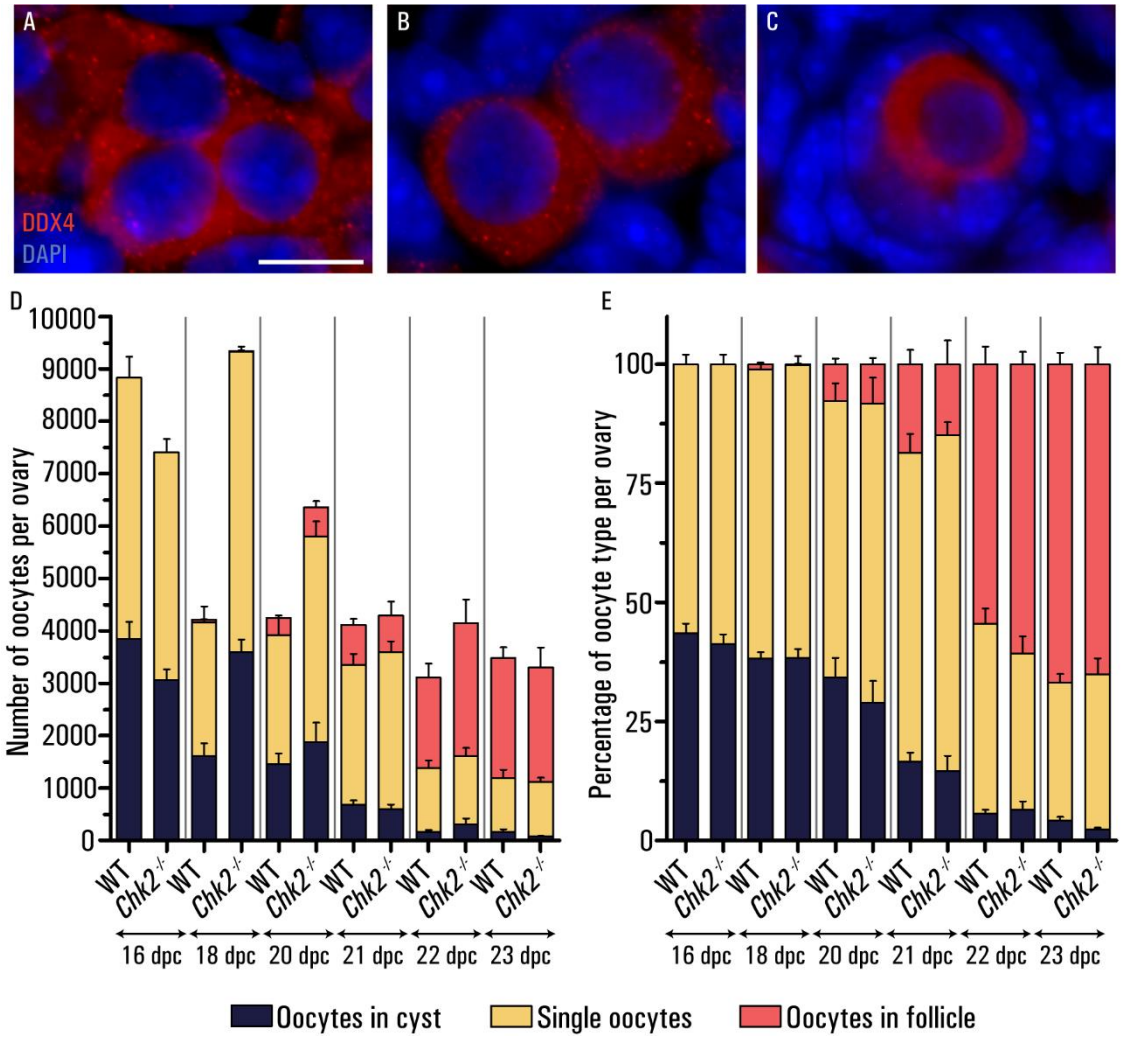

Figure 4.7 CHK2 does not regulate the cyst breakdown and follicle formation. A-C) Representative oocytes immunostained against DDX4 of three oocytes forming a cyst (A), two single oocytes (B) and an oocyte forming a follicle (C). The DNA is counterstained with DAPI (blue). Scale bar represent 10 µm and applies to all images. **D-E)** Number (D) and percentage (E) of oocyte type per ovary in WT and *Chk2*$^{-/-}$ mice. The lines represent the mean ± SEM. As the days pass, cysts breakdown and follicles form with no differences between both genotypes.

Table 4.4 Number and percentage of the different classes of oocytes found on the WT and *Chk2*$^{-/-}$ ovaries analyzed. The numbers express the average ± SEM. N indicates the number of ovaries counted, * represents the statistical difference between the two genotypes.

Age	WT				*Chk2*$^{-/-}$			
	N		Cysts	Single oocytes	Follicles	N	Cysts	Single oocytes	Follicles
16 dpc	5	#	3844±335.3	4987±398.8	0	4	# 3057±210.5	4351±251.7	0
		%	43.6±2%	56.4±2%	0%		% 41.2±2%	58.8±2%	0%
18 dpc	4	#	1620±236.2*	2539±310.9*	48.6±18	4	# 3591±242.9*	5735±105.8*	19.25±7.5
		%	38.2±1.4%	60.7±1.4%	1.1%±0.3%*		% 38.3±1.8%	61.5±1.8%	0.2±0.1%*
20 dpc (1 dpp)	8	#	1456±203.6	2466±323.9*	324.3±46.8	5	# 1875±372.7	3929±283.2*	550.8±119.8
		%	34.3±4.1%	57.9±3.7%	7.8±1.1%		% 28.9±4.6%	62.7±5.5%	8.3±1.3%
21 dpc (2 dpp)	6	#	677.7±86.2	2675±207.1	763.8±117.5	4	# 593.8±90.9	3005±202.3	691.4±269.7
		%	16.5±2%	64.9±3.9%	18.6±3%		% 14.6±3.3%	70.5±2.7%	14.9±5%
22 dpc (3 dpp)	6	#	167.7±32.07	1212±149.4	1728±271.2	4	# 304.1±118.4	1308±153	2533±458.1
		%	5.6±0.9%	40±3.1%	54.5±3.7%		% 6.4±1.8%	32.9±3.5%	60.7±2.6%
23 dpc (4 dpp)	8	#	163.9±47.9	1028±158.2	2288±205.2	4	# 74±14.07	1040±84.3	2183±381.7
		%	4.2±0.8%	29±1.8%	66.8±2.4%		% 2.3±0.4%	32.6±3.3%	65.1±3.6%

4.1.3.1. Evaluation of the efficiency of the cyst breakdown and follicle formation in absence of SPO11

After finding that the oocyte number in the *Spo11*$^{-/-}$ ovaries was already very low at 20 dpc, we wanted to know if the cyst breakdown and follicle formation were affected in this mutant. For that reason, we classified the oocytes from 20 dpc *Spo11*$^{-/-}$ ovaries in the different 3 sub-types, and compared them to the WT. We expressed the results in both absolut numbers and percentages for each genotype. There was an 80% decrease in the number of cysts in the *Spo11*$^{-/-}$ ovaries, compared to the WT (p=0.0029 t-test, Fig. 4.8, Table 4.5), far superior than the 62% of reduction from the total number of oocytes. These results indicate that the *Spo11*$^{-/-}$ ovaries are breaking their cysts before the WT ovaries, maybe as a consequence of the increase in the oocyte death.

Previously, we found that *Chk2* mutation rescues the number of oocytes found in *Spo11*$^{-/-}$ mouse ovaries, postulating that the *Spo11*$^{-/-}$ oocytes may be able to create SPO11-independent DSBs (Carofiglio et al., 2013). Furthermore, we saw how the absence of CHK2 had no effect on cyst breakdown or follicle formation in WT ovaries. Thus, we next wanted to test if the absence of CHK2 could rescue the number of oocytes in cyst in *Spo11*$^{-/-}$ ovaries. Indeed, both numbers and percentages of cysts were significantly increased in *Spo11*$^{-/-}$ *Chk2*$^{-}$

$^{-/-}$ ovaries, being similar to the ones found in WT ovaries (p=0.0025 t-test, Fig. 4.8, Table 4.5). However, the number of single oocytes and follicles remains the same comparing both genotypes (p=0.0557 t-test for single oocytes, and p=0.7439 for follicles, Fig. 4.8, Table 4.5). These data suggest that the increase of oocytes found in the double mutant, primarly comes from rescueing oocytes in cyst. Thus, this finding indicates that CHK2 regulates the cyst breakdown in *Spo11*$^{-/-}$ ovaries, probably in relation with the higher oocyte death.

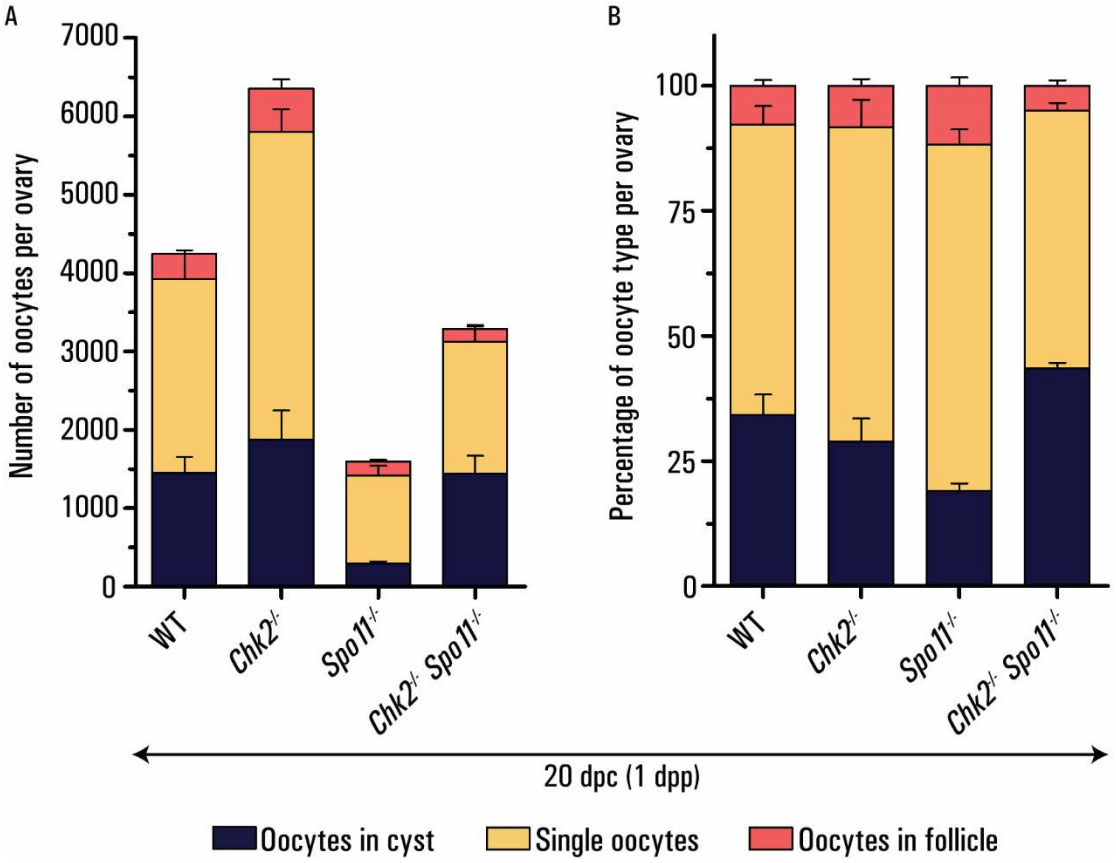

Figure 4.8 CHK2 rescues the number of cysts in a SPO11 background. A) Number of types of oocytes per ovary in WT and *Chk2*$^{-/-}$, *Spo11*$^{-/-}$, *Spo11*$^{-/-}$ *Chk2*$^{-/-}$ mice. **B)** Percentage of the different types of oocytes per ovary in WT and *Chk2*$^{-/-}$, *Spo11*$^{-/-}$, *Spo11*$^{-/-}$ *Chk2*$^{-/-}$mice. The lines represents the mean ± SEM. The data of WT and *Chk2*$^{-/-}$ was extracted from Figure 4.7. The number of cyst is rescued in the double mutant to WT levels.

Table 4.5 Number and percentage of the different classes of oocytes found at 20 dpc^{-} ovaries from the different indicated genotypes. The numbers express the average ± SEM. N indicates the number of ovaries counted. a, b and c represent the statistical difference between the different genotypes. The data of WT and *Chk2*$^{-/-}$ was extracted from Table 4.4.

		20 dpc (1 dpp)		
Genotype	N	Cysts	Single oocytes	Follicles
Spo11$^{-/-}$	4	# 300.6 ± 22.3^{abc}	1116.9 ± 128.3^{bc}	183.5 ± 20.7^{b}
		% 19 ± 1.5%^{ab}	69.2 ± 3%^{a}	11.8 ± 1.7%^{a}
Spo11$^{-/-}$ *Chk2*$^{-/-}$	4	# 1441 ± 228.1^{a}	1680 ± 200.8^{a}	165.8 ± 47.6^{a}
		% 43.5 ± 1.1%^{ac}	51.5 ± 1.6%^{a}	5 ± 1%^{a}
WT	8	# 1456 ± 203.6^{b}	2466 ± 323.9^{bd}	324.3 ± 46.8
		% 34.3 ± 4.1%^{b}	57.9 ± 3.7%	7.8 ± 1.1%
Chk2$^{-/-}$	5	# 1875 ± 372.7^{c}	3929 ± 283.2^{acd}	550.8 ± 119.8^{ab}
		% 28.9 ± 4.6%^{c}	62.7 ± 5.5%	8.3 ± 1.3%

4.1.4. Analysis of the use of pharmacological inhibitors to study the oocyte loss and folliculogenesis *in vitro*

Since the number of oocytes in *Chk2*$^{-/-}$ levels to the one found in WT ovaries at 21 dpc, we thought that there should be an alternative mechanism causing this belated perinatal death in the absence of CHK2. Hence, we aimed to find out the mechanisms responsible for this oocyte loss. For that reason we used a previously described ovarian culture technique (Morgan et al., 2015) in order to use farmacological inhibitors of putative candidates and evaluate their effect *in vitro*.

Previous unpublished work of our lab (Guillot and Roig, 2017) evaluated the efficiency of the follicle development *in vitro* culturing 20 dpc (1 dpp) WT mouse ovaries. Our lab data suggests that after 5 days of culture, the proportion of follicle formation was equivalent to 22 dpc (3 dpp) ovaries (Fig. 4.9A).

4.1.4.1. The Notch2 signaling pathway does not participate in the oocyte loss *in vitro*

Several studies have reported that the proteins involved in the Notch pathway are required for cyst breakdown and follicle formation (Trombly et al., 2009; Xu and Gridley, 2013). Trombly et al., found that the inhibition of the Notch pathway in cultured newborn ovaries increases the percentage of cysts and decreases the percentage of primordial follicles. Xu and Gridley found that in 18 dpp conditional *Notch2* mutants there was a 20% increase in oocyte number, associated to the presence of MOFs. Thus, we decided to

investigate if the Notch2 pathway was involved in the perinatal control of the population of oocytes. To do so, we selected the DAPT, N-[N-(3,5-Difluorophennacetyl)-L-alanyl]-S-phenylglycine-t-butyl ester inhibitor, which inhibits the γ-secretase, a protease complex that cleaves the Notch receptor releasing the intracellular domain into the nucleus regulating gene transcription (Zhang et al., 2014). DAPT has been repeateadly used as a Notch inhibitor in different scenarios, including the study of female oogenesis (Jing et al., 2017; Li et al., 2016; Trombly et al., 2009; Zhang et al., 2011) and male spermatogenesis (Murta et al., 2014).

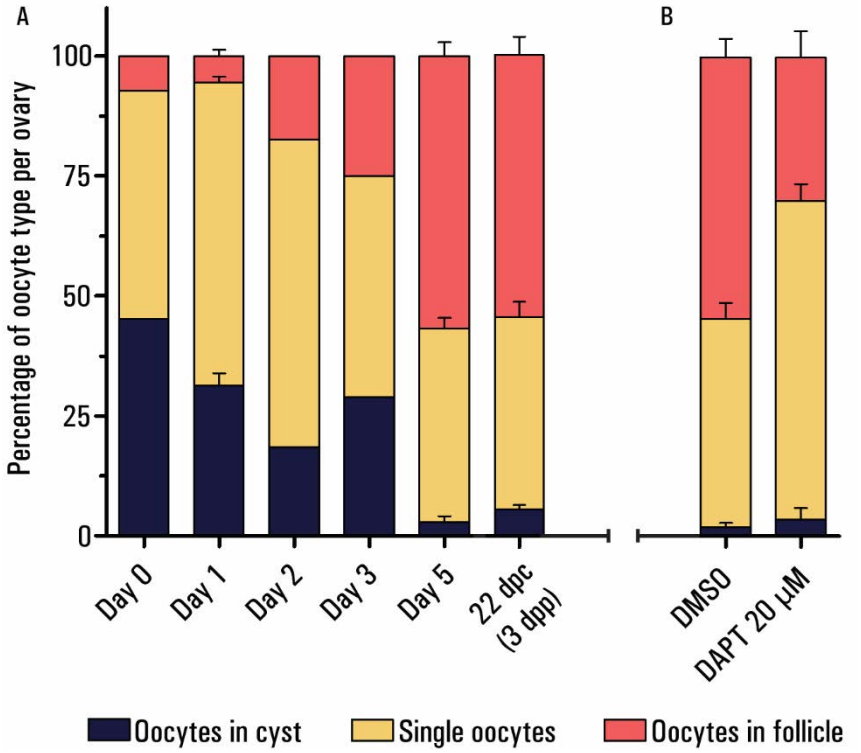

Figure 4.9 The organotypic culture allows folliculogenesis initiation *in vitro*. A) After 5 days of culture, the ovaries of WT females present the same percentage of follicles as the 22 dpc ovaries (3 dpp). **B)** Introducing the DAPT inhibitor of the Notch pathway in the culture decreases the proportion of follicles of WT ovaries. The lines represents the mean ± SEM. Modified from Guillot and Roig, 2017.

We cultured *Chk2*$^{-/-}$ ovaries with DAPT, to check if in absence of CHK2 and inhibition of Notch signaling, we were able to see a rescue in the oocyte number. In our previous work the DAPT inhibitor was tested in WT ovaries, determining the concentration to 20 µM (Jing et al., 2017; Li et al., 2016; Trombly et al., 2009; Zhang et al., 2011) and confirming the effects of the inhibitor in folliculogenesis. We observed a decrease in the percentage of follicles, from 54.7% of the controls to a 29.9% of the inhibited ovaries (p=0.0120 t-test, Fig. 4.9B). Histologicaly, the inhibited ovaries were different compared to the controls. They accumulated single oocytes, the majority, near the cortex, while the medulla of the ovary was practically empty, since that is normally where the follicles lay. Furthermore, the

follicles found had flatter, smaller and discontinous surrounding follicular cells, compared to the controls, with bigger and continuous layer of granulosa cells (Fig. 4.10). When we tested it on *Chk2*$^{-/-}$ ovaries, we found that both the control and the inhibited cultured ovaries had statistically the same oocyte number (Fig. 4.10, Table 4.6). We also found that the inhibited mutant ovaries had a significant decrease in both the number and the percentage of follicles (p=0.0163 for the numbers; p=0.0016 for the percentages, t-test, Fig. 4.10, Table 4.6). The number of single oocytes remained the same in both conditions, even though the percentage was higher in the inhibited ones due to the reduced presence of follicles (p=0.9897 for the numbers; p=0.0013 for the percentages, t-test, Fig. 4.10, Table 4.6). Surprisingly, we did not found any differences in the number nor in the proportion of cysts. With these obtained data, we can conclude that the Notch pathway does not regulate the process of oocyte death after birth, even though it has a role in follicle formation.

Table 4.6 Number and percentage of the different classes of oocytes found at 20 dpc *Chk2*$^{-/-}$ cultured ovaries at the indicated conditions. The numbers express the average ± SEM. N indicates the number of ovaries counted. * represents the statistical difference between the two conditions.

Chk2$^{-/-}$	N		Cysts	Single oocytes	Follicles	Total
DMSO	9	#	94.6±25.7	559.8±46.7	824.8±67.6*	1479±124.4
		%	5.9±1.2%	38.1±1.5%*	56±1.9%*	-
DAPT 20 µM	3	#	83±23.97	558.2±172.4	421.6±136.2*	1063±325.5
		%	7.9±0.2%	53.5±4.3%*	38.6±4.5%*	-

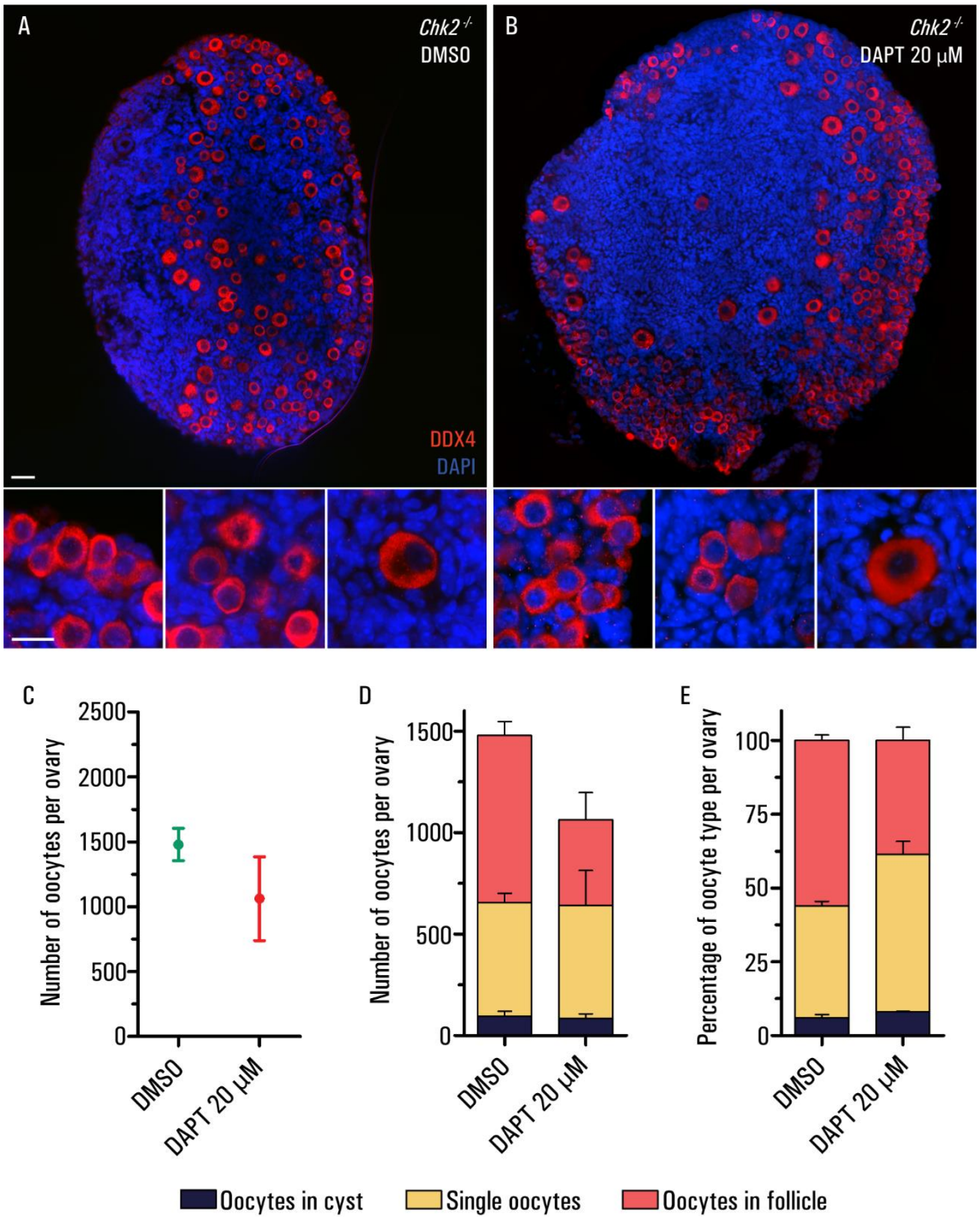

Figure 4.10 Addition of the DAPT inhibitor decreases the proportion of follicles in absence of CHK2 but does not rescue the oocyte number. A-B) Histological sections of *Chk2*$^{-/-}$ DMSO-treated ovaries (A) and 20 µM DAPT-inhibited ovaries (B) immunostained against DDX4 (red) and with the DNA counterstained with DAPI (blue). The inserts show the detail of oocytes in cyst (left), single oocytes (center) and a follicle (right). The scale bar in the top image represent 40 µm and applies to both images. The scale bar in the insert represents 20 µm and applies to all bottom images. **C**) Number of oocytes per ovary after 5 days of culture, for controls and DAPT-inhibited ovaries of *Chk2*$^{-/-}$ 20 dpc females. The round symbols represent the mean and the lines the SEM. **D-E)** Number (D) and percentage (E) of the different oocyte types for the same ovaries. The lines represent the mean ± SEM. There is a decrease in the proportion of follicles in the inhibited mutant ovaries, and there is no rescue of the oocyte number.

4.1.4.2. The Chk1 signaling pathway participates in the *in vitro* oocyte loss

The CHK1 protein is an effector kinase of the DDR activated mainly by ATR in response to single stranded DNA, although there is some overlap between the ATM-CHK2 and the ATR-CHK1 axis (Cuadrado et al., 2006; Kastan and Lim, 2000; Stracker et al., 2013; Wang et al., 2006). CHK1 function has been studied primarly in cell cycle and cancer (Bartek and Lukas, 2001, 2003; L. Chen et al., 2012), and even though conditional mutants have been created and studied in male fertility (Abe et al., 2018), the role of CHK1 in the ovarian development and oocyte pool remains unknown. LY2603618 is a potent and selective small molecule inhibitor of CHK1 protein kinase activity *in vitro* (King et al., 2014), mostly used in cancer studies (Liang et al., 2017), but also used to study meiosis (Pacheco et al., 2018).

To check the effects of this inhibitor in our *in vitro* ovary development system, we cultured 20 dpc *Chk2*$^{-/-}$ for 5 days in presence of different concentrations of the CHK1 inhibitor LY2603618 (Chk1i) and compared them to ovaries cultured in the presence of DMSO (as controls). We analyzed the total oocyte number and the propotion of oocyte types. At the lower concentration (1 µM) the number of oocytes was statistically the same as the controls (Fig. 4.11, Table 4.7); also, the number and proportion of cyst and follicles were the same, but we found a little decrease in the percentage of single oocytes from a 38.1 to a 30.3% (p=0.0472 t-test, Fig. 4.11, Table 4.7). This lack of difference in both the oocyte number and the follicle and cyst proportion may indicate that the concentration of the inhibitor was too low. For that reason, we increase it to 5 µM and we observed a significant 38% increase in the total number of oocytes in the CHK1 inhibited ovaries, (p=0.0473 t-test, Fig. 4.11, Table 4.7). There was also more than a 3-fold increase in the number of cyst (p=0.0049 t-test, Fig. 4.11, Table 4.7), resulting in a 2-fold increase in the proportion of cysts (p=0.0081 t-test, Fig. 4.11, Table 4.7). Regarding the number of follicles, there was a tendency of the inhibited ovaries to have less follicles (p=0.2687 t-test, Fig. 4.11, Table 4.7), with a significant reduction on the percentage (p=0.0006 t-test, Fig. 4.11, Table 4.7). We found that increasing the concentration of Chk1i to 10 µM, it was toxic for the ovaries. Histologically, in both ovaries the majority of the ovarian cells looked dead, with one of them presenting no oocytes, and the other one only 823 (Fig. 4.11, Table 4.7).

All together, these results suggest that the DDR regulates the number of oocytes, cyst breakdown and follicle formation in the perinatal development.

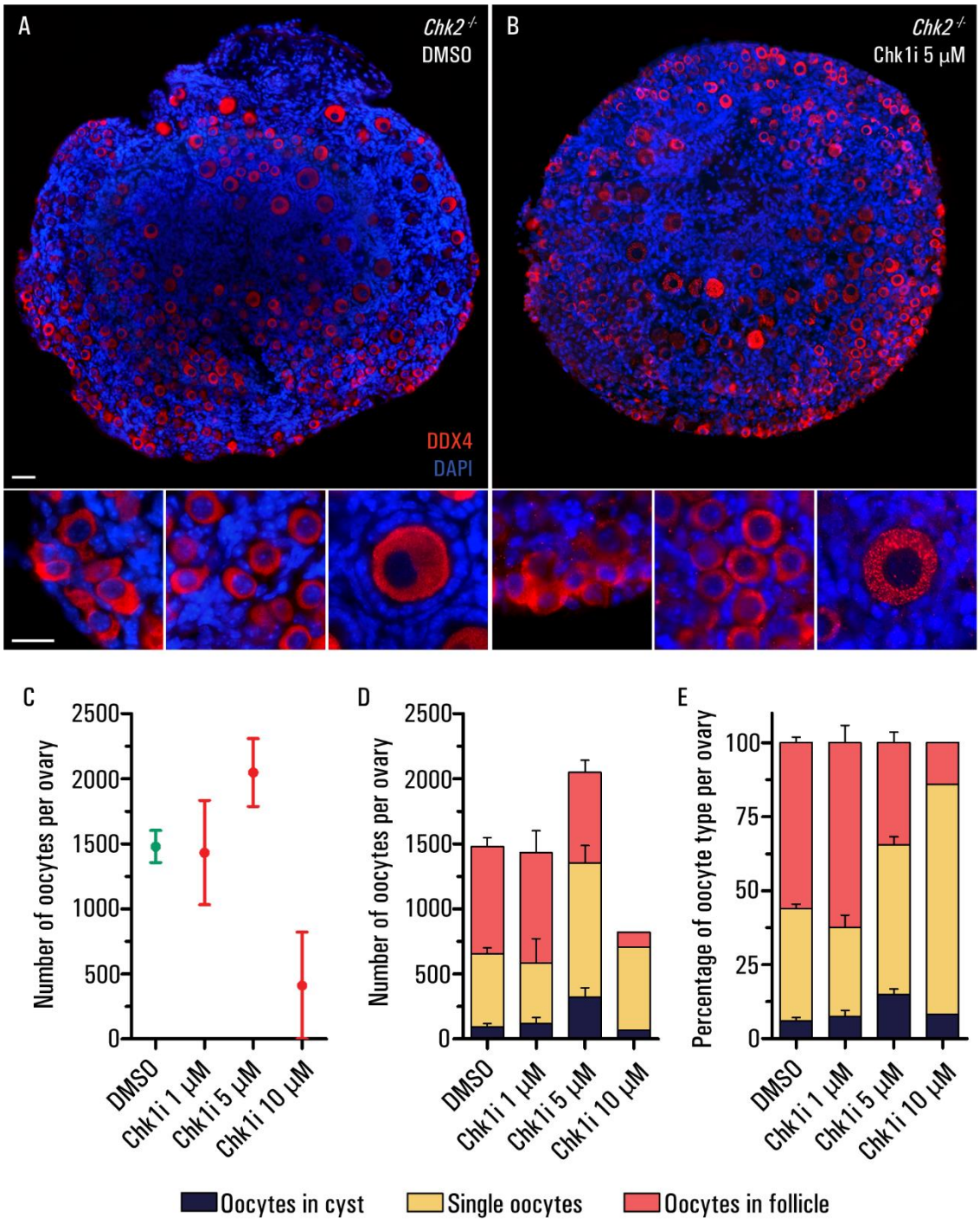

Figure 4.11 The inhibition of CHK1 rescues the oocyte number in *Chk2*$^{-/-}$ ovaries. A-B) Histological sections of *Chk2*$^{-/-}$ DMSO-treated ovaries (A) and 5 µM LY2603618 inhibited ovaries (B) immunostained against DDX4 (red) and with the DNA counterstained with DAPI (blue). The inserts show the detail of oocytes in cyst (left), single oocytes (center) and a follicle (right). The scale bar in the top image represent 40 µm and applies to both images. The scale bar in the insert represents 20 µm and applies to all bottom images. **C)** Number of oocytes per ovary after 5 days of culture, for controls and CHK1-inhibited ovaries of *Chk2*$^{-/-}$ 20 dpc females. The round symbols represent the mean and the lines the SEM. **D-E)** Number (D) and percentage (E) of the different oocyte types for the same ovaries. The lines represents the mean ± SEM. In the Chk1i 10 µM, only the data of the ovary with oocytes is shown. There is an increase in the oocyte number in the CHK1 inhibited ovaries, accompanied by an increase in the cyst and a decrease in the proportion of follicles.

Table 4.7 Number and percentage of the different classes of oocytes found at 20 dpc *Chk2*$^{-/-}$ cultured ovaries at the indicated conditions. The numbers express the average ± SEM. N indicates the number of ovaries counted. a, b and c represent the statistical difference between the different genotypes.

Chk2$^{-/-}$	N		Cysts	Single oocytes	Follicles	Total
DMSO	9	#	94.6 ± 25.7^{b}	559.8 ± 46.7^{b}	824.8 ± 67.6^{c}	1479 ± 124.4^{bc}
		%	5.9 ± 1.2%^{a}	38.1 ± 1.5%^{ab}	56 ± 1.9%^{bc}	-
Chk1i 1 µM	3	#	116.8 ± 48.6	467.3 ± 187.5	848.5 ± 168.7	1433 ± 401.3
		%	7.4 ± 2.2%	30.3 ± 4.1%^{a}	62.3 ± 5.8%^{a}	-
Chk1i 5 µM	6	#	320.6 ± 73.4^{b}	1033 ± 134.2^{b}	693.8 ± 95.5	2047 ± 260.5^{b}
		%	14.9 ± 1.9%^{ab}	50.6 ± 2.6%^{b}	34.4 ± 3.7%^{b}	-
Chk1i 10 µM	2	#	33.5 ± 33.5	320.5 ± 320.5	57.5 ± 57.5^{c}	411.5 ± 411.5^{c}
		%	4.1 ± 4.1%^{b}	39 ± 39%	7 ± 7%^{abc}	-

4.2. Study of the role of the DDR pathway in adult mammalian ovaries

It's been known for a long time that the pool of follicles of adult females is sensitive to external radiation (Baker, 1971). Hence, there is a DNA damage response that is activated in case of an external or an endogenous disruption of the DNA in adult oocytes. Therefore, we wanted to test if CHK2, responsible of the fetal oocyte death, was also mediating some kind of response in the follicles of adult mice females.

4.2.1. Analysis of the variation of follicle number during adulthood

In order to evaluate the effects of the DDR in adult females, we collected ovaries from young (40 dpp) and elder (400 dpp) WT and *Chk2*$^{-/-}$ females and counted the oocyte number in histological sections stained with PAS-Hematoxylin. At 40 dpp, there was no significant difference between both genotypes regarding the total oocyte number, both having around 1000 oocytes per ovary (Fig. 4.12, Table 4.8). Nonetheless, there was a tendency of the mutant ovaries to have more oocytes. We also classified these oocytes in primordial, primary, secondary, antral an abnormal follicles. We found that most of the oocytes were enclosed in primordial follicles, but there were also a high quantity of primary, secondary and antral follicles, as expected from a young ovary. We found no differences between WT and mutant samples (Fig. 4.12, Table 4.8).

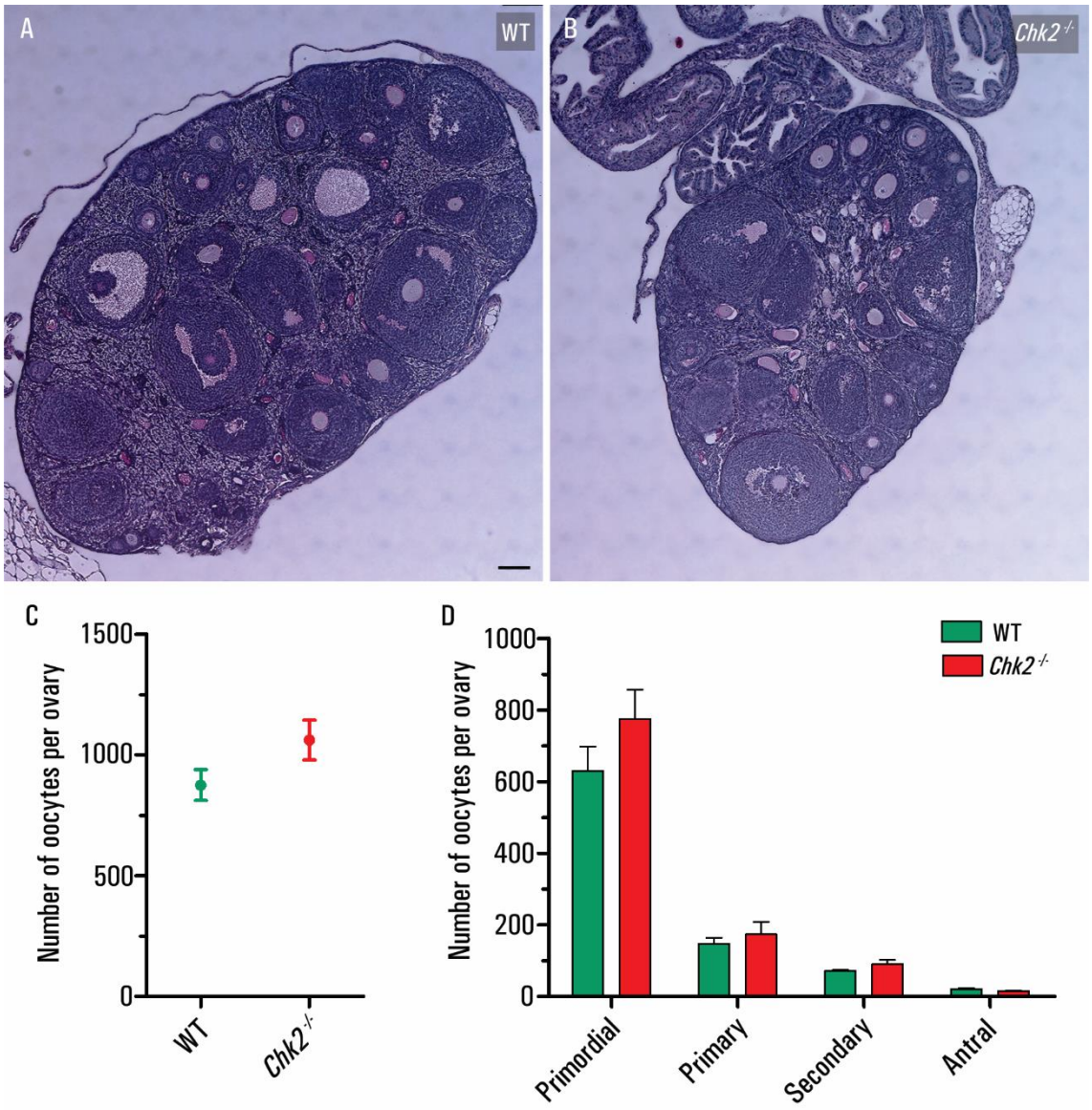

Figure 4.12 40 dpp WT and *Chk2*$^{-/-}$ ovaries have silimar number of oocytes. A-B) Histological sections of WT (A) and *Chk2*$^{-/-}$ (B) ovaries stained with PAS-Hematoxylin. Scale bar represent 100 µm and applies to both images **C)** Number of oocytes per ovary in 40 dpp WT and *Chk2*$^{-/-}$ ovaries. The round symbols represent the mean and the lines the SEM. **D)** Number of oocytes classified in all the follicle types. The lines represent the mean ± SEM. Both genotypes present the same oocyte number with the ovaries of the same appearance.

Analyzing the elder ovaries (400 dpp), we found that the WT ones presented a very low follicle pool, with around 100 oocytes per ovary, and with an equivalent number of primordial and primary follicles (p=0.1951 t-test, Fig. 4.13, Table 4.8). This phenotype is the expected from an ovary from old mice, with the oocyte pool almost exhausted.

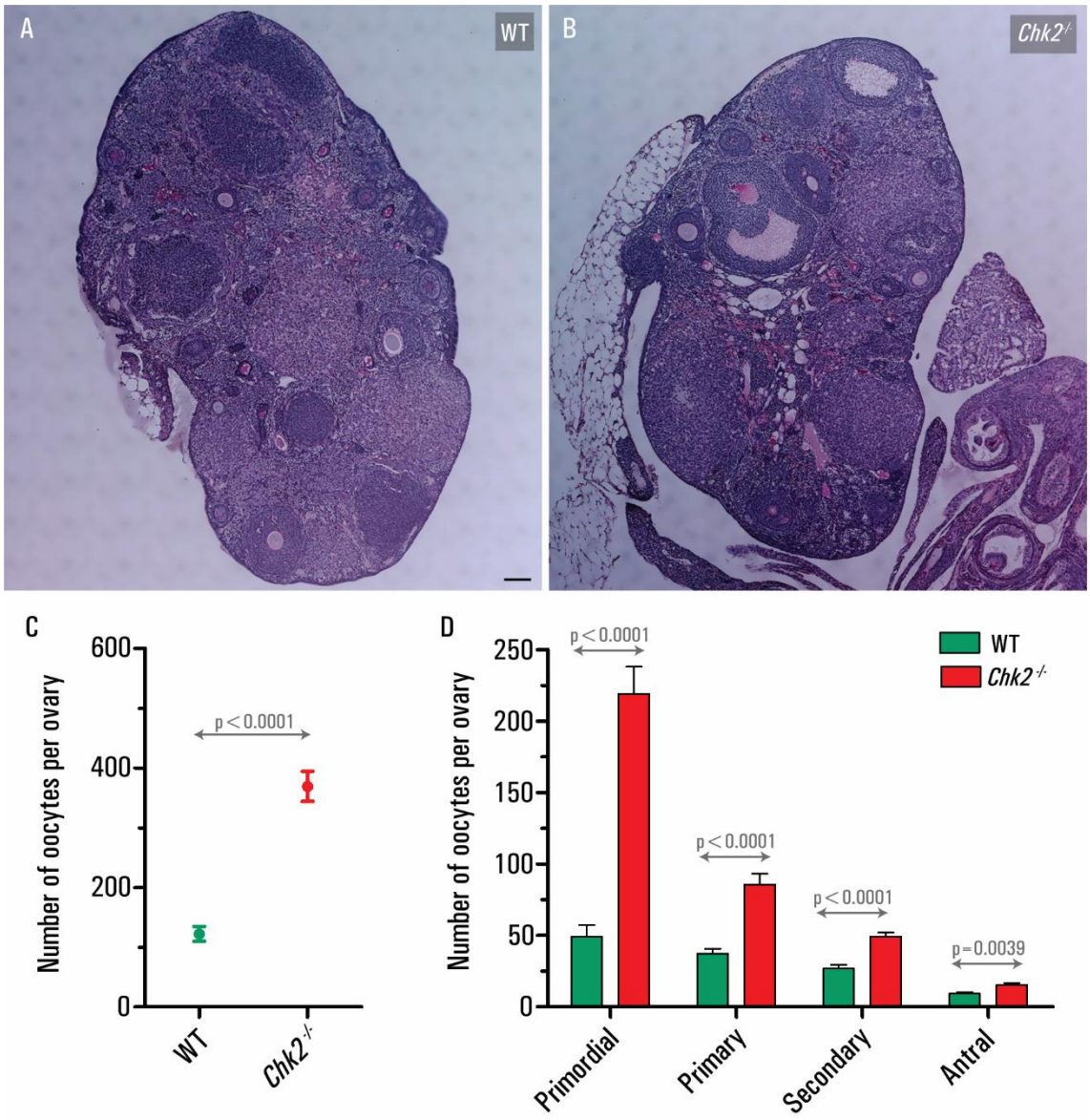

Figure 4.13 400 dpp *Chk2*$^{-/-}$ ovaries have a 3-fold increase in the oocyte number. A-B) Histological sections of WT (A) and *Chk2*$^{-/-}$ (B) ovaries stained with PAS-Hematoxylin. Scale bar represent 100 µm and applies to all images **C)** Number of oocytes per ovary in 400 dpp WT and *Chk2*$^{-/-}$ ovaries. The round symbols represent the mean and the lines the SEM. **D)** Number of oocytes classified in all the follicle types. The lines represent the mean ± SEM. The ovaries at 400 dpp present a higher number of all the follicle types.

We found that the Chk2$^{-/-}$ mutants had a 3-fold increase in the oocyte number compared to the controls ($p<0.0001$ t-test, Fig. 4.13, Table 4.8). This increase in the total number is translated to an increase in all the different follicle types: the mutant ovaries had 4 times more primordial follicles ($p<0.0001$ t-test, Fig. 4.13, Table 4.8), 2 times more primary ($p<0.0001$ t-test, Fig. 4.13, Table 4.8) and secondary follicles ($p<0.0001$ t-test, Fig. 4.13, Table 4.8) and almost 2 times more antral follicles ($p=0.0039$ t-test, Fig. 4.13, Table 4.8). Hence, with this observed increase in elder *Chk2*$^{-/-}$ females we postulate that CHK2 eliminates the oocytes in follicle in the adult females. We hypothesize that as the females get old, the

oocytes accumulate oxidative damage, increasing the DNA damage. In absence of CHK2 these oocytes cannot be killed, therefore there is a higher number of oocytes in *Chk2*$^{-/-}$ mice. Importantly, this could lead to an extension in the reproductive lifespan.

Table 4.8 Number and percentage of the different follicle types found at 40 and 400 dpp WT and *Chk2*$^{-/-}$ ovaries. The numbers express the average ± SEM. N indicates the number of ovaries counted. * represents the statistical difference between the two genotypes.

		N	Primordial	Primary	Secondary	Antral	Abnormal	Total
40 dpp	WT	7	# 629.3±68	147.1±17.2	71.4±3.8	20.43±3.6	6.6±0.6	874.9±64.2
			% 71±3.2%	17.4±2.5%	8.3±0.4%	2.5±0.5%	0.8±0.1%	-
	Chk2$^{-/-}$	8	# 775±82.3	174±34.9	89.9±12.8	15.8±1.8	7.1±2	1062±82.6
			% 72.5±4%	16.9±3.5%	8.3±0.9%	1.6±0.2%	0.8±0.3%	-
400 dpp	WT	14	# 49.2±8.4*	37.1±3.7*	26.8±2.7*	9.1±1.2*	0.2±0.2	122.4±12.3*
			% 37.6±3.6%*	31.1±1.7%*	23.3±2.2%*	7.9±1.3%*	0.1±0.1%	-
	Chk2$^{-/-}$	14	# 218.9±19.1*	85.7±7.6*	49.3±2.7*	15.3±1.5*	0	369.2±25.1*
			% 58.4±2.2%*	23.3±1.4%*	14±1.1%*	4.3±0.5%*	0%	-

Furthermore while analyzing the ovaries, we found the presence of some multi-oocyte follicles (MOFs). Those are follicles with 2 or more oocytes that have been associated to cyst breakdown defects. We previously described how CHK2 was mostly dispensable for cyst breakdown, but we wanted to analyze if in CHK2 absence, the cyst breakdown process was done correctly. For that, we measured the percentage of oocytes sharing follicle in 40 and 400 dpp WT and *Chk2*$^{-/-}$ ovaries. At 40 dpp, even though the mutants had a higher percentage of oocytes sharing follicle, the difference was non significant (Fig. 4.14, Table 4.9). At 400 dpp we found a 3-fold increase in the percentage of MOFs in *Chk2*$^{-/-}$ ovaries (p=0.0068 t-test, Fig. 4.14, Table 4.9). Because it has been reported that the presence of MOFs is related to an incomplete cyst breakdown (reviewed in Pepling, 2006, 2012; Tingen, et al., 2009), these data suggest that in absence of CHK2, the cyst breakdown could be, in part, compromised.

Table 4.9 Number and percentage of the different follicle types found at 40 and 400 dpp WT and *Chk2*$^{-/-}$ ovaries. The numbers express the average ± SEM. N indicates the number of ovaries counted. * represents the statistical difference between the two genotypes.

	N	40 dpp	N	400 dpp
WT	7	# 33.9±6.7*	14	1.4±0.4*
		% 4.1±0.9%		1.1±0.3%*
Chk2$^{-/-}$	8	# 70.4±8.6*	14	14.2±3.2*
		% 7.1±1.2%		3.6±0.8%*

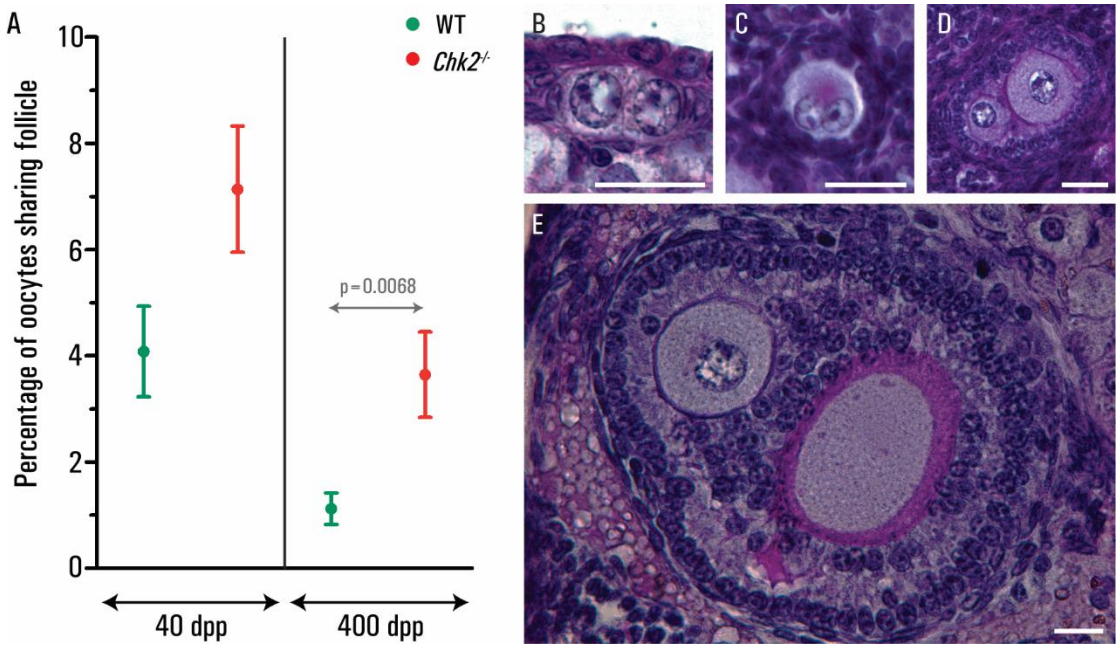

Figure 4.14 400 dpp *Chk2*$^{-/-}$ ovaries have a 3-fold increase in the percentage of oocytes sharing follicle. A) Percentage of oocytes sharing follicle in 40 and 400 dpp WT and *Chk2*$^{-/-}$ ovaries. The round symbols represent the mean and the lines the SEM. **B-E)** Representative images of oocytes sharing follicle stained with PAS-Hematoxylin of primordial (B), primary (C-D) and secondary (E) follicles. Scale bars in all images represent 30 µm. The MOFs can be found in the ovaries as two or more oocytes inside a single follicle.

4.2.2. Analysis of the fertility and reproductive lifespan of *Chk2*$^{-/-}$ females

Since we saw an increase in the oocyte number in elder *Chk2*$^{-/-}$ females, we studied if the absence of CHK2 had an impact in the fertility and reproductive lifespan of these females.

We set matings of approximately 2 months old WT and *Chk2*$^{-/-}$ females with males of proven fertility for one year; and matings of 12 months old WT and *Chk2*$^{-/-}$ females with

males of proven fertility for 6 months. All the data from the two experiments was pooled together (Fig. 4.15). We found no differences in the number of pups per litter, in the number of litters, nor in the number of pups per female. Furthermore we correlated the age of the mother at the birth of the pups with the number of pups from the litter, and in general, as expected, there is a decrese of the number of pups per litter as the mothers grow older. This decrease is equivalent in both control and mutants for the first 400 dpp, but in the last 6 months there is a tendency for the *Chk2*$^{-/-}$ females to increase the number of pups compared to the controls. At that age, beyond one year, the females are very old and they had a lot of difficulties to get pregnant and deliver the pups, so the mating analysis are unreliable. With these data, we can confirm that CHK2 does not obviously interfere in the fertility (Bolcun-Filas et al., 2014; Hirao et al., 2002; Takai et al., 2002) but its absence produces a younger ovarian phenotype, allowing the presence of more follicles and hence most likely, delaying the end of the reproductive life.

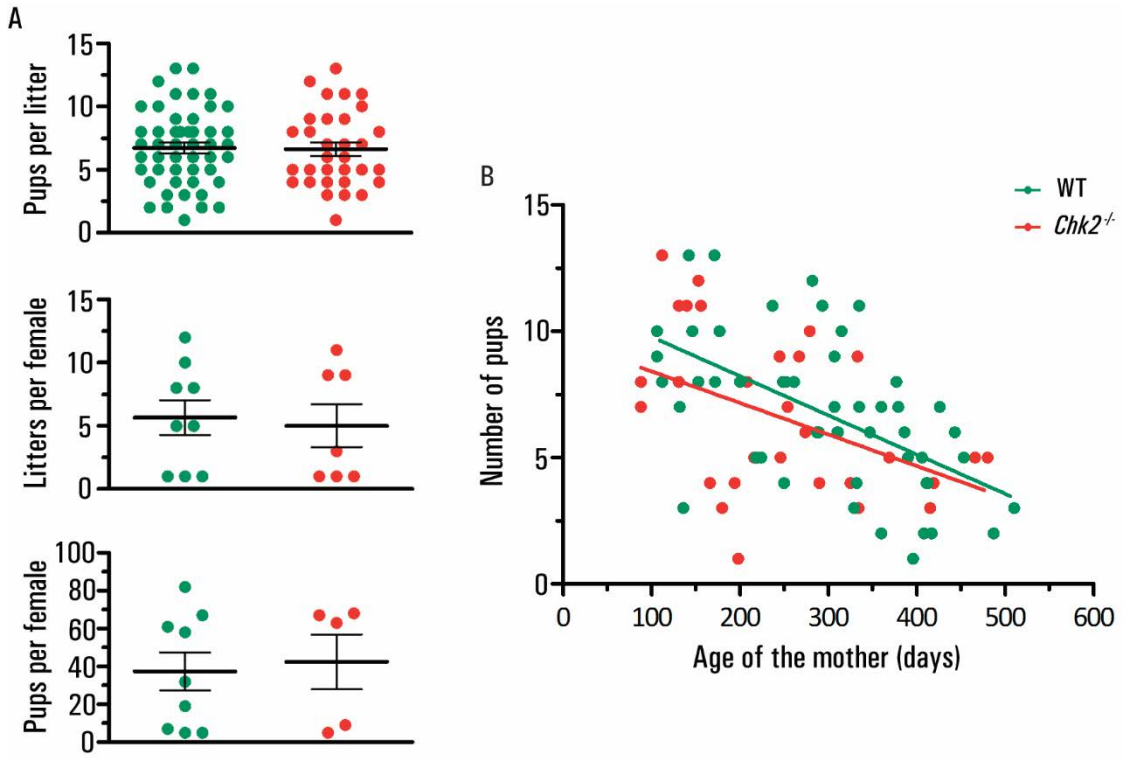

Figure 4.15 The *Chk2*$^{-/-}$ mice have no remarkable fertility problems. A) Number of pups per litter, litters per female and pups per female for WT and Chk2$^{-/-}$ mice. The horizontal lines represent the means ± SEM. **B)** Lineal regression with the number of pups related to the age of the mother (in days) at the time of the birth. There is no difference in the fertility in mutants compared to WT.

4.3. Study of the synapsis checkpoint in mammalian oocytes

The DNA-damage-independent, or synapsis checkpoint has been studied in male mice mostly, due to the presence of the sex body and the meiotic sex chromosome inactivation (MSCI) (Turner, 2007). The activation of this checkpoint in females is believed to be triggered by the meiotic silencing of unsynapsed chromomes (MSUC). The presence of HORMAD1/2, ɣH2AFX, and other proteins like ATR and BRCA1 on the unsynapsed axes produces a transcriptional silencing that it is supposed to trigger the oocyte death due to synapsis problems in the MSUC mechanism (Cloutier et al., 2015; Turner, 2007). TRIP13 is required for the depletion of HORMAD1/2 from synapsed regions in males and females (Wojtasz et al., 2009b). Moreover, studies with TRIP13 homologues in other species like *S. cerevisiae*, *C. elegans* or *D. melanogaster* shows a checkpoint-related role of this protein (Bhalla and Dernburg, 2005; Joyce and McKim, 2009; San-Segundo and Roeder, 1999). However, it's been proposed that TRIP13 is not involved in the pachytene checkpoint control in mice since it is not required to implement the synaptic checkpoint in males or females (Li and Schimenti, 2007). That postulation was made without providing oocyte counts, so we wanted to double-check it and extend the data.

We wanted to check if TRIP13 can rescue two mutants that are thought to arrest due to the synapsis checkpoint, *Spo11*$^{-/-}$, and *Dmc1*$^{-/-}$ *Chk2*$^{-/-}$. First, we analyzed the oocyte number in young 30 dpp *Trip13*$^{mod/mod}$ *Spo11*$^{-/-}$ double mutant ovaries using *Spo11*$^{-/-}$ ovaries as controls. We used this mutant because we know that at least a part of its oocytes die by synapsis errors (Di Giacomo et al., 2005; Vera D. Rinaldi et al., 2017). Our hypothesis is that if TRIP13 participates in this synapsis checkpoint, there should be a rescue in the number of oocytes in these double mutant. However, as it was previously reported (Li and Schimenti, 2007), in the *Trip13*$^{mod/mod}$ *Spo11*$^{-/-}$ there was no rescue of the oocyte numbers. The double mutant had the same low number of oocytes than the *Spo11*$^{-/-}$ (Fig. 4.16, Table 4.10). Similarly, we did not found any difference for any of the follicle types between both genotypes (Fig. 4.16, Table 4.10). This lack of rescue was previously reported (Li and Schimenti, 2007), confirming our results in absence of SPO11-induced DSBs.

Table 4.10 Number and percentage of the different follicle types found at 30 dpp *Spo11*$^{+/+}$ and Spo11 Trip13$^{mod/mod}$ ovaries. The numbers express the average ± SEM. N indicates the number of ovaries counted.

30 dpp	N	Primordial	Primary	Secondary	Antral	Abnormal	Total
Dmc1$^{-/-}$ *Chk2*$^{-/-}$	8	# 108.4±11.8*	59.9±7.2*	127±4.6	42.1±2.9	28.9±4.2*	366.6±16.3*
		% 29±2.3%*	16.1±1.6%	35.2±2.1%*	11.8±1.2%*	7.9±1%*	-
Dmc1$^{-/-}$ *Chk2*$^{-/-}$ *Trip13*$^{mod/mod}$	8	# 366.5±84.4*	109.9±11.1*	123.6±15.4	32.9±4.8	16±1.8*	648.9±110.8*
		% 52.6±3.7%*	18.5±1.7%	20.6±1.9%*	5.5±0.8%*	2.8±0.4%*	-

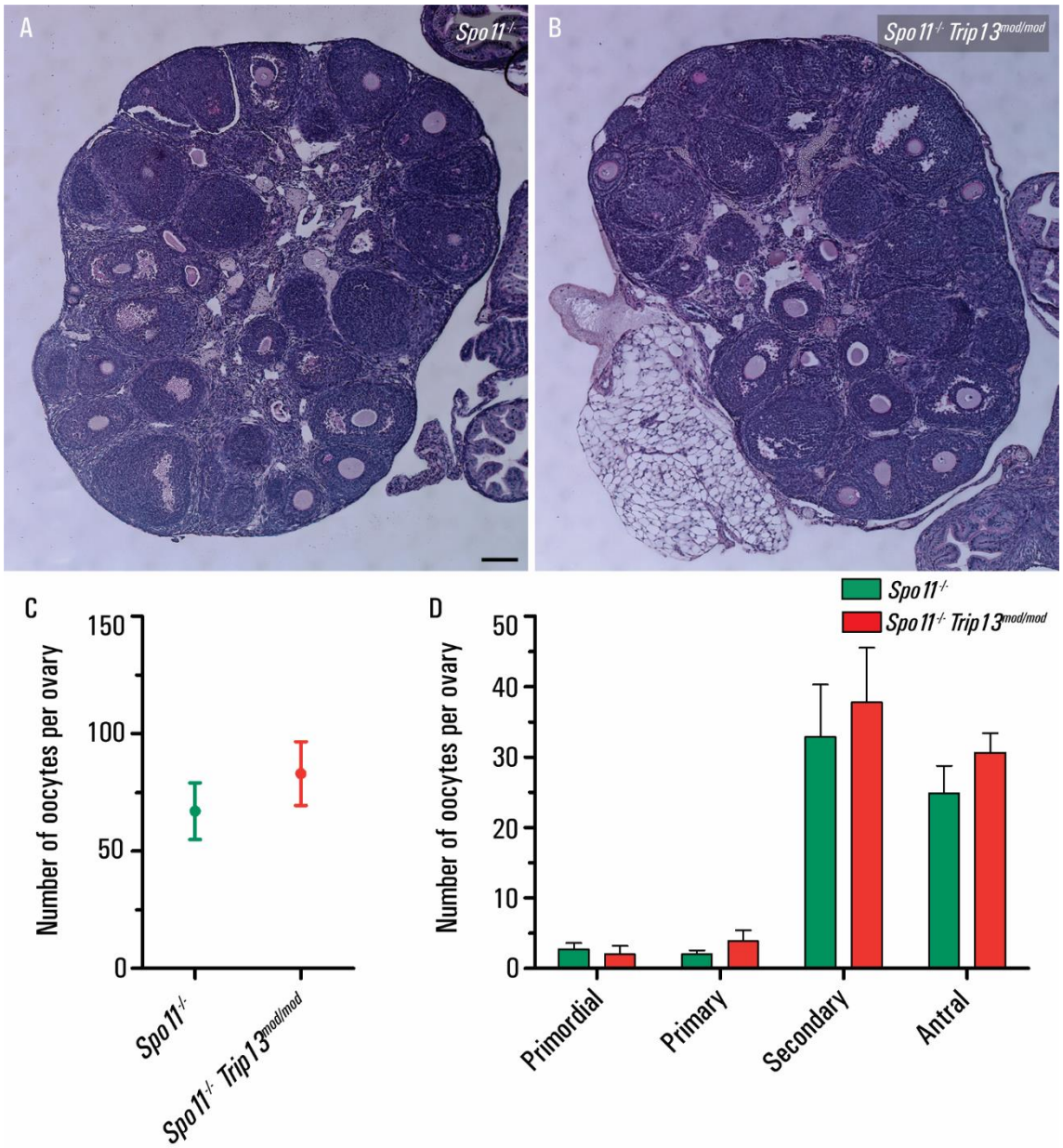

Figure 4.16 30 dpp *Spo11*$^{-/-}$ and *Spo11*$^{-/-}$ *Trip13*$^{mod/mod}$ ovaries have the same oocyte number. **A-B)** Histological sections of control *Spo11*$^{-/-}$ (A) and *Spo11*$^{-/-}$ *Trip13*$^{mod/mod}$ (B) ovaries stained with PAS-Hematoxylin. Scale bar represent 100 µm and applies to all images. **C)** Number of oocytes per ovary in 30 dpp *Spo11*$^{-/-}$ and *Spo11*$^{-/-}$ *Trip13*$^{mod/mod}$ ovaries. The round symbols represent the mean and the lines the SEM. **D)** Number of oocytes classified in all the follicle types. The lines represent the mean ± SEM. The ovaries from the two genotypes present no differences between them.

Furthermore, knowing that TRIP13 does not eliminate the *Spo11*$^{-/-}$ oocytes with synapsis problems and without SPO11-induced DSBs, we wanted to check if TRIP13 is involved in the synapsis checkpoint, but this time, in presence of DSBs. For that reason, we obtained ovaries from 30 dpp *Chk2*$^{-/-}$ *Dmc1*$^{-/-}$ *Trip13*$^{mod/mod}$ females. In absence of CHK2 the recombination-dependent checkpoint is skipped, resulting in a partial rescue of these double *Chk2*$^{-/-}$ *Dmc1*$^{-/-}$ mutants. In the triple mutant, if TRIP13 is participating in the synapsis checkpoint there should be a higher rescue of these oocytes compared to the double mutants. Indeed, we saw a higher rescue in the oocyte number in the triple mutants

compared with the double mutants (p=0.0245 t-test, Fig. 4.17, Table 4.11), wich corresponded mainly to the increase in the number of primordial (p=0.0090 t-test, Fig. 4.17, Table 4.11) and primary follicles (p=0.0020 t-test, Fig. 4.17, Table 4.11). We also observed a reduction in the triple mutant of the number and percentage of abnormal follicles (p=0.0137 for the numbers; p=0.0003 for the percentages, t-test, Fig. 4.7, Table 4.4), the ones that are presumably dying. These results show the role of TRIP13 in the synapsis checkpoint regulating the oocyte number, but only in the oocytes with presence of DSBs. Other interpretation of these results will also be presented in the discussion section.

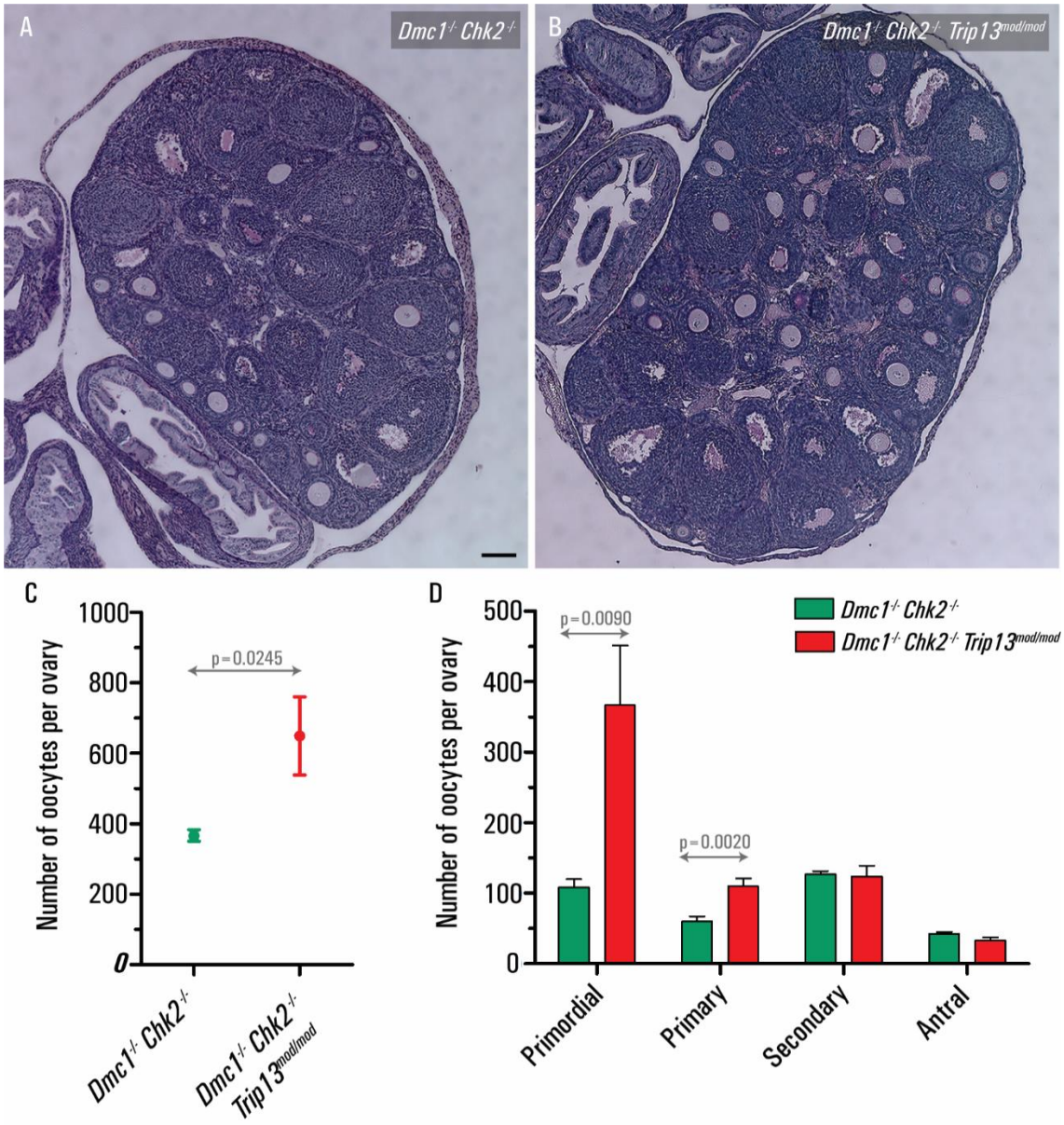

Figure 4.17 There is a rescue of the oocyte number in 30 dpp *Dmc1*$^{-/-}$ *Chk2*$^{-/-}$ *Trip13*$^{mod/mod}$ ovaries compared to the *Dmc1*$^{-/-}$ *Chk2*$^{-/-}$ ones. A-B) Histological sections of 30 dpp *Dmc1*$^{-/-}$ *Chk2*$^{-/-}$ and *Dmc1*$^{-/-}$ *Chk2*$^{-/-}$ *Trip13*$^{mod/mod}$ ovaries stained with PAS-Hematoxylin. Scale bar represent 100 µm and applies to all images **C)** Number of oocytes per ovary in 30 dpp *Chk2*$^{-/-}$ *Dmc1*$^{-/-}$ and *Chk2*$^{-/-}$ *Dmc1*$^{-/-}$ *Trip13*$^{mod/mod}$ ovaries. The round symbols represent the mean and the lines the SEM. **D)** Number of oocytes classified in all the follicle types. The lines represent the mean ± SEM. There is an increase of the oocyte number in the triple mutant ovaries.

Table 4.11 Oocyte number and follicle type in 30 dpp *Chk2*$^{-/-}$ *Dmc1*$^{-/-}$ and *Chk2*$^{-/-}$ *Dmc1*$^{-/-}$ *Trip13*$^{mod/mod}$ ovaries. The numbers express the average ± SEM. N indicates the number of ovaries counted.

30 dpp	N	Primordial	Primary	Secondary	Antral	Abnormal	Total
Dmc1$^{-/-}$ *Chk2*$^{-/-}$	8	# 108.4±11.8*	59.9±7.2*	127±4.6	42.1±2.9	28.9±4.2*	366.6±16.3*
		% 29±2.3%*	16.1±1.6%	35.2±2.1%*	11.8±1.2%*	7.9±1%*	-
Dmc1$^{-/-}$ *Chk2*$^{-/-}$ *Trip13*$^{mod/mod}$	8	# 366.5±84.4*	109.9±11.1*	123.6±15.4	32.9±4.8	16±1.8*	648.9±110.8*
		% 52.6±3.7%*	18.5±1.7%	20.6±1.9%*	5.5±0.8%*	2.8±0.4%*	-

DISCUSSION

Chapter 5

5.1. Study of meiosis in female mammals

Meiosis is an evolutionary conserved cell division fundamental for the proliferation of the species with sexual reproduction. In mammals, it has been studied for several years, for example, with the generation of multiple mutants lacking proteins that are involved in meiosis and fertility but are dispensable for embryo viability. This study has been harder due to the major sexual dimorphism existing throughout all the steps of meiosis. In females the recombination and synapsis take place during the fetal development. The control mechanisms regulating these important events, in which we focus on this work, are a top priority of study for understanding female meiosis and fertility.

In order to learn about female mammalian meiosis, different approaches have been taken. They go from the attempt to generate functional germ cells *in vitro* (reviewed in Hayashi and Saitou, 2014; Sun et al., 2014), to the organotypic culture of perinatal ovaries to study meiosis I (Morgan et al., 2015; Rinaldi et al., 2018), or to the techniques used for imaging oocytes during meiosis II (Zielinska and Schuh, 2018).

In our work, we mainly focused in the observation and quantification of oocytes in fetal, newborn and adult ovaries combining different techniques. We aimed to relate the developmental processes of the establishment of the oocyte pool, the cyst breakdown and the follicle formation with the checkpoint mechanisms surveilling the recombination and synapsis of the homologous chromosomes during prophase I.

5.1.1. Methods to count oocytes in fetal and adult ovaries

The quantification of oocytes in ovarian sections is a classical technique used to evaluate, for example, the effects of several mutations on the ovarian pool establishment and on fertility. Although the procedure is easy, the reported oocyte numbers vary a lot depending on the age or the strain of the analyzed animals, and the study (Myers et al., 2004; Pepling et al., 2010; Tilly, 2003).

The markers and techniques used to identify the oocytes are diverse. For the study of perinatal ovaries, the labeling of oocytes is usually done by immunofluorescence or immunohistochemistry marking the germ cell cytoplasmic markers DDX4 (MVH) (Song et al., 2016), STAT3 (Murphy et al., 2005) and c-KIT (Manova et al., 1990); or the nuclear marker GCNA (GCNA-1 and TRA98) (Carmell et al., 2016; Enders and May, 1994; McClellan et al., 2003). In the study of adult ovaries the oocyte detection is easier, the follicles can be counted with a simple hematoxylin based staining, or labeled with an immunohistochemistry against PCNA (Muskhelishvili et al., 2005).

In order to estimate the oocyte or follicle number, usually the ovary is cut at 6-8 µm thick and one every two to five sections are counted in the perinatal ovaries; and one every five to ten sections are counted in the adults (Tilly, 2003). Other techniques involve the counting of a single representative section with a posterior estimation related to the measuring of the volume (Pepling and Spradling, 2001); and the clearing treatment of the

ovaries to get confocal images allowing a software estimation of the number of the oocytes without sectioning the tissue (Malki et al., 2015; Rinaldi et al., 2018; Rinaldi et al., 2017b).

In this work, we tried to use cytometry techniques to simplify the tedious and time-consuming task of ovary processing, immunolabeling and manual counting. Unfortunately, any of the two different techniques performed, with either alive or immunostained fixed cells, it could not differentiate between the somatic cell population and the germ cells. Hence, it could not be used to estimate the number of oocytes. Maybe further testing in cytometry with other cell processing and labeling techniques would allow the success of this approach.

Instead, we sectioned all the ovaries at 7 µm and performed an immunofluorescence against DDX4 (MVH) in perinatal ovaries; and a PAS-Hematoxylin staining in the adult ovaries. We decided to count one every two sections in the perinatal ovaries in order to ensure an accurate estimation of the total oocyte number. We think that the number of oocytes should be estimated counting from one every two sections to one every five sections. This is because there is a high variability in the total oocyte number comparing different ovaries from the same age and genotype; the distribution of the oocytes in the ovary is not homogeneous, and the number of sections is low due to the small size of the ovaries (McClellan et al., 2003). In adult ovaries, we counted the oocytes with visible nuclei from one every five sections in order to avoid the overestimation of the big follicles. We decided not to multiply the number obtained by five since we think that the estimation could be correct for the small follicles but not for the larger ones (Hirshfield and Midgley, 1978).

5.1.2. The ovarian organotypic culture is a useful tool to study the oocyte death, cyst breakdown and follicle formation

The use of culture techniques allows the study of several biological processes, mostly using somatic cells. The culture of meiotic cells, though, is harder. For example, the culture of different types of stem cells and germ cells has been performed for years in order to attempt the reconstitution of gametogenesis from both males and females to obtain functional gametes. But so far the *in vitro* reconstitution of the entire process has not been possible to achieve through the culture of cells (Hayashi and Saitou, 2014; Sun et al., 2014).

Still, the use of *ex vivo* organ cultures has allowed the creation of procedures to the analysis of male and female gonad development. For example, in males, the culture of pups' testis fragments allowed the obtention of functional sperm (Sato et al., 2011). Similar to that, after doing a nuclear transfer from oocytes obtained through premeiotic cultured germ cells, healthy offspring has been achieved (Obata et al., 2002). Besides the creation of functional gametes, the *ex vivo* ovarian culture (Morgan et al., 2015; O'Brien et al., 2003; Rinaldi et al., 2018) has been used to evaluate the effects of some drugs in the development of the perinatal ovaries (Chen et al., 2007; Jefferson et al., 2006; Livera et al., 2008; Morgan et al., 2013; Rinaldi et al., 2017b; Trombly et al., 2009). Taking advantage of this technique, we validated the newborn ovarian culture for the study of the effects of two different

inhibitors in the perinatal oocyte death, cyst breakdown and follicle formation in *Chk2*$^{-/-}$ mutant mice (see 5.2.3).

Some considerations of this *ex vivo* culture technique are that the results obtained for the oocyte number counts cannot be compared with the ones obtained in the uncultured ovaries. First, because there is a delay of the ovarian development *in vitro*, showed by the equivalence in the different types of oocytes obtained after 5 days of culture compared with the uncultured ones at 3 dpp (see Fig. 4.9). And second, because there is a general reduction of the number of oocytes present in the cultured ovaries compared with the uncultured ones. This may reflect that culture conditions are not optimal for ovary development.

In conclusion, the use of *ex vivo* cultures is a simple technique that can be used, like in our work, to test the effect of different drugs in the perinatal ovaries. This allowed us to see the effects of the inhibition of the Notch pathway and CHK1, that otherwise, are very difficult to study through knockout mice, since the elimination of these proteins are embryonic lethal.

5.2. The role of CHK2 in the first meiotic division

One of the key processes of meiotic division takes place during prophase I, when the homologous chromosomes synapse and recombine in order to ensure the genetic variability of the offspring, but also to ensure the right alignment and segregation of the chromosomes in further stages of meiosis.

The effector kinase CHK2 plays a crucial role in the regulation of these events acting as a DDR checkpoint protein in several organisms. CHK2 role is attributed to the recombination checkpoint since its activation is dependent on the presence of DSBs, even the non-meiotic SPO11-independent ones (Bolcun-Filas et al., 2014, Rinaldi et al., 2017a).

5.2.1. CHK2 participates in the recombination checkpoint eliminating fetal oocytes

In order to analyze the dynamics of the DSB repair, we counted the number of γH2AX patches as a readout for unrepaired DSBs in WT and *Chk2*$^{-/-}$ oocytes. This marker has been widely used to evaluate the quantity of DSBs in meiotic cells in both males and females (Mahadevaiah et al., 2001; Rogakou et al., 1998). Remarkably, it has been reported that the number of γH2AX patches in oocytes at pachynema and diplonema is higher than the ones found in spermatocytes (Roig et al., 2004). Furthermore, in females the majority of these patches colocalize with RPA, another marker for DNA damage, while in males the colocalization is lower (Roig et al., 2004). These data suggest a delay in the DSB repair in oocytes compared to spermatocytes.

One of our objectives was to check if this delay in the DSB repair was related to the perinatal oocyte death and if it was mediated by the recombination checkpoint. Certainly, the observed increase in the number of γH2AX patches in *Chk2*$^{-/-}$ oocytes at pachynema and

early diplonema, suggests that CHK2 has a role in the recombination checkpoint triggering either the repair of the DSBs or the oocyte death. Moreover, the range of γH2AX patches is equivalent in both genotypes, suggesting that there is not an increased induction of DSBs in *Chk2*$^{-/-}$ female mice, as it was proven for males (Pacheco et al., 2015) This is important to consider, since in other mutants, like *Atm*$^{-/-}$ there is an increase of the number of DSBs in spermatocytes (Lange et al., 2011).

To assess if this increase in the number of *Chk2*$^{-/-}$ oocytes with more unrepaired DSBs is given by the lack of elimination of these oocytes, we quantify the total oocyte number in ovaries from 16 dpc to 23 dpc. Confirming our hypothesis, we found that the oocyte number was significantly higher in the mutants, but strikingly, only at 18 and 20 dpc. At 18 dpc the mutants had a two-fold increase in the number of oocytes compared to the controls, indicating that in WT ovaries, CHK2 is killing the oocytes between 17 and 18 dpc. At this time, the majority of the oocytes are at pachytene stage. This led us to confirm that CHK2 regulates the oocyte number by the activation of the pachytene checkpoint.

We know that the *Chk2* mutation does not interfere with the oocyte number prior to the pachytene checkpoint, since the numbers at 16 dpc were the same in both genotypes. We cannot explain why there is a 20% increase of oocytes from 16 dp to 18 dpc in the mutants, but it could be due to the high variability observed and the number of ovaries analyzed these two days. We cannot exclude that somehow, at this time, there are still oogonia that are dividing and can become oocytes.

Significantly, compared to WT, there is a reduction of the number of oocytes found in *Chk2*$^{-/-}$ ovaries at 20 dpc, suggesting that a mechanism independent of CHK2 is eliminating the oocytes, finally leveling the numbers to the WT ones at 21 dpc (2 dpp).

With all this information, we can confirm that the CHK2-dependent pachytene checkpoint eliminates half of the oocyte pool before birth in WT ovaries. In absence of CHK2, there is a CHK2-independent mechanism that is activated killing the oocytes after birth (Fig. 5.1).

5.2.2. CHK2 is dispensable for the cyst breakdown and follicle formation

Since we showed that the effector kinase CHK2 controls the oocyte number in fetal oocytes, and we know that the oocyte death is believed to be required for the cyst breakdown and the follicle formation (Pepling and Spradling, 2001), we wanted to find out if CHK2 was required for cyst breakdown and follicle formation. Analyzing the number and proportion of the different oocyte types in WT and mutant ovaries, we observed that there was a significant increase in the number of cysts and single oocytes in *Chk2*$^{-/-}$ females at 18 dpc, corresponding to a two-fold increase in the total number of oocytes. Nonetheless, we saw no differences in the percentage of oocyte types between both genotypes, suggesting that the regulation of the cyst breakdown and the follicle formation are both independent of CHK2 (Fig. 5.1).

In our counts, the maximum percentage of oocytes in cyst observed in both control and mutant ovaries was under 50% of the total oocytes. This could be explained by different reasons: one is given by the limitations of the technique used. Having in mind that cyst are 3D structures, and that we count 2D sections, this could lower the total number of cysts scored. Furthermore, there is a partial fragmentation of the cysts prior to meiosis, allowing the association of different cysts of unrelated progenitors (Lei and Spradling, 2013). This fragmentation narrows the bridges of cytoplasm connecting the oocytes, probably obstructing the scoring of cysts and over representing the individual oocyte. Another possible explanation is that there is a previous, CHK2-independent, oocyte death that breaks some cysts prior to 16 dpc. One possible candidate producing this early attrition could be related to the activation of LINE-1 elements (Hunter, 2017; Malki et al., 2014).

5.2.3. CHK1 compensates the absence of CHK2 regulating the number of oocytes *in vitro*

Since we found that there was a massive perinatal oocyte death even in absence of CHK2, we used an *ex vivo* culture to expose neonatal *Chk2*$^{-/-}$ ovaries to two different inhibitors of key proteins from two candidate pathways that could possibly contribute to this death.

After inhibiting the Notch pathway, known for its role regulating the cyst breakdown and follicle formation (Trombly et al., 2009; Xu and Gridley, 2013), we found no differences in the total oocyte number of the inhibited ovaries compared to the control ones. Nevertheless, the number of oocytes in follicles in the inhibited ovaries was two times lower than in the controls. This can be explained by the fact that the Notch signaling pathway regulates follicle formation, as previously reported *in vivo* and *in vitro* (Trombly et al., 2009; Xu and Gridley, 2013). Strikingly, it was reported that Notch is required for the cyst breakdown, but we did not observe an increase in the number or percentage of cysts in the inhibited *Chk2*$^{-/-}$ mutants.

On the other hand, after inhibiting CHK1, another effector kinase of the DDR, we observed an increase in the total number of oocytes, particularly in cysts and single oocytes. There was too a decrease in the number and percentage of oocytes in follicle, compared with the controls. These results show that CHK1 is regulating several aspects of oogenesis. First, CHK1 controls the oocyte number. Chk1 inhibition produces a rescue of the number of oocytes in absence of CHK2. Second, CHK1 regulates the cyst breakdown after birth. And third, just like Notch, CHK1 regulates the follicle formation. These data show that CHK1 has a role regulating the oocyte number in the *in vitro* cultured ovaries after birth, compensating the absence of CHK2. Furthermore, the lack of both proteins CHK1 and CHK2 produces an increase of cysts and a decrease of follicles, evidencing the role of the DDR pathway in the cyst breakdown and follicle formation (Fig. 5.1).

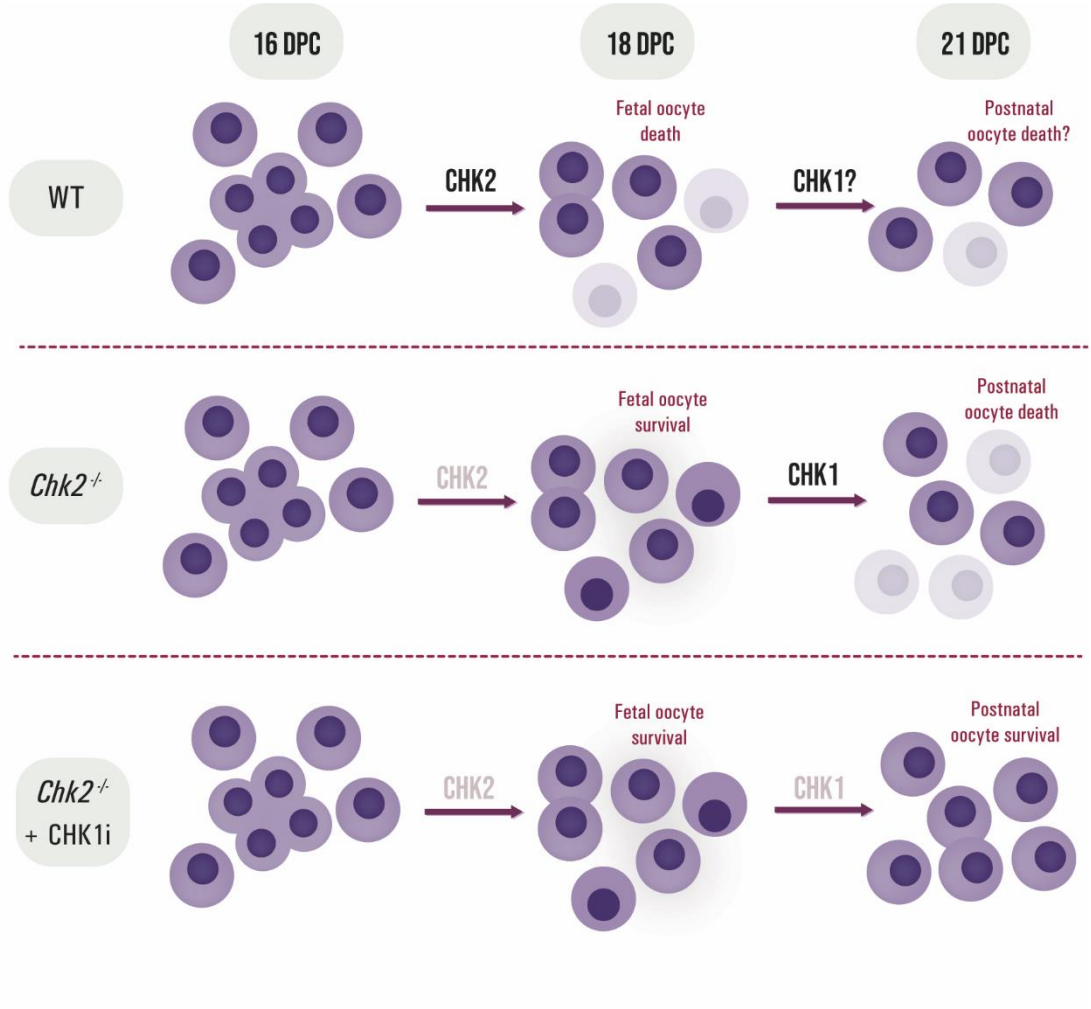

Figure 5.1 Dynamics of oocyte elimination in absence of CHK2 and inhibition of CHK1. In WT females (top panel), CHK2 triggers the oocyte death without regulating the cyst breakdown and follicle formation. In absence of CHK2 (middle panel) the oocytes surpass the fetal death, but they die later postnatally by the activation of CHK1. When CHK2 is absent and CHK1 inhibited, oocytes survive the postnatal death and decrease cyst breakdown and follicle formation.

5.2.4. CHK2 participates in the elimination of fetal oocytes in absence of SPO11-induced DSBs

As mentioned before, it has been recently reported that the CHK2-dependent recombination checkpoint can be activated also in absence of SPO11-induced DSBs (Rinaldi et al., 2017a). In that work they found a rescue of the young *Spo11*$^{-/-}$ depleted ovaries in absence of CHK2, even though the rescue was not to *Chk2*$^{-/-}$ levels, nor to WT levels. Before these results were published, we analyzed *Chk2*$^{-/-}$ *Spo11*$^{-/-}$ ovaries at 20 dpc (1 dpp) to test if CHK2 was involved in the elimination of DSB defective oocytes. We found that there was a partial rescue in the number of oocytes in the double mutants compared to the *Spo11*$^{-/-}$ single mutants. In the *Chk2*$^{-/-}$ *Spo11*$^{-/-}$ ovaries, though, the number of oocytes was lower than the one in *Chk2*$^{-/-}$ovaries, but it was statistically the same compared to the WT ones. The fact that these double mutants are unable to rescue the oocyte number to *Chk2*$^{-/-}$

numbers suggests the presence of another simultaneous perinatal mechanism eliminating Spo11$^{-/-}$ oocytes, probably sensing asynapsed chromosomes, independent of CHK2 (Burgoyne et al., 2009; Burgoyne and Baker, 1985).

Finding a partial rescue was unexpected since, classically, the loss of oocytes in the pachytene checkpoint was divided in two responses: one DNA damage-dependent and the other DNA damage-independent, determined by the differences in the ovarian phenotype of recombination- or synapsis- defective mutants (Di Giacomo et al., 2005). Thus, elimination of *Spo11*$^{-/-}$ oocytes was attributed to the activation of the DNA damage-independent response. Therefore, we did not expect that CHK2, which is only activated as a response to DNA damage, was responsible for the elimination of part of the *Spo11*$^{-/-}$ oocytes. The possible explanations for this rescue were postulated in Rinaldi et al., (2017a). If a recombination-checkpoint protein mutation is able to rescue the *Spo11*$^{-/-}$ oocytes, without SPO11-induced DSBs and with asynapsis, either CHK2 participates in both the recombination and the synapsis checkpoint, or somehow the *Spo11*$^{-/-}$ oocytes are eliminated due to the recombination checkpoint mediated by CHK2. They suggested that there is a DSB level that triggers the CHK2-dependent recombination checkpoint and the *Spo11*$^{-/-}$ oocytes are above this threshold. It is worth mentioning that other studies have reported the presence of DSBs of unknown origin in *Spo11*$^{-/-}$ oocytes at early pachynema (Carofiglio et al., 2013). It has been proposed that these SPO11-independent DSBs could be originated by the activation of the retrotransposon LINE-1 (Malki et al., 2014).

5.2.5. CHK2 rescues the cyst number in SPO11-deficient ovaries

We also analyzed cyst breakdown and follicle formation in *Spo11*$^{-/-}$ *Chk2*$^{-/-}$ ovaries. Double mutant, *Chk2*$^{-/-}$ and WT ovaries had the same number of cysts, significantly higher than the one found in *Spo11*$^{-/-}$ ovaries. Differently, the number of single oocytes and follicles in the double mutant was equivalent to the *Spo11*$^{-/-}$. The fact that the cysts are the only oocyte type rescued in the double mutant suggests that in absence of SPO11, the oocytes in cyst are the ones that are being eliminated by the CHK2-dependent checkpoint. Contrarily, the *Chk2*$^{-/-}$ ovaries contain the same number of oocytes in cyst as the WT, but an increase in the number of single oocytes. These results suggest that, in WT ovaries, the cysts are able to breakdown without dying, and that the single oocytes are the ones dying. This different response depending on the presence or absence of SPO11 shows different levels of regulation depending on the presence or absence of meiotic-induced DSBs.

5.2.6. The model of oocyte death

Taking into account the data presented here, and together with the published data, we would like to propose a model for the perinatal elimination of oocytes in female mammals. In this study, we found two response pathways responsible for the elimination of oocytes with high number of unrepaired DSBs: a CHK2-dependent pathway, detecting

and eliminating fetal oocytes with high unrepaired DSBs or recombination intermediates; and a CHK2-independent pathway, possibly eliminating oocytes with asynapsis. In absence of CHK2, a CHK1-dependent mechanism sensing unrepaired DSBs is responsible of the elimination of oocytes after birth.

The presence of an early oocyte attrition (EOA) and a late oocyte attrition (LOA) mechanisms have been proposed before (reviewed in Hunter et al., 2017). EOA is related with the activation of LINE-1 transposons, that would eliminate the early meiotic prophase oocytes in fetal ovaries (Malki et al., 2014). LOA would eliminate postnatally the oocytes with meiotic errors at prophase I, the ones with recombination failure in a DNA-damage-dependent checkpoint, and the ones with synapsis failure in a DNA-damage-independent checkpoint (Bolcun-Filas et al., 2014; Burgoyne and Baker, 1985; Cloutier et al., 2015; Di Giacomo et al., 2005).

Combining this information with our data, we propose that the CHK2-dependent checkpoint responds to the activation of LINE-1, belonging both to the same pathway in the EOA mechanism. LINE-1 (L1) is an autonomous retroelement and its transcripts are exported from the nucleus and translated. ORF1 and ORF2 proteins bind to the mRNA assembling ribonucleoprotein complexes, which enter the nucleus and mediate transposition. The endonuclease activity of ORF2 can generate DSBs and L1 expression is associated with the activation of the DNA-damage response (Hunter, 2018). Accordingly, the activity of L1 could generate the SPO11-independent DSBs triggering the CHK2-dependent response in the fetal ovaries of WT and *Spo11*$^{-/-}$ mice and causing the massive oocyte elimination around 17 dpc (Fig. 5.2). The timing of death and the oocyte numbers found in Malki et al., 2014 using a retrotransposon inhibitor, fits our data with the *Chk2* mutants, with an increase in the oocyte number in the fetal period and the posterior reduction after birth. However, as mentioned before, different mice backgrounds and oocyte counts can yield different results that cannot be compared. In order to know if these two pathways are related, further experiments are required. This CHK2-dependent checkpoint is activated in fetal oocytes in response to DSBs, eliminating presumably the oocytes with higher unrepaired DSBs or recombination intermediates. Moreover, the EOA is also triggered by a CHK2-independent mechanism, probably sensing synapsis errors, as seen by the lack of a complete rescue in newborn *Spo11*$^{-/-}$ *Chk2*$^{-/-}$ ovaries (Fig. 5.2). This checkpoint has been related to HORMAD proteins sensing asynapsis and triggering oocyte death mediated by the MSUC (Fig. 5.2). The presence of asynapsed axes containing HORMAD1/2 triggers the recruitment of other proteins like BRCA1, ATR and γH2AFX at these axes. The accumulation of these proteins may produce a transcriptional silence of genes required for the survival of the oocyte, triggering their death (Cloutier et al., 2015).

The LOA would be triggered after birth by a CHK2-independent checkpoint. It is possible that CHK1 would regulate this death, even though we only found evidences of a CHK1-dependent oocyte elimination in absence of CHK2 (Fig. 5.2). Furthermore, it was discovered recently that the protein RNF212 is a SUMO ligase required for CO formation that also promotes oocyte apoptosis at late prophase I. RNF212 promotes reloading of HORMADs in the axes at diplonema, and the authors propose that this reloading impede

the DSB repair due to the IH bias, that inhibits the repair with the sister chromatid (Qiao et al., 2018). The persistence of recombination intermediates could also ultimately activate a CHK1-dependent elimination (Fig. 5.2).

The fact that in mammals, recombination and synapsis of the homologous chromosomes are two very close and related events makes more difficult their study, especially, with the available mouse models in which, for example, the absence of recombination produces synapsis errors. This difficulty in the study is enhanced in females by the fact that the meiotic prophase I occurs only once in the perinatal period, and in normal conditions there is a massive oocyte death that could work as a selection for the best oocytes to survive. Hence the mechanisms regulating this death have to go through a high number of oocytes in a short time period and ensure the best possible outcome. As showed, the regulation of the perinatal oocyte population is a high regulated and complex process with its own special features and with still a lot of questions to be answered.

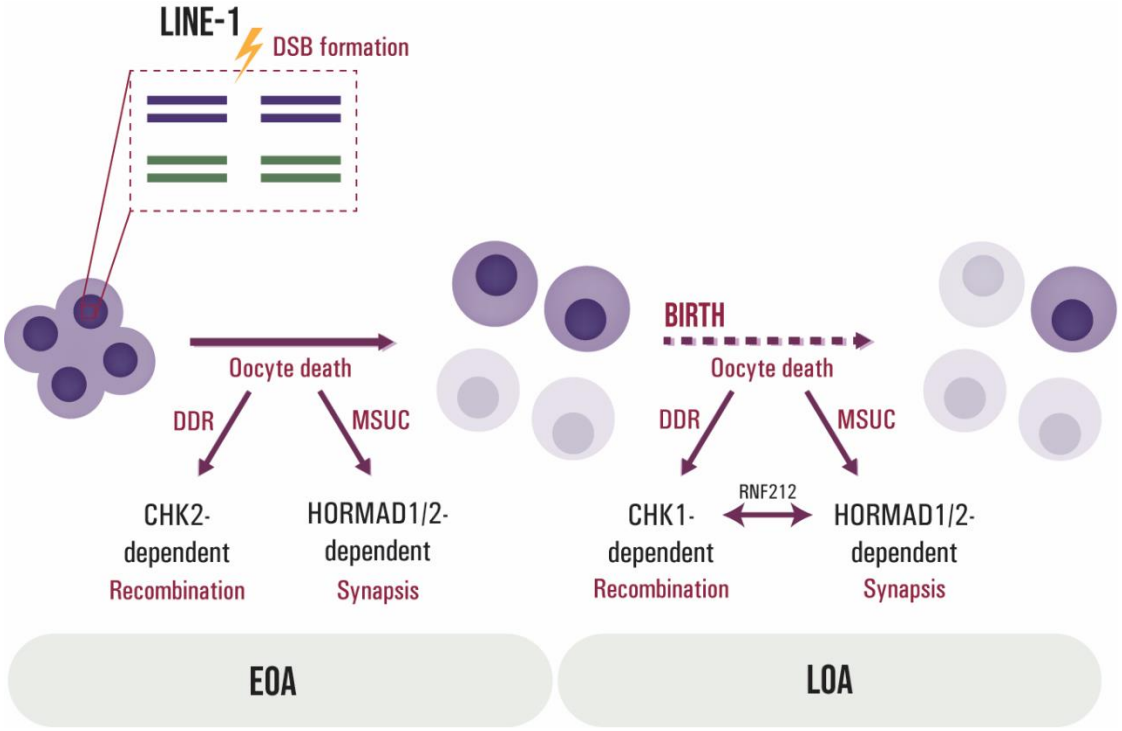

Figure 5.2 Model of oocyte elimination. LINE-1 induces DSBs that would ensure the activation of the CHK2-dependent checkpoint mediated by the DDR, eliminating a high number of oocytes before birth. In addition to this recombination checkpoint, there would be also a CHK2-independent mechanism sensing asynapsed fetal oocytes. After birth the LOA is activated, eliminating oocytes with recombination and synapsis defects, mediated probably by CHK1, RNF212 and HORMADs.

5.3. The role of CHK2 in adult ovaries

After discovering that CHK2 controls the fetal oocyte population, we wanted to check if this DDR checkpoint protein was also involved in the elimination of oocytes in adult females, hence, in dormant and growing follicles. Counting the oocytes present in ovaries of young 40 dpp and elder 400 dpp, WT and *Chk2*$^{-/-}$ females, we found that at young age, the oocyte number is equivalent in both genotypes, but it is three times higher in the mutants at elder age. This difference is significant for all the follicle types, showing that the role of CHK2 does not involve only the elimination of recruited follicles, but it is also eliminating the resting primordial follicles. One of the special features in the oogenesis is that the oocytes block at dictyate stage perinatally and remain quiescent until they are recruited to grow and resume meiosis. This means that the oocytes recruited at elder ages have been blocked for most of the female life. We propose that during this long dormant state, the oocytes are vulnerable, accumulating progressively DNA damage that triggers their elimination by a CHK2-dependent mechanism. Accordingly, the absence of CHK2 should produce an increase in the oocyte number, but these oocytes should present more DNA damage compared to the WT ones.

The finding of this increase of oocytes in elder mutant females led us to study if this higher oocyte number would translate into an increase of the fertility, having more offspring, or into a longer reproductive lifespan. After setting up several matings in cages with control and *Chk2*$^{-/-}$ females with males of proven fertility, we observed that there was no evidence of an increase in fertility during 18 months of life of the females. Moreover, we tried to find if there was an increase in the reproductive lifespan, but the advanced age of the females that were breeding made the study very difficult. They had a lot of physical difficulties to get pregnant and for deliver the pups, like uterus prolapse or even death at delivery, which resulted in a reduced sample size that impeded reaching firm conclusions.

The rescued *Chk2*$^{-/-}$ oocytes could present DNA damage, which could involve an increase in aneuploidies, leading, possibly, to embryo failure after the oocyte is fertilized. Moreover, there is an increase of MOFs in Chk2$^{-/-}$ elder mice. The oocyte in those MOFs have been prove to be less fertile (Iguchi et al., 1991), which would produce decrease in the success in fertilization and even problems in embryo development.

To solve this, in collaboration with the group of Dr. Anna Pujol (CBATEG-UAB), we performed an IVF on WT and *Chk2*$^{-/-}$ 15-17-month-old mice in order to check the efficiency of fertilization and blastocyst formation. According to our previous results, the number of oocytes collected after ovarian stimulation was higher in the mutants than in the WT; the fertilization rates (obtainment of 2-cell embryos) were also higher in the mutants compared to the WT; but oppositely, the percentage of embryos developing intro blastocysts was higher in the WT, with all of the 2-cell embryo progressing to blastocyst (Fig. 5.3). These data suggest that, indeed, the mutant oocytes are less able to develop into a blastocyst than the WT ones, most likely because they accumulate some sort of unrepaired DNA damage.

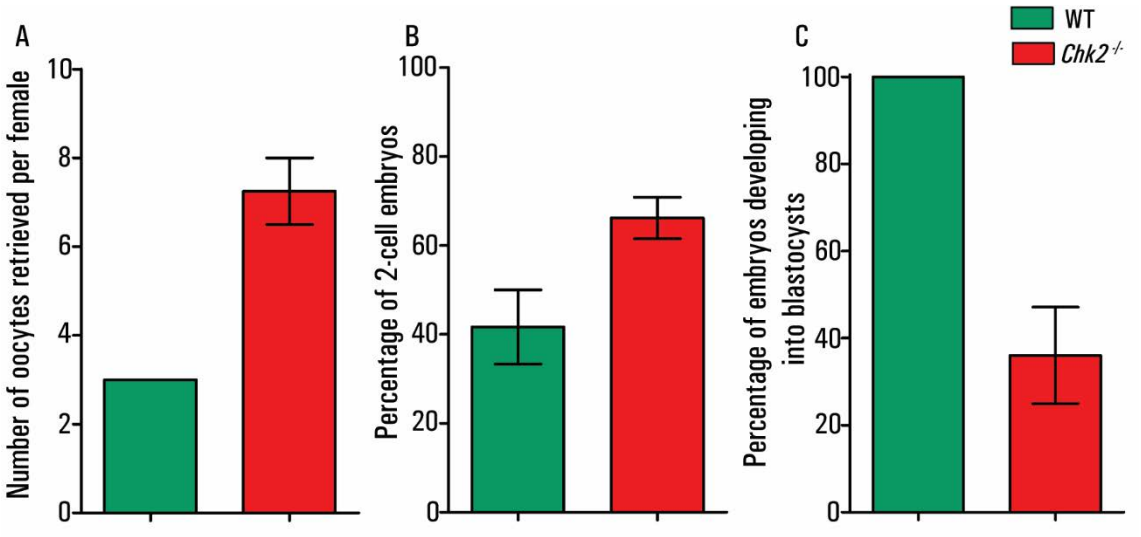

Figure 5.3 After IVF, *Chk2*$^{-/-}$ elder females have a low percentage of embryos developing into blastocysts. A) Number of oocytes retrieved per female in *Chk2*$^{-/-}$ and WT elder mice. **B)** Percentage of 2-cell embryos. **C)** Percentage of embryos developing into blastocysts. The lines represent the mean ± SEM.

Taking all this information in mice, it would be interesting to check the possible applications of these data in humans. At the end of the reproductive lifespan, and as a consequence of the follicle pool exhaustion, women go through menopause. The low number of oocytes at elder age produce a decrease of the ovarian negative feedback on FSH, increasing the levels of that hormone, accelerating the recruitment and the consequent follicular loss resulting in the decline of the estrogen levels. These changes involve several physical symptoms and affections, for example vasomotor alterations, genitourinary affections, cardiovascular diseases, osteoporosis or other conditions like depression (Takahashi and Johnson, 2015). Women with an abnormally low pool of follicles will reach menopause at an early age, going through these alterations prematurely. Thus, an increase of the follicle pool in women would be very interesting for extending their reproductive lifespan and delaying menopause onset. The establishment of the timing of menopause age has been related with variations in proteins of the DDR, including CHK2, among others. (Day et al., 2015)

In that direction, the study of the function of proteins like CHK2 is very interesting due to their potential to be used as a therapeutic target of pharmacological drugs. For example, in the above-mentioned menopause, the inhibition of CHK2 could presumably result in an increase of the follicle pool, delaying menopause onset. Similar to that, the use of chemotherapeutics and other treatments in cancer patients decreases the oocyte pool causing a reduction of the reproductive lifespan, even in young women. Already in the first investigations using *Chk2*$^{-/-}$ mice, it was evident that their cells exhibit a resistance to ionizing radiation, avoiding the apoptosis even in presence of DNA damage that normally would be fatal (Takai et al., 2002). Hence, taking advantage of that information, the use of drugs that inhibit or activate CHK2 and other DDR pathway proteins have been the focus of study to

either try to preserve the ovarian reserve, or in an opposite but related function, to try to kill cancer cells. The existence of different tumors, ones that express functional CHK2, and others that present a decrease or lack of CHK2 function, allows the potential use of inhibitors or activators of DDR proteins, depending on the tumor type, to eliminate it. Nonetheless, there is still a lot of steps to be done in order to benefit cancer patients with this therapy (Antoni et al., 2007; Bartek and Lukas, 2003; Chen et al., 2012; King et al., 2014; Tao and Lin, 2006). Regarding the fertility preservation, studies with some mice mutants for p63 or PUMA (a pro-apoptotic protein member of the BCL-2 family) showed a protection of the ovarian reserve after irradiation or chemotherapeutic treatments (Livera et al., 2008; Nguyen et al., 2018). Similarly, the use of pharmacological inhibitors, like the ones targeting CHK2 and TAp63 also protects the ovarian follicle pool after radiation or chemotherapeutics (Gonfloni et al., 2009; Morgan et al., 2013; Rinaldi et al., 2017b). As with the cancer potential treatments, the use of these inhibitors for avoiding the loss of oocytes has a lot of potential, but it has to be further tested in different conditions, and in a future, with humans. Even though, our data suggest that these oocytes may accumulate DNA damage and won't be able to develop into a healthy embryo. Another alternative to the inhibition treatment for the restoration of fertility is the use of printed 3D ovarian scaffolds that allows the follicle survival in surgically sterilized mice (Laronda et al., 2017).

5.4. The role of TRIP13 in the synapsis checkpoint

In order to know if TRIP13 is participating in the elimination of oocytes as a consequence of the synapsis checkpoint activation, we checked if TRIP13 is necessary for the elimination of oocytes from *Spo11*$^{-/-}$ and *Dmc1*$^{-/-}$ *Chk2*$^{-/-}$ ovaries.

Due to the absence of SPO11-induced DSBs, the *Spo11*$^{-/-}$ mutant has been widely used to study the oocyte death triggered by asynapsis problems. In that direction, we hypothesized that if TRIP13 participates in this synapsis checkpoint, in absence of both SPO11 and TRIP13 proteins, there should be a rescue of the number of oocytes. It was reported previously that this rescue was not effective, with the double mutant ovaries being the same as the *Spo11*$^{-/-}$ single mutants, but without actual quantification of the follicle population (Li and Schimenti, 2007). Confirming these results, we found no differences in the oocyte number nor in the number of follicle types between both genotypes.

Going one step further, we wanted to check the oocyte number in the *Dmc1*$^{-/-}$ *Chk2*$^{-/-}$ *Trip13*$^{mod/mod}$ triple mutants. *Dmc1*$^{-/-}$ single mutant oocytes are unable to recombine, leading to a total oocyte depletion due to the activation of the recombination checkpoint (Di Giacomo et al., 2005; Pittman et al., 1998). By removing CHK2 in these mutants, the defective oocytes can skip the CHK2-dependent recombination checkpoint, with one fraction of them escaping death and surviving. The rescue is not complete, probably because the surviving oocytes die at the recombination-independent checkpoint most likely due to synapsis problems (Bolcun-Filas et al., 2014). Thus, if TRIP13 participates in this synapsis checkpoint, its absence should be able to rescue the *Dmc1*$^{-/-}$ *Chk2*$^{-/-}$ ovaries to a higher

extent. Contradicting the results with the *Spo11*$^{-/-}$ *Trip13*$^{mod/mod}$ mutants, we found a rescue of the oocyte number, reflected by the increase of primordial and primary follicles. This rescue shows that TRIP13 eliminates the oocytes with synaptic defects, but only in presence of SPO11-induced DSBs.

We postulate two possible explanations for this rescue. First, is possible that TRIP13 participates in the synapsis checkpoint, but requires the presence of SPO11-induced DNA damage. The formation of hundreds of DSBs all over the genome would activate a global response that could activate TRIP13 function. This is supported by the fact that TRIP13 has an evolutionary conserved S/T-Q domain, which is a target for the ATM/ATR effector kinases of the DDR (Data not shown, AM and IR). Additionally, it is known that TRIP13, besides its function in recombination, is required in males for sex body formation in the MSCI (Marcet-Ortega et al., 2017; Pacheco et al., 2015). This mechanism triggers death in spermatocytes with asynapsis problems or sex body defects and has been associated to synapsis checkpoint activation in oocytes (Cloutier et al., 2015; Turner, 2007). Also, comparing our results with the ones obtained in *Dmc1*$^{-/-}$ *Chk2*$^{-/-}$ *Hormad2*$^{-/-}$ ovaries, they were very similar, showing a rescue of the *Dmc1*$^{-/-}$ *Chk2*$^{-/-}$ oocytes (Rinaldi et al., 2017a). HORMAD proteins participate in the elimination of oocytes in the synapsis checkpoint, proven by the rescue in the triple mutant, and by fact that the absence of either HORMAD1 or HORMAD2 produces an oocyte rescue in the *Spo11*$^{-/-}$ ovaries (Daniel et al., 2011; Kogo et al., 2012b, 2012a; Wojtasz et al., 2012). Furthermore, supporting their role in synapsis, HORMADs are present on unsynapsed axes and participates in the MSCI and transcriptional silencing sensing asynapsis and promoting the loading of γH2AX, ATR and BRCA1 (Shin et al., 2010; Wojtasz et al., 2009a). HORMAD1/2 are depleted from the chromosomal axes by TRIP13 at the time that the homologous chromosome synapse. Hence, the oocytes from *Hormad1/2* mutants present no protein on the axes, while the oocytes from *Trip13*$^{mod/mod}$ are not able to remove HORMADs from the axes, having these proteins remaining in the synapsed chromosomes (Wojtasz et al., 2009a). As explained in the introduction, the presence of HORMAD1/2 on the axes regulates the interhomolog bias, inhibiting the intersister recombination. In absence of HORMAD1/2, the DSBs that normally trigger the checkpoint in the *Spo11*$^{-/-}$ would be repaired by intersister recombination, saving those oocytes from the death and producing the rescue of the double mutants (Rinaldi et., al 2017a). Another similar case we found it in the *Hormad2*$^{-/-}$ *Trip13*$^{mod/mod}$ double mutant, with a partial rescue of the follicles as well as a rescue in the fertility. In these ovaries the absence of HORMAD2 would reduce the DSBs allowing the surpassing of the checkpoint and the posterior repair of the remaining oocytes (Rinaldi et., al 2017a). Hence, TRIP13 has similar and overlapping functions with HORMADs supporting its participation in the synapsis checkpoint.

Looking in other species, like *Saccharomyces cerevisiae,* TRIP13 ortholog Pch2 has a demonstrated role in the synapsis checkpoint, suggesting that this function could be conserved in mammals. Pch2 localizes to synapsed chromosomes and to the unsynapsed rDNA region in the nucleolus. The PCH2 null mutant in yeast present no obvious phenotype, with the same sporulation efficiency and only a subtle decrease in spore viability compared to the WT (San-Segundo and Roeder, 1999). On the contrary, the mutation of the

synaptonemal complex protein Zip1 causes a pachytene arrest due to synapsis defects (Sym et al., 1993). Showing the checkpoint function of Pch2, the lack of this protein in the Zip1 mutant abolishes the meiotic arrest by synapsis defects. Moreover, Pch2 repress the IH recombination in the ribosomal DNA by excluding Hop1 from the nucleolus (San-Segundo and Roeder, 1999)

Alternatively, the inability of TRIP13 to rescue the *Spo11*$^{-/-}$ oocytes, questions its participation in the synapsis checkpoint. For that reason, we present a second hypothesis to explain the triple mutant oocyte rescue. TRIP13 could participate in the DSB repair pathway choice, inhibiting NHEJ and enhancing HR. In the *Dmc1*$^{-/-}$ *Chk2*$^{-/-}$ mutant, there is a small rescue of oocytes, but they are far from having WT or *Chk2*$^{-/-}$ oocyte numbers. We described that in the absence of CHK2, there is a CHK1-dependent oocyte elimination after birth, which could be responsible of this poor rescue in the double mutant. If TRIP13 participates in the repair pathway choice, and not in the synapsis checkpoint, it would be able to repair most of the DSBs, which cannot be repair by meiotic recombination in absence of DMC1, by NHEJ. Hence, the CHK1-dependent checkpoint would not be activated, rescuing most of the oocytes, as we saw. This hypothesis would explain the death of *Spo11*$^{-/-}$ *Trip13*$^{mod/mod}$ oocytes by asynapsis problems. There are some evidences of this function in somatic cells supporting this hypothesis. TRIP13 remodels HORMA-domain proteins, like MAD2 or HORMAD1. Recently, it was found that the shieldin complex, containing SHLD1, SHLD2, SHLD3 and the HORMA-domain REV7, protects DSBs from extensive resection preventing them from being repaired by HR and promoting NHEJ (Ghezraoui et al., 2018; Gupta et al., 2018; Mirman et al., 2018; Noordermeer et al., 2018). REV7 interacts with p31^{COMET}, which is required by TRIP13 to switch the conformation of MAD2, the HORMA-domain spindle assembly checkpoint protein (Alfieri et al., 2018; Rizzo et al., 2018; Ye et al., 2015). Therefore, it is possible that TRIP13 function in the repair pathway choice could be mediated by the remodeling of REV7.

Summarizing, with this work we were able to contribute to the knowledge of the checkpoint functions in mammalian females. We evidenced that there is not a straight answer to the multiple doubts that have been created through the years about the functioning of the recombination and synapsis checkpoint eliminating abnormal oocytes. We were able to unravel some of the mechanisms mediated by CHK1, CHK2 and TRIP13 in the regulation of the oocyte number in perinatal and adult ovaries. Nonetheless, several questions still remain unanswered, like the overlapping or independence of these mechanisms.

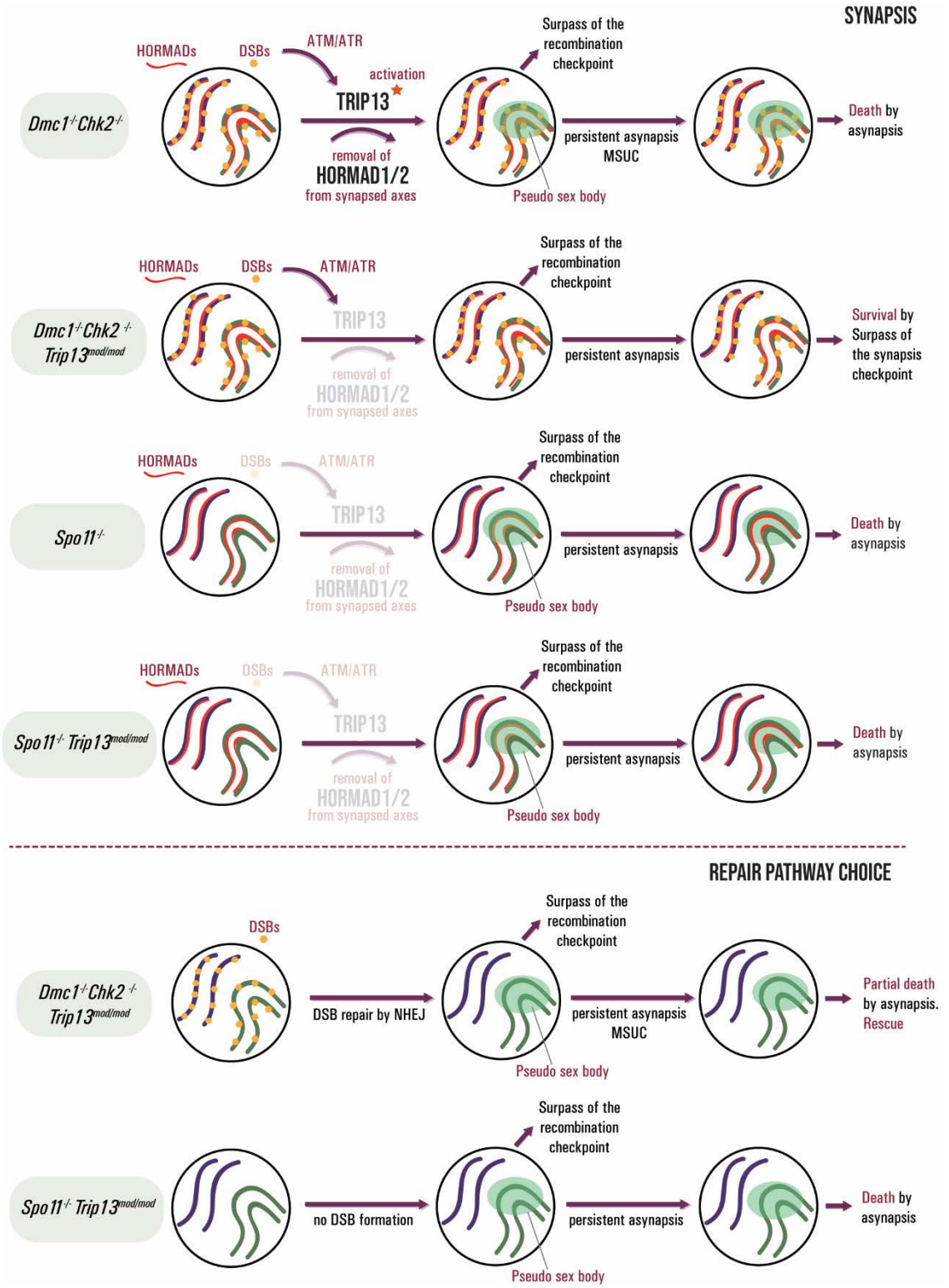

Figure 5.4 Models showing the two possible functions of TRIP13 eliminating oocytes. We postulated two different models explaining the oocyte loss in different mutants. In the mechanism sensing asynapsis (top panel), TRIP13 would be activated in presence of DSBs (*Dmc1*$^{-/-}$ *Chk2*$^{-/-}$), killing the asynapsed oocytes. In absence of TRIP13 (*Dmc1*$^{-/-}$ *Chk2*$^{-/-}$ *Trip13*$^{mod/mod}$), the pseudo sex body cannot be formed and the MSUC cannot be activated, producing a rescue of the oocytes. In absence of SPO11 (*Spo11*$^{-/-}$ *and Spo11*$^{-/-}$ *Trip13*$^{mod/mod}$), hence in absence of DSBs, TRIP13 is not activated and the oocytes die by asynapsis due to the MSUC. If TRIP13 is involved in the repair pathway choice (bottom panel), it would promote the NHEJ repair. In presence of unrepaired DSBs that are not able to be repaired by HR (*Dmc1*$^{-/-}$ *Chk2*$^{-/-}$ *Trip13*$^{mod/mod}$), the absence of TRIP13 would allow the repair by NHEJ, resulting in a partial rescue, with some oocytes dying by asynapsis. In absence of DSBs (*Spo11*$^{-/-}$ *Trip13*$^{mod/mod}$) a normal synapsis checkpoint would be activated, even in absence of TRIP13.

CONCLUSIONS

Chapter 6

1. The lack of CHK2 in mouse ovaries produces an increase in the number of unrepaired DSBs at late pachynema and early diplonema oocytes. At late diplonema, though, the number of DSBs present in *Chk2*$^{-/-}$ oocytes are equivalent to a WT.

2. Cell cytometry is not a reliable technique for separate and count oocytes from perinatal ovaries.

3. CHK2 regulates the oocyte population in fetal ovaries, eliminating approximately half of the oocyte pool just before birth.

4. The CHK2-dependent checkpoint eliminates oocytes lacking SPO11-induced DSBs.

5. CHK2 is dispensable for the correct timing of cyst breakdown and follicle formation, but it is necessary for cyst breakdown in the absence of SPO11.

6. The use of ex vivo ovary cultures is a valid model to study the perinatal oocyte death, the cyst breakdown and the follicle formation.

7. The Notch signaling pathway does not regulate the oocyte loss in perinatal mice, but it regulates the follicle formation.

8. CHK1 eliminates the oocytes after birth in absence of CHK2. It also regulates the cyst breakdown and follicle formation.

9. CHK2 eliminates primordial follicles during adulthood.

10. CHK2 is dispensable for fertility, but in its absence, the oocytes from elder females are less able to develop into blastocysts after fertilization.

11. The absence of TRIP13 does not rescue *Spo11*$^{-/-}$ ovaries, but it rescues *Dmc1*$^{-/-}$ *Chk2*$^{-/-}$ ovaries, suggesting a role in the elimination of oocytes with synaptic defects and unrepaired DSBs

REFERENCES

Chapter 7

Abe, H., Alavattam, K.G., Kato, Y., Castrillon, D.H., Pang, Q., Andreassen, P.R., Namekawa, S.H., 2018. CHEK1 coordinates DNA damage signaling and meiotic progression in the male germline of mice. Hum. Mol. Genet. 27 (7), 1136–1149. https://doi.org/10.1093/hmg/ddy022

Abreu, C.M., Prakash, R., Romanienko, P.J., Roig, I., Keeney, S., Jasin, M., 2018. Shu complex SWS1-SWSAP1 promotes early steps in mouse meiotic recombination. Nat. Commun. 9, 3961. https://doi.org/10.1038/s41467-018-06384-x

Alfieri, C., Chang, L., Barford, D., 2018. Mechanism for remodelling of the cell cycle checkpoint protein MAD2 by the ATPase TRIP13. Nature 559, 274–278. https://doi.org/10.1038/s41586-018-0281-1

Antoni, L., Sodha, N., Collins, I., Garrett, M.D., 2007. CHK2 kinase: cancer susceptibility and cancer therapy - two sides of the same coin? Nat. Rev. Cancer 7, 925–936. https://doi.org/10.1038/nrc2251

Baarends, W.M., Wassenaar, E., van der Laan, R., Hoogerbrugge, J., Sleddens-Linkels, E., Hoeijmakers, J.H.J., de Boer, P., Grootegoed, J.A., 2005. Silencing of Unpaired Chromatin and Histone H2A Ubiquitination in Mammalian Meiosis. Mol. Cell. Biol. 25 (3), 1041–1053. https://doi.org/10.1128/MCB.25.3.1041-1053.2005

Bailis, J.M., Smith, A. V, Roeder, G.S., 2000. Bypass of a Neiotic Checkpoint by Overproduction of Meiotic Chromosomal Proteins. Mol. Cell. Biol. 20, 4838–4848. https://doi.org/10.1128/MCB.20.13.4838-4848.2000

Baker, S.M., Plug, A.W., Prolla, T.A., Bronner, C.E., Harris, A.C., Yao, X., Christie, D.M., Monell, C., Arnheim, N., Bradley, A., Ashley, T., Liskay, R.M., 1996. Involvement of mouse *Mlh1* in DNA mismatch repair and meiotic crossing over. Nat. Genet. 13, 336–342. https://doi.org/10.1038/ng0796-336

Baker, T.G., 1971. Comparative aspects of the effects of radiation during oogenesis. Mutat. Res. Mol. Mech. Mutagen. 11 (1), 9–22. https://doi.org/10.1016/0027-5107(71)90028-5

Banin, S., Moyal, L., Shieh, S., Taya, Y., Anderson, C.W., Chessa, L., Smorodinsky, N.I., Prives, C., Reiss, Y., Shiloh, Y., Ziv, Y., 1998. Enhanced Phosphorylation of p53 by ATM in Response to DNA Damage. Science 281 (5383), 1674–1677. https://doi.org/10.1126/SCIENCE.281.5383.1674

Barchi, M., Mahadevaiah, S., Di Giacomo, M., Baudat, F., de Rooij, D.G., Burgoyne, P.S., Jasin, M., Keeney, S., 2005. Surveillance of Different Recombination Defects in Mouse Spermatocytes Yields Distinct Responses Despite Elimination at an Identical Developmental Stage. Mol. Cell. Biol. 25 (16), 7203–7215. https://doi.org/10.1128/MCB.25.16.7203-7215.2005

Barlow, C., Brown, K.D., Deng, C.X., Tagle, D.A., Wynshaw-Boris, A., 1997. Atm selectively regulates distinct p53-dependent cell-cycle checkpoint and apoptotic pathways. Nat. Genet. 17, 453–456. https://doi.org/10.1038/ng1297-453

Barlow, C., Hirotsune, S., Paylor, R., Liyanage, M., Eckhaus, M., Collins, F., Shiloh, Y., Crawley, J.N., Ried, T., Tagle, D., Wynshaw-Boris, A., 1996. Atm-Deficient Mice: A Paradigm of Ataxia Telangiectasia. Cell 86 (1), 159–171. https://doi.org/10.1016/S0092-8674(00)80086-0

Barlow, C., Liyanage, M., Moens, P.B., Tarsounas, M., Nagashima, K., Brown, K., Rottinghaus, S., Jackson, S.P., Tagle, D., Ried, T., Wynshaw-Boris, A., 1998. Atm deficiency results in severe meiotic disruption as early as leptonema of

prophase I. Development 125 (20), 4007–4017.

Bartek, J., Lukas, J., 2003. Chk1 and Chk2 kinases in checkpoint control and cancer. Cancer Cell 3 (5) 421–429. https://doi.org/10.1016/S1535-6108(03)00110-7

Bartek, J., Lukas, J., 2001. Mammalian G1-and S-phase checkpoints in response to DNA damage 739 738–747. Curr. Opin. Cell Biol. 13 (6) 738-747. https://doi.org/10.1016/S0955-0674(00)00280-5

Baudat, F., de Massy, B., 2007. Regulating double-stranded DNA break repair towards crossover or non-crossover during mammalian meiosis. Chromosom. Res. 15 (5), 565–577. https://doi.org/10.1007/s10577-007-1140-3

Baudat, F., Imai, Y., Massy, B. De, 2013. Meiotic recombination in mammals: localization and regulation. Nat. Rev. Genet. 14, 794–806. https://doi.org/10.1038/nrg3573

Baudat, F., Manova, K., Yuen, J.P., Jasin, M., Keeney, S., 2000. Chromosome Synapsis Defects and Sexually Dimorphic Meiotic Progression in Mice Lacking Spo11. Mol. Cell 6 (5), 989–998. https://doi.org/10.1016/S1097-2765(00)00098-8

Belgnaoui, S.M., Gosden, R.G., Semmes, O.J., Haoudi, A., 2006. Human LINE-1 retrotransposon induces DNA damage and apoptosis in cancer cells. Cancer Cell Int. 6, 13. https://doi.org/10.1186/1475-2867-6-13

Bellani, M.A., Romanienko, P.J., Cairatti, D.A., Camerini-Otero, R.D., 2005. SPO11 is required for sex-body formation, and Spo11 heterozygosity rescues the prophase arrest of $Atm^{-/-}$ spermatocytes. J. Cell Sci. 118, 3233–3245. https://doi.org/10.1242/jcs.02466

Bhalla, N., Dernburg, A.F., 2005. A Conserved Checkpoint Monitors Chromosome Synapsis in *Caenorhabditis elegans*. Science 310 (5754), 1683–1686. https://doi.org/10.1126/science.1117468

Boekhout, M., Karasu, M.E., Wang, J., Acquaviva, L., Pratto, F., Brick, K., Eng, D.Y., Xu, J., Camerini-Otero, R.D., Patel, D.J., Keeney, S., 2019. REC114 Partner ANKRD31 Controls Number, Timing, and Location of Meiotic DNA Breaks. Mol. Cell. https://doi.org/10.1016/J.MOLCEL.2019.03.023

Bogdanov, Y.F., Grishaeva, T.M., Dadashev, S.Y., 2007. Similarity of the Domain Structure of Proteins as a Basis for the Conservation of Meiosis. Int. Rev. Cytol. 257, 83–142. https://doi.org/10.1016/S0074-7696(07)57003-8

Bolcun-Filas, E., Rinaldi, V.D., White, M.E., Schimenti, J.C., 2014. Reversal of Female Infertility by *Chk2* Ablation Reveals the Oocyte DNA Damage Checkpoint Pathway. Science 343 (6170), 533–536. https://doi.org/10.1126/science.1247671

Borum, K., 1961. Oogenesis in the mouse: A study of the meiòtic prophase. Exp. Cell Res. 24 (3), 495–507. https://doi.org/10.1016/0014-4827(61)90449-9

Bowles, J., Koopman, P., 2013. Precious cargo: Regulation of sex-Specific Germ Cell Development in Mice. Sex. Dev. 7, 46–60. https://doi.org/10.1159/000342072

Bowles, J., Koopman, P., 2007. Retinoic acid, meiosis and germ cell fate in mammals. Development 134, 3401–3411. https://doi.org/10.1242/dev.001107

Bray, S.J., 2006. Notch signalling: a simple pathway becomes complex. Nat. Rev. Mol. Cell Biol. 7, 678–689. https://doi.org/10.1038/nrm2009

Brown, E.J., Baltimore, D., 2000. ATR disruption leads to chromosomal

fragmentation and early embryonic lethality. Genes Dev. 14 (4), 397–402.

Bullejos, M., Koopman, P., 2004. Germ cells enter meiosis in a rostro-caudal wave during development of the mouse ovary. Mol. Reprod. Dev. 68 (4), 422–428. https://doi.org/10.1002/mrd.20105

Byskov, A.G., Guoliang, X., Andersen, C.Y., 1997. The cortex-medulla oocyte growth pattern is organized during fetal life: an in-vitro study of the mouse ovary. Mol. Hum. Reprod. 3 (9), 795–800.

Callender, T.L., Hollingsworth, N.M., 2010. Mek1 Suppression of Meiotic Double-Strand Break Repair Is Specific to Sister Chromatids, Chromosome Autonomous and Independent of Rec8 Cohesin Complexes. Genetics 185 (3), 771–782. https://doi.org/10.1534/genetics.110.117523

Canman, C.E., Lim, D.S., Cimprich, K.A., Taya, Y., Tamai, K., Sakaguchi, K., Appella, E., Kastan, M.B., Siliciano, J.D., 1998. Activation of the ATM Kinase by Ionizing Radiation and Phosphorylation of p53. Science 281 (5383), 1677–1679. https://doi.org/10.1126/SCIENCE.281.5383.1677

Carballo, J.A., Johnson, A.L., Sedgwick, S.G., Cha, R.S., 2008. Phosphorylation of the Axial Element Protein Hop1 by Mec1/Tel1 Ensures Meiotic Interhomolog Recombination. Cell 132 (5), 758–770. https://doi.org/10.1016/j.cell.2008.01.035

Carmell, M.A., Dokshin, G.A., Skaletsky, H., Hu, Y.-C., van Wolfswinkel, J.C., Igarashi, K.J., Bellott, D.W., Nefedov, M., Reddien, P.W., Enders, G.C., Uversky, V.N., Mello, C.C., Page, D.C., 2016. A widely employed germ cell marker is an ancient disordered protein with reproductive functions in diverse eukaryotes. Elife 5, e19993. https://doi.org/10.7554/eLife.19993

Chen, L., Chao, S.-B., Wang, Z.-B., Qi, S.-T., Zhu, X.-L., Yang, S.-W., Yang, C.-R., Zhang, Q.-H., Ouyang, Y.-C., Hou, Y., Schatten, H., Sun, Q.-Y., 2012. Checkpoint kinase 1 is essential for meiotic cell cycle regulation in mouse oocytes. Cell Cycle 11 (10), 1948–1955. https://doi.org/10.4161/cc.20279

Carofiglio, F., Inagaki, A., de Vries, S., Wassenaar, E., Schoenmakers, S., Vermeulen, C., van Cappellen, W.A., Sleddens-Linkels, E., Grootegoed, J.A., te Riele, H.P.J., de Massy, B., Baarends, W.M., 2013. SPO11-Independent DNA Repair Foci and Their Role in Meiotic Silencing. PLoS Genet. 9 (6), 1003538. https://doi.org/10.1371/journal.pgen.1003538

Carofiglio, F., Sleddens-Linkels, E., Wassenaar, E., Inagaki, A., van Cappellen, W.A., Grootegoed, J.A., Toth, A., Baarends, W.M., 2018. Repair of exogenous DNA double-strand breaks promotes chromosome synapsis in SPO11-mutant mouse meiocytes, and is altered in the absence of HORMAD1. DNA Repair. 63, 25–38. https://doi.org/10.1016/j.dnarep.2018.01.007

Chaturvedi, P., Eng, W.K., Zhu, Y., Mattern, M.R., Mishra, R., Hurle, M.R., Zhang, X., Annan, R.S., Lu, Q., Faucette, L.F., Scott, G.F., Li, X., Carr, S.A., Johnson, R.K., Winkler, J.D., Zhou, B.-B.S., 1999. Mammalian Chk2 is a downstream effector of the ATM-dependent DNA damage checkpoint pathway. Oncogene 18, 4047–4054. https://doi.org/10.1038/sj.onc.1202925

Chen, T., Stephens, P.A., Middleton, F.K., Curtin, N.J., 2012. Targeting the S and G2 checkpoint to treat cancer. Drug Discov. Today 17 (5-6), 194–202. https://doi.org/10.1016/j.drudis.2011.12.009

Chen, Y., Jefferson, W.N., Newbold, R.R., Padilla-Banks, E., Pepling, M.E., 2007. Estradiol, Progesterone, and Genistein Inhibit Oocyte Nest Breakdown and Primordial Follicle Assembly in the Neonatal Mouse Ovary *in Vitro* and *in Vivo*.

Endocrinology 148 (8), 3580–3590. https://doi.org/10.1210/en.2007-0088

Cherry, S.M., Adelman, C.A., Theunissen, J.W., Hassold, T.J., Hunt, P.A., Petrini, J.H.J., 2007. The Mre11 Complex Influences DNA Repair, Synapsis, and Crossing Over in Murine Meiosis. Curr. Biol. 17 (4), 373–378. https://doi.org/10.1016/J.CUB.2006.12.048

Chesnel, F., Eppig, J.J., 1995. Synthesis and accumulation of $p34^{cdc2}$ and cyclin B in mouse oocytes during acquisition of competence to resume meiosis. Mol. Reprod. Dev. 40 (4), 503–508. https://doi.org/10.1002/mrd.1080400414

Cimprich, K.A., Cortez, D., 2008. ATR: an essential regulator of genome integrity. Nat. Rev. Mol. Cell Biol. 9, 616–627. https://doi.org/10.1038/nrm2450

Cloutier, J.M., Mahadevaiah, S.K., ElInati, E., Nussenzweig, A., Tóth, A., Turner, J.M.A., 2015. Histone H2AFX Links Meiotic Chromosome Asynapsis to Prophase I Oocyte Loss in Mammals. PLOS Genet. 11 (10), e1005462. https://doi.org/10.1371/journal.pgen.1005462

Cole, F., Kauppi, L., Lange, J., Roig, I., Wang, R., Keeney, S., Jasin, M., 2012. Homeostatic control of recombination is implemented progressively in mouse meiosis. Nat. Cell Biol. 14, 424–430. https://doi.org/10.1038/ncb2451

Cooke, H.J., Lee, M., Kerr, S., Ruggiu, M., 1996. A Murine Homologue of the Human Daz Gene is Autosomal and Expressed only in Male and Female Gonads. Hum. Mol. Genet. 5 (4), 513–516. https://doi.org/10.1093/hmg/5.4.513

Cordaux, R., Batzer, M.A., 2009. The impact of retrotransposons on human genome evolution. Nat. Rev. Genet. 10, 691–703. https://doi.org/10.1038/nrg2640

Costa, Y., Speed, R., Ollinger, R., Alsheimer, M., Semple, C.A., Gautier, P., Maratou, K., Novak, I., Höög, C., Benavente, R., Cooke, H.J., 2005. Two novel proteins recruited by synaptonemal complex protein 1 (SYCP1) are at the centre of meiosis. J. Cell Sci. 118, 2755–2762. https://doi.org/10.1242/jcs.02402

Couteau, F., Belzile, F., Horlow, C., Grandjean, O., Vezon, D., Doutriaux, M.P., 1999. Random Chromosome Segregation without Meiotic Arrest in Both Male and Female Meiocytes of a *dmc1* Mutant of Arabidopsis. Plant Cell 11, 1623–1634. https://doi.org/10.1105/TPC.11.9.1623

Cuadrado, M., Martinez-Pastor, B., Murga, M., Toledo, L.I., Gutierrez-Martinez, P., Lopez, E., Fernandez-Capetillo, O., 2006. ATM regulates ATR chromatin loading in response to DNA double-strand breaks. J. Exp. Med. 203 (2), 297–303. https://doi.org/10.1084/jem.20051923

Daniel, K., Lange, J., Hached, K., Fu, J., Anastassiadis, K., Roig, I., Cooke, H.J., Stewart, A.F., Wassmann, K., Jasin, M., Keeney, S., Tóth, A., 2011. Meiotic homologue alignment and its quality surveillance are controlled by mouse HORMAD1. Nat. Cell Biol. 13, 599–610. https://doi.org/10.1038/ncb2213

Day, F.R., et al., 2015. Large-scale genomic analyses link reproductive aging to hypothalamic signaling, breast cancer susceptibility and BRCA1-mediated DNA repair. Nat. Genet. 47, 1294–1303. https://doi.org/10.1038/ng.3412

de Cuevas, M., Lilly, M., Spradling, A., 1997. GERMLINE CYST FORMATION IN DROSOPHILA. Annu. Rev. Genet. 31, 405-428. https://doi.org/10.1146/annurev.genet.31.1.405

De Felici, M., Di Carlo, A., Pesce, M., Iona, S., Farrace, M.G., Piacentini, M., 1999. Bcl-2 and Bax regulation of apoptosis in germ cells during prenatal oogenesis in the mouse embryo. Cell Death Differ. 6, 908–915. https://doi.org/10.1038/sj.cdd.4400561

Dernburg, A.F., McDonald, K., Moulder, G., Barstead, R., Dresser, M., Villeneuve, A.M., 1998. Meiotic Recombination in C. elegans Initiates by a Conserved Mechanism and Is Dispensable for Homologous Chromosome Synapsis. Cell 94 (3), 387–398. https://doi.org/10.1016/S0092-8674(00)81481-6

Di Carlo, A.D., Travia, G., De Felici, M., 2000. The meiotic specific synaptonemal complex protein SCP3 is expressed by female and male primordial germ cells of the mouse embryo. Int. J. Dev. Biol. 44 (2), 241–244.

Di Giacomo, M., Barchi, M., Baudat, F., Edelmann, W., Keeney, S., Jasin, M., 2005. Distinct DNA-damage-dependent and -independent responses drive the loss of oocytes in recombination-defective mouse mutants. Proc. Natl. Acad. Sci. U.S.A. 102 (3), 737–742. https://doi.org/10.1073/pnas.0406212102

Donehower, L.A., Harvey, M., Slagle, B.L., McArthur, M.J., Montgomery, C.A., Butel, J.S., Bradley, A., 1992. Mice deficient for p53 are developmentally normal but susceptible to spontaneous tumours. Nature 356, 215–221. https://doi.org/10.1038/356215a0

Eaker, S., Cobb, J., Pyle, A., Handel, M.A., 2002. Meiotic Prophase Abnormalities and Metaphase Cell Death in MLH1-Deficient Mouse Spermatocytes: Insights into Regulation of Spermatogenic Progress. Dev. Biol. 249 (1), 85–95. https://doi.org/10.1006/DBIO.2002.0708

Edelmann, W., Cohen, P.E., Kane, M., Lau, K., Morrow, B., Bennett, S., Umar, A., Kunkel, T., Cattoretti, G., Chaganti, R., Pollard, J.W., Kolodner, R.D., Kucherlapati, R., 1996. Meiotic Pachytene Arrest in MLH1-Deficient Mice 85 (7), 1125–1134. https://doi.org/10.1016/S0092-8674(00)81312-4

Enders, G.C., May, J.J., 1994. Developmentally Regulated Expression of a Mouse Germ Cell Nuclear Antigen Examined from Embryonic Day 11 to Adult in Male and Female Mice. Dev. Biol. 163 (2), 331–340. https://doi.org/10.1006/DBIO.1994.1152

Enguita-Marruedo, A., Martín-Ruiz, M., García, E., Gil-Fernández, A., Parra, M.T., Viera, A., Rufas, J.S., Page, J., 2019. Transition from a meiotic to a somatic-like DNA damage response during the pachytene stage in mouse meiosis. PLoS Genet. 15, e1007439. https://doi.org/10.1371/journal.pgen.1007439

Fernandez-Capetillo, O., Mahadevaiah, S.K., Celeste, A., Romanienko, P.J., Camerini-Otero, R.D., Bonner, W.M., Manova, K., Burgoyne, P., Nussenzweig, A., 2003. H2AX Is Required for Chromatin Remodeling and Inactivation of Sex Chromosomes in Male Mouse Meiosis. Dev. Cell 4 (4), 497–508. https://doi.org/10.1016/S1534-5807(03)00093-5

Finsterbusch, F., Ravindranathan, R., Dereli, I., Stanzione, M., Tränkner, D., Tóth, A., 2016. Alignment of Homologous Chromosomes and Effective Repair of Programmed DNA Double-Strand Breaks during Mouse Meiosis Require the Minichromosome Maintenance Domain Containing 2 (MCMDC2) Protein. PLoS Genet. 12 (10), e1006393. https://doi.org/10.1371/journal.pgen.1006393

Fraune, J., Schramm, S., Alsheimer, M., Benavente, R., 2012. The mammalian synaptonemal complex: Protein components, assembly and role in meiotic recombination. Exp. Cell Res. 318, 1340–1346. https://doi.org/10.1016/J.YEXCR.2012.02.018

Fujiwara, Y., Komiya, T., Kawabata, H., Sato, M., Fujimoto, H., Furusawa, M., Noce, T., 1994. Isolation of a DEAD-family protein gene that encodes a murine homolog of Drosophila vasa and its specific expression in germ cell lineage. Proc. Natl. Acad. Sci.

U.S.A. 91 (25), 12258–12262. https://doi.org/10.1073/PNAS.91.25.12258

Fukuda, T., Daniel, K., Wojtasz, L., Toth, A., Höög, C., 2010. A novel mammalian HORMA domain-containing protein, HORMAD1, preferentially associates with unsynapsed meiotic chromosomes. Exp. Cell Res. 316 (2), 158–171. https://doi.org/10.1016/J.YEXCR.2009.08.007

Fukuda, T., Pratto, F., Schimenti, J.C., Turner, J.M.A., Camerini-Otero, R.D., Höög, C., 2012. Phosphorylation of Chromosome Core Components May Serve as Axis Marks for the Status of Chromosomal Events during Mammalian Meiosis. PLoS Genet. 8, e1002485. https://doi.org/10.1371/journal.pgen.1002485

Gartner, A., Milstein, S., Ahmed, S., Hodgkin, J., Hengartner, M.O., 2000. A Conserved Checkpoint Pathway Mediates DNA Damage–Induced Apoptosis and Cell Cycle Arrest in *C. elegans*. Mol. Cell 5 (3), 435–443. https://doi.org/10.1016/S1097-2765(00)80438-4

Gasior, S.L., Wakeman, T.P., Xu, B., Deininger, P.L., 2006. The Human LINE-1 Retrotransposon Creates DNA Double-Strand Breaks. J. Mol. Biol. 357 (5), 1383–1393. https://doi.org/10.1016/j.jmb.2006.01.089

Ghafari, F., Gutierrez, C.G., Hartshorne, G.M., 2007. Apoptosis in mouse fetal and neonatal oocytes during meiotic prophase one. BMC Dev. Biol. 7, 87. https://doi.org/10.1186/1471-213X-7-87

Ghezraoui, H., Oliveira, C., Becker, J.R., Bilham, K., Moralli, D., Anzilotti, C., Fischer, R., Deobagkar-Lele, M., Sanchiz-Calvo, M., Fueyo-Marcos, E., Bonham, S., Kessler, B.M., Rottenberg, S., Cornall, R.J., Green, C.M., Chapman, J.R., 2018. 53BP1 cooperation with the REV7–shieldin complex underpins DNA structure-specific NHEJ. Nature 560, 122–127. https://doi.org/10.1038/s41586-018-0362-1

Goedecke, W., Eijpe, M., Offenberg, H.H., Aalderen, M. van, Heyting, C., 1999. Mre11 and Ku70 interact in somatic cells, but are differentially expressed in early meiosis. Nat. Genet. 23, 194–198. https://doi.org/10.1038/13821

Gonfloni, S., Di Tella, L., Caldarola, S., Cannata, S.M., Klinger, F.G., Di Bartolomeo, C., Mattei, M., Candi, E., De Felici, M., Melino, G., Cesareni, G., 2009. Inhibition of the c-Abl–TAp63 pathway protects mouse oocytes from chemotherapy-induced death. Nat. Med. 15, 1179–1185. https://doi.org/10.1038/nm.2033

Goodyer, W., Kaitna, S., Couteau, F., Ward, J.D., Boulton, S.J., Zetka, M., 2008. HTP-3 Links DSB Formation with Homolog Pairing and Crossing Over during C. elegans Meiosis. Dev. Cell 14 (2), 263–274. https://doi.org/10.1016/j.devcel.2007.11.016

Gosden, R.G., 2002. Oogenesis as a foundation for embryogenesis. Mol. Cell. Endocrinol. 186 (2), 149–153. https://doi.org/10.1016/S0303-7207(01)00683-9

Greenfeld, C.R., Pepling, M.E., Babus, J.K., Furth, P.A., Flaws, J.A., 2007. BAX regulates follicular endowment in mice. Reproduction 133 (5), 865–876. https://doi.org/10.1530/REP-06-0270

Guillon, H., De Massy, B., 2002. An initiation site for meiotic crossing-over and gene conversion in the mouse. Nat. Genet. 32, 296-299. https://doi.org/10.1038/ng990

Guillot, M. T., Roig, I., 2017. Estudi de la formació dels fol·licles de mamífer *in vitro* (master's thesis). Universitat Autònoma de Barcelona, Cerdanyola del Vallès, Spain.

Gupta, R., Somyajit, K., Narita, T., Maskey, E., Stanlie, A., Kremer, M., Typas, D., Lammers, M., Mailand, N., Nussenzweig, A., Lukas, J., Choudhary, C., 2018. DNA Repair Network Analysis Reveals Shieldin as a Key Regulator

of NHEJ and PARP Inhibitor Sensitivity. Cell 173, 972-988.e23. https://doi.org/10.1016/j.cell.2018.03.050

Hahn, K.L., 2005. Lunatic fringe null female mice are infertile due to defects in meiotic maturation. Development 132, 817–828. https://doi.org/10.1242/dev.01601

Hamer, G., Gell, K., Kouznetsova, A., Novak, I., Benavente, R., Höög, C., 2006. Characterization of a novel meiosis-specific protein within the central element of the synaptonemal complex. J. Cell Sci. 119, 4025–4032. https://doi.org/10.1242/JCS.03182

Handel, M.A., Schimenti, J.C., 2010. Genetics of mammalian meiosis: regulation, dynamics and impact on fertility. Nat. Rev. Genet. 11, 124–136. https://doi.org/10.1038/nrg2723

Hartshorne, G.M., Lyrakou, S., Hamoda, H., Oloto, E., Ghafari, F., 2009. Oogenesis and cell death in human prenatal ovaries: what are the criteria for oocyte selection? Mol. Hum. Reprod. 15 (12), 805–819. https://doi.org/10.1093/molehr/gap055

Hartwell, L.H., Weinert, T.A., 1989. Checkpoints: controls that ensure the order of cell cycle events. Science 246 (4930), 629–634. https://doi.org/10.1126/SCIENCE.2683079

Hassold, T., Hunt, P., 2001. To Err (Meiotically) Is Human : the Genesis of Human Aneuploidy. Nat. Rev. Genet 2 (4), 280–291. https://doi.org/10.1038/35066065

Hassold, T., Sherman, S., Hunt, P., 2000. Counting cross-overs: characterizing meiotic recombination in mammals. Hum. Mol. Genet. 9 (16), 2409–2419. https://doi.org/10.1093/hmg/9.16.2409

Hayashi, K., Saitou, M., 2014. Perspectives of germ cell development *in vitro* in mammals. Anim. Sci. J. 85 (6), 617–626. https://doi.org/10.1111/asj.12199

Hirao, A., Cheung, A., Duncan, G., Girard, P-M., A.J., Wakeham, A., Okada, H., Sarkissian, T., Wong, J. A, Sakai, T., de Stanchina, E., Bristow, R.G., Suda, T., Lowe, S.W., Jeggo, P.A, Elledge, S.J., Mak, T.W., 2002. Chk2 Is a Tumor Suppressor That Regulates Apoptosis in both an Ataxia Telangiectasia Mutated (ATM)-Dependent and an ATM-Independent Manner. Mol. Cell. Biol. 22 (18), 6521–6532. https://doi.org/10.1128/MCB.22.18.6521-6532.2002

Hirota, T., Blakeley, P., Sangrithi, M.N., Mahadevaiah, S.K., Encheva, V., Snijders, A.P., ElInati, E., Ojarikre, O.A., de Rooij, D.G., Niakan, K.K., Turner, J.M.A., 2018. SETDB1 Links the Meiotic DNA Damage Response to Sex Chromosome Silencing in Mice. Dev. Cell 47 (5), 645-659. https://doi.org/10.1016/j.devcel.2018.10.004

Hirshfield, A.N., 1991. Development of follicles in the mammalian ovary. Int. Rev. Cytol. 124, 43–101.

Hirshfield, A.N., Midgley, A.R., 1978. Morphometric analysis of follicular development in the rat. Biol. Reprod. 19 (3), 597–605.

Hochwagen, A., Amon, A., 2006. Checking your Breaks: Surveillance Mechanisms of Meiotic Recombination. Curr. Biol. 16 (6), 217–228. https://doi.org/10.1016/j.cub.2006.03.009

Hodges, C. A, LeMaire-Adkins, R., Hunt, P., 2001. Coordinating the segregation of sister chromatids during the first meiotic division: evidence for sexual dimorphism. J. Cell Sci. 114, 2417–2426.

Hollingsworth, N.M., Byers, B., 1989. HOP1: a yeast meiotic pairing gene. Genetics 121 (3), 445–462.

Hsueh, A.J.W., Billig, H., Tsafriri, A., 1994. Ovarian Follicle Atresia: A Hormonally Controlled Apoptotic Process. Endocr. Rev. 15 (6), 707–724. https://doi.org/10.1210/edrv-15-6-707

Hunter, N., 2017. Oocyte Quality Control: Causes, Mechanisms, and Consequences. Cold Spring Harb. Symp. Quant. Biol. 82, 235–247. https://doi.org/10.1101/sqb.2017.82.035394

Iguchi, T., Kamiya, K., Uesugi, Y., Sayama, K., Takasugi, N., 1991. In vitro fertilization of oocytes from polyovular follicles in mouse ovaries exposed neonatally to diethylstilbestrol. In Vivo 5, 359–363.

Jacks, T., Remington, L., Williams, B.O., Schmitt, E.M., Halachmi, S., Bronson, R.T., Weinberg, R.A., 1994. Tumor spectrum analysis in *p53*-mutant mice. Curr. Biol. 4 (1), 1–7. https://doi.org/10.1016/S0960-9822(00)00002-6

Jefferson, W., Newbold, R., Padilla-Banks, E., Pepling, M., 2006. Neonatal Genistein Treatment Alters Ovarian Differentiation in the Mouse: Inhibition of Oocyte Nest Breakdown and Increased Oocyte Survival. Biol. Reprod. 74 (1), 161–168. https://doi.org/10.1095/biolreprod.105.045724

Jing, J., Jiang, X., Chen, J., Yao, X., Zhao, M., Li, P., Pan, Y., Ren, Y., Liu, W., Lyu, L., 2017. Notch signaling pathway promotes the development of ovine ovarian follicular granulosa cells. Anim. Reprod. Sci. 181, 69–78. https://doi.org/10.1016/j.anireprosci.2017.03.017

Joyce, E.F., McKim, K.S., 2009. Drosophila PCH2 Is Required for a Pachytene Checkpoint That Monitors Double-Strand-Break-Independent Events Leading to Meiotic Crossover Formation. Genetics 181, 39–51. https://doi.org/10.1534/genetics.108.093112

Kastan, M.B., Lim, D.-S., 2000. The many substrates and functions of ATM. Nat. Rev. Mol. Cell Biol. 1, 179-186. https://doi.org/10.1038/35043058

Kauppi, L., Barchi, M., Baudat, F., Romanienko, P.J., Keeney, S., Jasin, M., 2011. Distinct properties of the XY pseudoautosomal region crucial for male meiosis. Science 331, 916–920. https://doi.org/10.1126/science.1195774

Keeney, S., Giroux, C.N., Kleckner, N., 1997. Meiosis-Specific DNA Double-Strand Breaks Are Catalyzed by Spo11, a Member of a Widely Conserved Protein Family. Cell 88 (3), 375–384. https://doi.org/10.1016/S0092-8674(00)81876-0

Kent, H.A., 1960. Polyovular follicles and multinucleate ova in the ovaries of young mice. Anat. Rec. 137, 521–4.

Khanna, K.K., Keating, K.E., Kozlov, S., Scott, S., Gatei, M., Hobson, K., Taya, Y., Gabrielli, B., Chan, D., Lees-miller, S.P., Lavin, M.F., 1998. ATM associates with and phosphorylates p53: mapping the region of interaction. Nat. Genet. 20 (4), 398–400.

King, C., Diaz, H., Barnard, D., Barda, D., Clawson, D., Blosser, W., Cox, K., Guo, S., Marshall, M., 2014. Characterization and preclinical development of LY2603618: A selective and potent Chk1 inhibitor. Invest. New Drugs 32 (2), 213–226. https://doi.org/10.1007/s10637-013-0036-7

King, C., Diaz, H., Barnard, D., Barda, D., Clawson, D., Blosser, W., Cox, K., Guo, S., Marshall, M., 2014. Characterization and preclinical development of LY2603618: A selective and potent Chk1 inhibitor. Invest. New Drugs 32 (3), 213–226. https://doi.org/10.1007/s10637-013-0036-7

Kleckner, N., 1996. Meiosis: how could it work? Proc. Natl. Acad. Sci. U.S.A. 93 (16), 8167–8174. https://doi.org/10.1073/pnas.93.16.8167

Kogo, H., Tsutsumi, M., Inagaki, H., Ohye, T., Kiyonari, H., Kurahashi, H., 2012a. HORMAD2 is essential for synapsis surveillance during meiotic prophase via

the recruitment of ATR activity. Genes to Cells 17 (11), 897–912. https://doi.org/10.1111/gtc.12005

Kogo, H., Tsutsumi, M., Ohye, T., Inagaki, H., Abe, T., Kurahashi, H., 2012b. HORMAD1-dependent checkpoint/surveillance mechanism eliminates asynaptic oocytes. Genes to Cells 17 (6), 439–454. https://doi.org/10.1111/j.1365-2443.2012.01600.x

Kolas, N.K., Marcon, E., Crackower, M.A., Höög, C., Penninger, J.M., Spyropoulos, B., Moens, P.B., 2005. Mutant meiotic chromosome core components in mice can cause apparent sexual dimorphic endpoints at prophase or X–Y defective male-specific sterility. Chromosoma 114 (2), 92–102. https://doi.org/10.1007/s00412-005-0334-8

Kolp, R., Sorenson, C.M., Flaws, J.A., Tilly, J.L., Ratts, V.S., 2014. Ablation of bcl-2 gene expression decreases the numbers of oocytes and primordial follicles established in the post-natal female mouse gonad. Endocrinology 136 (8), 3665–3668. https://doi.org/10.1210/endo.136.8.7628407

Kouznetsova, A., Wang, H., Bellani, M., Camerini-Otero, R.D., Jessberger, R., Höög, C., 2009. BRCA1-mediated chromatin silencing is limited to oocytes with a small number of asynapsed chromosomes. J. Cell Sci. 122, 2446–2452. https://doi.org/10.1242/jcs.049353

Krakauer, D.C., Mira, A., 1999. Mitochondria and germ-cell death. Nature 400, 125–126. https://doi.org/10.1038/22026

Lam, I., Keeney, S., 2014. Mechanism and Regulation of Meiotic Recombination Initiation. Cold Spring Harb. Perspect. Biol. 7, a016634. https://doi.org/10.1101/cshperspect.a016634

Lange, J., Pan, J., Cole, F., Thelen, M.P., Jasin, M., Keeney, S., 2011. ATM controls meiotic double-strand-break formation. Nature 479, 237–240. https://doi.org/10.1038/nature10508

Lao, J.P., Hunter, N., 2010. Trying to Avoid Your Sister. PLoS Biol. 8, e1000519. https://doi.org/10.1371/journal.pbio.1000519

Laronda, M.M., Rutz, A.L., Xiao, S., Whelan, K.A., Duncan, F.E., Roth, E.W., Woodruff, T.K., Shah, R.N., 2017. A bioprosthetic ovary created using 3D printed microporous scaffolds restores ovarian function in sterilized mice. Nat. Commun. 8, 15261. https://doi.org/10.1038/ncomms15261

Lei, L., Spradling, A.C., 2016. Mouse oocytes differentiate through organelle enrichment from sister cyst germ cells. Science. 352 (6281), 95–99. https://doi.org/10.1126/science.aad2156

Lei, L., Spradling, A.C., 2013. Mouse primordial germ cells produce cysts that partially fragment prior to meiosis. Development 140, 2075–2081. https://doi.org/10.1242/dev.093864

Li, J., Zhao, D., Guo, C., Li, J., Mi, Y., Zhang, C., 2016. Involvement of Notch signaling in early chick ovarian follicle development. Cell Biol. Int. 40 (1), 65–73. https://doi.org/10.1002/cbin.10538

Li, R., Albertini, D.F., 2013. The road to maturation: Somatic cell interaction and self-organization of the mammalian oocyte. Nat. Rev. Mol. Cell Biol. 14, 141-152. https://doi.org/10.1038/nrm3531

Li, X., Schimenti, J.C., 2007. Mouse Pachytene Checkpoint 2 (*Trip13*) Is Required for Completing Meiotic Recombination but Not Synapsis. PLoS Genet. 3 (8), e130. https://doi.org/10.1371/journal.pgen.0030130

Li, X.C., Bolcun-Filas, E., Schimenti, J.C., 2011. Genetic Evidence That Synaptonemal Complex Axial Elements Govern Recombination Pathway Choice in Mice. Genetics 189 (1), 71–82. https://doi.org/10.1534/genetics.111.130674

Liang, M., Zhao, T., Ma, L., Guo, Y., 2017. CHK1 inhibition sensitizes pancreatic cancer cells to gemcitabine via promoting CDK-dependent DNA damage and ribonucleotide reductase downregulation. Oncol. Rep. 39 (3), 1322–1330. https://doi.org/10.3892/or.2017.6168

Liu, J.-G., Yuan, L., Brundell, E., Björkroth, B., Daneholt, B., Höög, C., 1996. Localization of the N-terminus of SCP1 to the Central Element of the Synaptonemal Complex and Evidence for Direct Interactions between the N-termini of SCP1 Molecules Organized Head-to-Head. Exp. Cell Res. 226 (1), 11–19. https://doi.org/10.1006/EXCR.1996.0197

Livera, G., Petre-Lazar, B., Guerquin, M.J., Trautmann, E., Coffigny, H., Habert, R., 2008. p63 null mutation protects mouse oocytes from radio-induced apoptosis. Reproduction 135 (1), 3–12. https://doi.org/10.1530/REP-07-0054

Lobascio, A.M., Klinger, F.G., Scaldaferri, M.L., Farini, D., De Felici, M., 2007. Analysis of programmed cell death in mouse fetal oocytes. Reproduction 134 (2), 241–252. https://doi.org/10.1530/REP-07-0141

Longhese, M.P., Bonetti, D., Guerini, I., Manfrini, N., Clerici, M., 2009. DNA double-strand breaks in meiosis: Checking their formation, processing and repair. DNA Repair 8 (9), 1127–1138. https://doi.org/10.1016/J.DNAREP.2009.04.005

Maatouk, D.M., Kellam, L.D., Mann, M.R.W., Lei, H., Li, E., Bartolomei, M.S., Resnick, J.L., 2006. DNA methylation is a primary mechanism for silencing postmigratory primordial germ cell genes in both germ cell and somatic cell lineages. Development 133, 3411–3418. https://doi.org/10.1242/dev.02500

MacQueen, A.J., Hochwagen, A., 2011. Checkpoint mechanisms: the puppet masters of meiotic prophase. Trends Cell Biol. 21 (7), 393–400. https://doi.org/10.1016/j.tcb.2011.03.004

MacQueen, A.J., Villeneuve, A.M., 2001. Nuclear reorganization and homologous chromosome pairing during meiotic prophase require C. elegans chk-2. Genes Dev. 15, 1674–1687. https://doi.org/10.1101/gad.902601

Mahadevaiah, S.K., Bourc'his, D., de Rooij, D.G., Bestor, T.H., Turner, J.M.A., Burgoyne, P.S., 2008. Extensive meiotic asynapsis in mice antagonises meiotic silencing of unsynapsed chromatin and consequently disrupts meiotic sex chromosome inactivation. J. Cell Biol. 182 (2), 263–276. https://doi.org/10.1083/jcb.200710195

Mahadevaiah, S.K., Turner, J.M.A., Baudat, F., Rogakou, E.P., de Boer, P., Blanco-Rodríguez, J., Jasin, M., Keeney, S., Bonner, W.M., Burgoyne, P.S., 2001. Recombinational DNA double-strand breaks in mice precede synapsis. Nat. Genet. 27, 271–276. https://doi.org/10.1038/85830

Malki, S., Tharp, M.E., Bortvin, A., 2015. A Whole-Mount Approach for Accurate Quantitative and Spatial Assessment of Fetal Oocyte Dynamics in Mice. Biol. Reprod. 93 (5), 113, 1-9. https://doi.org/10.1095/biolreprod.115.132118

Malki, S., van der Heijden, G.W., O'Donnell, K.A., Martin, S.L., Bortvin, A., 2014. A Role for Retrotransposon LINE-1 in Fetal Oocyte Attrition in Mice. Dev. Cell 29 (5), 521–533. https://doi.org/10.1016/j.devcel.2014.04.027

Manova, K., Nocka, K., Besmer, P., Bachvarova, R.F., 1990. Gonadal expression of c-kit encoded at the W locus of the mouse. Development 110 (4), 1057-1069.

Marcet-Ortega, M., Pacheco, S., Martínez-Marchal, A., Castillo, H., Flores, E., Jasin, M., Keeney, S., Roig, I., 2017. p53 and TAp63 participate in the recombination-dependent pachytene arrest in mouse spermatocytes. PLoS Genet. 13, e1006845. https://doi.org/10.1371/journal.pgen.1006845

Maréchal, A., Zou, L., 2013. DNA Damage Sensing by the ATM and ATR kinases. Cold Spring Harb. Perspect. Biol. 5 (9), a012716 https://doi.org/10.1101/cshperspect.a012716

Matova, N., Cooley, L., 2001. Comparative Aspects of Animal Oogenesis. Dev. Biol. 231 (2), 291–320. https://doi.org/10.1006/DBIO.2000.0120

Matsuoka, S., Rotman, G., Ogawa, A., Shiloh, Y., Tamai, K., Elledge, S.J., 2000. Ataxia telangiectasia-mutated phosphorylates Chk2 in vivo and in vitro. Proc. Natl. Acad. Sci. U.S.A. 97 (19), 10389–10394. https://doi.org/10.1073/pnas.190030497

McClellan, K.A., Gosden, R., Taketo, T., 2003. Continuous loss of oocytes throughout meiotic prophase in the normal mouse ovary. Dev. Biol. 258 (2), 334–348. https://doi.org/10.1016/S0012-1606(03)00132-5

McGee, E.A., Hsueh, A.J.W., 2000. Initial and Cyclic Recruitment of Ovarian Follicles. Endocr. Rev. 21 (2), 200-214. https://doi.org/10.1210/edrv.21.2.0394

McKee, B.D., Handel, M.A., 1993. Sex chromosomes, recombination, and chromatin conformation. Chromosoma 102 (2), 71–80. https://doi.org/10.1007/BF00356023

McKim, K.S., Green-Marroquin, B.L., Sekelsky, J.J., Chin, G., Steinberg, C., Khodosh, R., Hawley, R.S., 1998. Meiotic Synapsis in the Absence of Recombination. Science 279 (5352), 876–878. https://doi.org/10.1126/SCIENCE.279.5352.876

McLaren, A., 1984. Meiosis and differentiation of mouse germ cells. Symp. Soc. Exp. Biol. 38, 7–23.

McNairn, A.J., Rinaldi, V.D., Schimenti, J.C., 2017. Repair of Meiotic DNA Breaks and Homolog Pairing in Mouse Meiosis Requires a Minichromosome Maintenance (MCM) Paralog. Genetics 205, 529–537. https://doi.org/10.1534/genetics.116.196808

Menke, D.B., Koubova, J., Page, D.C., 2003. Sexual differentiation of germ cells in XX mouse gonads occurs in an anterior-to-posterior wave. Dev. Biol. 262 (2), 303–312. https://doi.org/10.1016/S0012-1606(03)00391-9

Meuwissen, R.L., Offenberg, H.H., Dietrich, A.J., Riesewijk, A., van Iersel, M., Heyting, C., 1992. A coiled-coil related protein specific for synapsed regions of meiotic prophase chromosomes. EMBO J. 11 (13), 5091–5100.

Mintz, B., Rusell, E.S., 1957. Gene-induced embryological modifications of primordial germ cells in the mouse. J. Exp. Zool. 134 (2), 207–237.

Mirman, Z., Lottersberger, F., Takai, H., Kibe, T., Gong, Y., Takai, K., Bianchi, A., Zimmermann, M., Durocher, D., de Lange, T., 2018. 53BP1–RIF1–shieldin counteracts DSB resection through CST- and Polα-dependent fill-in. Nature 560, 112–116. https://doi.org/10.1038/s41586-018-0324-7

Mitra, N., Roeder, G.S., 2007. A Novel Nonnull *ZIP1* Allele Triggers Meiotic Arrest With Synapsed Chromosomes in *Saccharomyces cerevisiae*. Genetics 176 (2), 773–787. https://doi.org/10.1534/GENETICS.107.071100

Moens, P.B., Chen, D.J., Shen, Z., Kolas, N., Tarsounas, M., Heng, H.H.Q., Spyropoulos, B., 1997. Rad51 immunocytology in rat and mouse spermatocytes and oocytes. Chromosoma 106 (4), 207–215. https://doi.org/10.1007/s004120050241

Moens, P.B., Kolas, N., Tarsounas, M., Marcon, E., Cohen, P.E., Spyropoulos, B., 2002. The time course and chromosomal localization of recombination-related proteins at meiosis in the mouse are compatible with models that can resolve the early DNA-DNA interactions without

reciprocal recombination. J. Cell Sci. 115 (8), 1611-1622.

Moens, P.B., Spyropoulos, B., 1995. Immunocytology of chiasmata and chromosomal disjunction at mouse meiosis. Chromosoma 104 (3), 175–182. https://doi.org/10.1007/BF00352182

Molyneaux, K.A., Stallock, J., Schaible, K., Wylie, C., 2001. Time-Lapse Analysis of Living Mouse Germ Cell Migration. Dev. Biol. 240 (2), 488–498. https://doi.org/10.1006/DBIO.2001.0436

Monk, M., McLaren, A., 1981. X-chromosome activity in foetal germ cells of the mouse. J. Embryol. Exp. Morphol. 63, 75–84.

Morelli, M. A., Cohen, P.E., 2005. Not all germ cells are created equal: Aspects of sexual dimorphism in mammalian meiosis. Reproduction 130 (6), 761–781. https://doi.org/10.1530/rep.1.00865

Morgan, S., Campbell, L., Allison, V., Murray, A., Spears, N., 2015. Culture and Co-Culture of Mouse Ovaries and Ovarian Follicles. J. Vis. Exp. 97, e52458 https://doi.org/10.3791/52458

Morgan, S., Lopes, F., Gourley, C., Anderson, R.A., Spears, N., 2013. Cisplatin and Doxorubicin Induce Distinct Mechanisms of Ovarian Follicle Loss: Imatinib Provides Selective Protection Only against Cisplatin. PLoS One 8 (7), e70117. https://doi.org/10.1371/journal.pone.0070117

Morita, Y., Maravei, D. V, Bergeron, L., Wang, S., Perez, G.I., Tsutsumi, O., Taketani, Y., Asano, M., Horai, R., Korsmeyer, S.J., Iwakura, Y., Yuan, J., Tilly, J.L., 2001. Caspase-2 deficiency prevents programmed germ cell death resulting from cytokine insufficiency but not meiotic defects caused by loss of *ataxia telangiectasia-mutated* (*Atm*) gene function. Cell Death Differ. 8, 614–620. https://doi.org/10.1038/sj.cdd.4400845

Mork, L., Tang, H., Batchvarov, I., Capel, B., 2012. Mouse germ cell clusters form by aggregation as well as clonal divisions. Mech. Dev. 128 (11-12), 591–596. https://doi.org/10.1016/j.mod.2011.12.005

Murga, M., Bunting, S., Montaña, M.F., Soria, R., Mulero, F., Cañamero, M., Lee, Y., McKinnon, P.J., Nussenzweig, A., Fernandez-Capetillo, O., 2009. A mouse model of ATR-Seckel shows embryonic replicative stress and accelerated aging. Nat. Genet. 41, 891–898. https://doi.org/10.1038/ng.420

Murphy, K., Carvajal, L., Medico, L., Pepling, M., 2005. Expression of Stat3 in germ cells of developing and adult mouse ovaries and testes. Gene Expr. Patterns 5 (4), 475–482. https://doi.org/10.1016/J.MODGEP.2004.12.007

Murta, D., Batista, M., Trindade, A., Silva, E., Henrique, D., Duarte, A., Lopes-da-Costa, L., 2014. *In Vivo* Notch Signaling Blockade Induces Abnormal Spermatogenesis in the Mouse. PLoS One 9 (11), e113365. https://doi.org/10.1371/journal.pone.0113365

Muskhelishvili, L., Wingard, S.K., Latendresse, J.R., 2005. Proliferating Cell Nuclear antigen – A Marker for Ovarian Follicle Counts. Toxicol. Pathol. 33 (3), 365–368. https://doi.org/10.1080/01926230590930164

Myers, M., Britt, K.L., Wreford, N.G.M., Ebling, F.J.P., Kerr, J.B., 2004. Methods for quantifying follicular numbers within the mouse ovary. Reproduction 127 (5), 569–580. https://doi.org/10.1530/rep.1.00095

Nandedkar, T., Dharma, S., Modi, D., Dsouza, S., 2007. Differential gene expression in transition of primordial to preantral follicles in mouse ovary. Soc. Reprod. Fertil. Suppl. 63, 57-67.

Nguyen, Q.N., Zerafa, N., Liew, S.H., Morgan, F.H., Strasser, A., Scott, C.L., Findlay, J.K., Hickey, M., Hutt, K.J., 2018. Loss of PUMA protects the ovarian reserve during DNA-damaging chemotherapy and preserves fertility. Cell Death Dis. 9, 618.

https://doi.org/10.1038/s41419-018-0633-7

Niu, H., Li, X., Job, E., Park, C., Moazed, D., Gygi, S.P., Hollingsworth, N.M., 2007. Mek1 Kinase is Regulated to Suppress Double-Strand Break Repair between Sister Chromatids during Budding Yeast Meiosis. Mol. Cell. Biol. 27, 5456–5467. https://doi.org/10.1128/MCB.00416-07

Niu, H., Wan, L., Baumgartner, B., Schaefer, D., Loidl, J., Hollingsworth, N.M., 2005. Partner Choice during Meiosis Is Regulated by Hop1-promoted Dimerization of Mek1. Mol. Biol. Cell 16 (12), 5804–5818. https://doi.org/10.1091/mbc.e05-05-0465

Niu, H., Wan, L., Busygina, V., Kwon, Y., Allen, J.A., Li, X., Kunz, R.C., Kubota, K., Wang, B., Sung, P., Shokat, K.M., Gygi, S.P., Hollingsworth, N.M., 2009. Regulation of Meiotic Recombination via Mek1-Mediated Rad54 Phosphorylation. Mol. Cell 36 (3), 393–404. https://doi.org/10.1016/J.MOLCEL.2009.09.029

Noordermeer, S.M., Adam, S., Setiaputra, D., Barazas, M., Pettitt, S.J., Ling, A.K., Olivieri, M., Álvarez-Quilón, A., Moatti, N., Zimmermann, M., Annunziato, S., Krastev, D.B., Song, F., Brandsma, I., Frankum, J., Brough, R., Sherker, A., Landry, S., Szilard, R.K., Munro, M.M., McEwan, A., Goullet de Rugy, T., Lin, Z.-Y., Hart, T., Moffat, J., Gingras, A.-C., Martin, A., van Attikum, H., Jonkers, J., Lord, C.J., Rottenberg, S., Durocher, D., 2018. The shieldin complex mediates 53BP1-dependent DNA repair. Nature 560, 117–121. https://doi.org/10.1038/s41586-018-0340-7

O'Brien, M.J., Pendola, J.K., Eppig, J.J., 2003. A Revised Protocol for In Vitro Development of Mouse Oocytes from Primordial Follicles Dramatically Improves Their Developmental Competence. Biol. Reprod. 68, 1682–1686. https://doi.org/10.1095/biolreprod.102.013029

Obata, Y., Kono, T., Hatada, I., 2002. Maturation of mouse fetal germ cells in vitro. Nature 418, 497. https://doi.org/10.1038/418497a

Oh, J., Symington, L.S., 2018. Role of the Mre11 Complex in Preserving Genome Integrity. Genes 9 (12), 589. https://doi.org/10.3390/genes9120589

Oren, M., 1994. Relationship of p53 to the control of apoptotic cell death. Semin. Cancer Biol. 5, 221–227.

Pacheco, S., Maldonado-Linares, A., Marcet-Ortega, M., Rojas, C., Martínez-Marchal, A., Fuentes-Lazaro, J., Lange, J., Jasin, M., Keeney, S., Fernández-Capetillo, O., Garcia-Caldés, M., Roig, I., 2018. ATR is required to complete meiotic recombination in mice. Nat. Commun. 9, 2622. https://doi.org/10.1038/s41467-018-04851-z

Pacheco, S., Marcet-Ortega, M., Lange, J., Jasin, M., Keeney, S., Roig, I., 2015. The ATM Signaling Cascade Promotes Recombination-Dependent Pachytene Arrest in Mouse Spermatocytes. PLoS Genet. 11 (3): e1005017. https://doi.org/10.1371/journal.pgen.1005017

Page, S.L., Hawley, R.S., 2003. Chromosome Choreography: the Meiotic Ballet. Science 301 (5634), 785–789. https://doi.org/10.1126/science.1086605

Papanikos, F., Clément, J.A.J., Testa, E., Ravindranathan, R., Grey, C., Dereli, I., Bondarieva, A., Valerio-Cabrera, S., Stanzione, M., Schleiffer, A., Jansa, P., Lustyk, D., Fei, J.-F., Adams, I.R., Forejt, J., Barchi, M., de Massy, B., Toth, A., 2019. Mouse ANKRD31 Regulates Spatiotemporal Patterning of Meiotic Recombination Initiation and Ensures Recombination between X and Y Sex Chromosomes. Mol. Cell. https://doi.org/10.1016/J.MOLCEL.2019.03.022

Paull, T.T., 2015. Mechanisms of ATM Activation. Annu. Rev. Biochem. 84, 711–738. https://doi.org/10.1146/annurev-biochem-060614-034335

Pepling, M.E., 2012. Follicular assembly: mechanisms of action. Reproduction 143 (2), 139–149. https://doi.org/10.1530/REP-11-0299

Pepling, M.E., 2006. From primordial germ cell to primordial follicle: mammalian female germ cell development. Genesis 44 (12), 622–632. https://doi.org/10.1002/dvg.20258

Pepling, M.E., Spradling, A.C., 2001. Mouse Ovarian Germ Cell Cysts Undergo Programmed Breakdown to Form Primordial Follicles. Dev. Biol. 234 (2), 339–351. https://doi.org/10.1006/dbio.2001.0269

Pepling, M.E., Spradling, A.C., 1998. Female mouse germ cells form synchronously dividing cysts. Development 125, 3323–3328.

Pepling, M.E., Sundman, E.A., Patterson, N.L., Gephardt, G.W., Medico, L., Wilson, K.I., 2010. Differences in oocyte development and estradiol sensitivity among mouse strains. Reproduction 139 (2), 349–357. https://doi.org/10.1530/REP-09-0392

Pepling, M.E., Wilhelm, J.E., O'Hara, A.L., Gephardt, G.W., Spradling, A.C., 2007. Mouse oocytes within germ cell cysts and primordial follicles contain a Balbiani body. Proc. Natl. Acad. Sci. 104 (1), 187–192. https://doi.org/10.1073/pnas.0609923104

Perez, G.I., Robles, R., Knudson, C.M., Flaws, J.A., Korsmeyer, S.J., Tilly, J.L., 1999. Prolongation of ovarian lifespan into advanced chronological age by Bax-deficiency. Nat. Genet. 21, 200–203. https://doi.org/10.1038/5985

Picton, H., Briggs, D., Gosden, R., 1998. The molecular basis of oocyte growth and development. Mol. Cell. Endocrinol. 145 (1-2) 27-37.

Pittman, D.L., Cobb, J., Schimenti, K.J., Wilson, L.A., Cooper, D.M., Brignull, E., Handel, M.A., Schimenti, J.C., 1998. Meiotic Prophase Arrest with Failure of Chromosome Synapsis in Mice Deficient for *Dmc1*, a Germline-Specific RecA Homolog. Mol. Cell 1 (5), 697–705. https://doi.org/10.1016/S1097-2765(00)80069-6

Qiao, H., Rao, H.B.D.P., Yun, Y., Sandhu, S., Fong, J.H., Sapre, M., Nguyen, M., Tham, A., Van, B.W., Chng, T.Y.H., Lee, A., Hunter, N., 2018. Impeding DNA Break Repair Enables Oocyte Quality Control. Mol. Cell 72 (2) 211-221. https://doi.org/10.1016/j.molcel.2018.08.031

Ratts, V.S., Flaws, J.A., Kolp, R., Sorenson, C.M., Tilly, J.L., 1995. Ablation of bcl-2 gene expression decreases the numbers of oocytes and primordial follicles established in the post-natal female mouse gonad. Endocrinology 136 (8), 3665–3668. https://doi.org/10.1210/endo.136.8.7628407

Revenkova, E., Jessberger, R., 2006. Shaping meiotic prophase chromosomes: cohesins and synaptonemal complex proteins. Chromosoma 115 (3), 235–240. https://doi.org/10.1007/s00412-006-0060-x

Rinaldi, V.D., Bloom, J.C., Schimenti, J.C., 2018. Whole Mount Immunofluorescence and Follicle Quantification of Cultured Mouse Ovaries. J. Vis. Exp. 135, e57593. https://doi.org/10.3791/57593

Rinaldi, V.D., Bolcun-Filas, E., Kogo, H., Kurahashi, H., Schimenti, J.C., 2017a. The DNA Damage Checkpoint Eliminates Mouse Oocytes with Chromosome Synapsis Failure. Mol. Cell 67 (6), 1026–1036.e2. https://doi.org/10.1016/j.molcel.2017.07.027

Rinaldi, V.D., Hsieh, K., Munroe, R., Bolcun-Filas, E., Schimenti, J.C., 2017b. Pharmacological Inhibition of the DNA Damage Checkpoint Prevents Radiation-

Induced Oocyte Death. Genetics 206 (4), 1823–1828. https://doi.org/10.1534/genetics.117.203455

Rizzo, A.A., Vassel, F.-M., Chatterjee, N., D'Souza, S., Li, Y., Hao, B., Hemann, M.T., Walker, G.C., Korzhnev, D.M., 2018. Rev7 dimerization is important for assembly and function of the Rev1/Polζ translesion synthesis complex. Proc. Natl. Acad. Sci. U. S. A. 115, E8191–E8200. https://doi.org/10.1073/pnas.1801149115

Robert, T., Nore, A., Brun, C., Maffre, C., Crimi, B., Bourbon, H.-M., de Massy, B., Massy, B. de, 2016. The TopoVIB-Like protein family is required for meiotic DNA double-strand break formation. Science. 351 (6276), 943-949. https://doi.org/10.1126/science.aad5309

Roeder, G., Bailis, J., 2000. The pachytene checkpoint. Trends Genet. 16 (9), 395–403. https://doi.org/10.1016/S0168-9525(00)02080-1

Rogakou, E.P., Pilch, D.R., Orr, A.H., Ivanova, V.S., Bonner, W.M., 1998. DNA Double-stranded Breaks Induce Histone H2AX Phosphorylation on Serine 139. J. Biol. Chem. 273, 5858–5868. https://doi.org/10.1074/JBC.273.10.5858

Rogakou, E.P., Pilch, D.R., Orr, A.H., Ivanova, V.S., Bonner, W.M., 1998. DNA double-stranded breaks induce histone H2AX phosphorylation on serine 139. J. Biol. Chem. 273, 5858–5668. https://doi.org/10.1074/JBC.273.10.5858

Roig, I., Dowdle, J. a, Toth, A., de Rooij, D.G., Jasin, M., Keeney, S., 2010. Mouse TRIP13/PCH2 is Required for Recombination and Normal Higher-Order Chromosome Structure during Meiosis. PLoS Genet. 6 (8), e1001062. https://doi.org/10.1371/journal.pgen.1001062

Roig, I., Liebe, B., Egozcue, J., Cabero, L., Garcia, M., Scherthan, H., 2004. Female-specific features of recombinational double-stranded DNA repair in relation to synapsis and telomere dynamics in human oocytes. Chromosoma 113, 22–33. https://doi.org/10.1007/s00412-004-0290-8

Romanienko, P.J., Camerini-Otero, R.D., 2000. The Mouse *Spo11* Gene Is Required for Meiotic Chromosome Synapsis. Mol. Cell 6 (5), 975–987. https://doi.org/10.1016/S1097-2765(00)00097-6

Roos, W.P., Kaina, B., 2006. DNA damage-induced cell death by apoptosis. Trends Mol. Med. 12 (9), 440–450. https://doi.org/10.1016/j.molmed.2006.07.007

Royo, H., Polikiewicz, G., Mahadevaiah, S.K., Prosser, H., Mitchell, M., Bradley, A., de Rooij, D.G., Burgoyne, P.S., Turner, J.M.A., 2010. Evidence that Meiotic Sex Chromosome Inactivation Is Essential for Male Fertility. Curr. Biol. 20 (23), 2117–2123. https://doi.org/10.1016/J.CUB.2010.11.010

Royo, H., Prosser, H., Ruzankina, Y., Mahadevaiah, S.K., Cloutier, J.M., Baumann, M., Fukuda, T., Höög, C., Tóth, A., de Rooij, D.G., Bradley, A., Brown, E.J., Turner, J.M.A., 2013. ATR acts stage specifically to regulate multiple aspects of mammalian meiotic silencing. Genes Dev. 27, 1484–1494. https://doi.org/10.1101/gad.219477.113

Rucker, E.B., Dierisseau, P., Wagner, K.-U., Garrett, L., Wynshaw-Boris, A., Flaws, J.A., Hennighausen, L., 2000. Bcl-x and Bax Regulate Mouse Primordial Germ Cell Survival and Apoptosis during Embryogenesis. Mol. Endocrinol. 14 (7), 1038–1052. https://doi.org/10.1210/mend.14.7.0465

Russell, D.L., Robker, R.L., 2007. Molecular mechanisms of ovulation: co-ordination through the cumulus complex. Hum. Reprod. Update 13 (3), 289–312. https://doi.org/10.1093/humupd/dml062

Salha, O., Abusheikha, N., Sharma, V., Abusheika, N., 1998. Dynamics of human follicular growth and *in-vitro* oocyte maturation. Hum. Reprod. Update 4 (6), 816–832.

San-Segundo, P.A., Roeder, G.S., 1999. Pch2 Links Chromatin Silencing to Meiotic Checkpoint Control. Cell 97 (3), 313–324. https://doi.org/10.1016/S0092-8674(00)80741-2

Sánchez, F., Smitz, J., 2012. Molecular control of oogenesis. Biochim. Biophys. Acta - Mol. Basis Dis. 1822 (12), 1896-1912. https://doi.org/10.1016/j.bbadis.2012.05.013

Sato, T., Katagiri, K., Gohbara, A., Inoue, K., Ogonuki, N., Ogura, A., Kubota, Y., Ogawa, T., 2011. *In vitro* production of functional sperm in cultured neonatal mouse testes. Nature 471, 504–507. https://doi.org/10.1038/nature09850

Schmekel, K., Meuwissen, R.L.J., Dietrich, A.J.J., Vink, A.C.G., van Marle, J., van Veen, H., Heyting, C., 1996. Organization of SCP1 Protein Molecules within Synaptonemal Complexes of the Rat. Exp. Cell Res. 226 (1), 20–30. https://doi.org/10.1006/EXCR.1996.0198

Schramm, S., Fraune, J., Naumann, R., Hernandez-Hernandez, A., Höög, C., Cooke, H.J., Alsheimer, M., Benavente, R., 2011. A Novel Mouse Synaptonemal Complex Protein Is Essential for Loading of Central Element Proteins, Recombination, and Fertility. PLoS Genet. 7, e1002088. https://doi.org/10.1371/journal.pgen.1002088

Schwacha, A., Kleckner, N., 1997. Interhomolog Bias during Meiotic Recombination: Meiotic Functions Promote a Highly Differentiated Interhomolog-Only Pathway. Cell 90 (6), 1123–1135. https://doi.org/10.1016/S0092-8674(00)80378-5

Schwacha, A., Kleckner, N., 1994. Identification of joint molecules that form frequently between homologs but rarely between sister chromatids during yeast meiosis. Cell 76 (1), 51–63.

Shimada, M., Nabeshima, K., Tougan, T., Nojima, H., 2002. The meiotic recombination checkpoint is regulated by checkpoint rad$^+$ genes in fission yeast. EMBO J. 21 (11), 2807–2818. https://doi.org/10.1093/emboj/21.11.2807

Shin, Y.-H., McGuire, M.M., Rajkovic, A., 2013. Mouse HORMAD1 is a Meiosis I CheckpointProtein That Modulates DNA Double- Strand Break Repair During Female Meiosis. Biol. Reprod. 89 (2), 29. https://doi.org/10.1095/biolreprod.112.106773

Shin, Y.H., Choi, Y., Erdin, S.U., Yatsenko, S.A., Kloc, M., Yang, F., Wang, P.J., Meistrich, M.L., Rajkovic, A., 2010. *Hormad1* Mutation Disrupts Synaptonemal Complex Formation, Recombination, and Chromosome Segregation in Mammalian meiosis. PLoS Genet. 6 (11), e1001190. https://doi.org/10.1371/journal.pgen.1001190

Song, K., Ma, W., Huang, C., Ding, J., Cui, D., Zhang, M., 2016. Expression Pattern of Mouse Vasa Homologue (MVH) in the Ovaries of C57BL/6 Female Mice. Med. Sci. Monit. 22, 2656-2663 https://doi.org/10.12659/MSM.899830

Speed, R.M., 1988. The possible role of meiotic pairing anomalies in the atresia of human fetal oocytes. Hum. Genet. 78 (3), 260–6.

Spiller, C., Koopman, P., Bowles, J., 2017. Sex Determination in the Mammalian Germline. Annu. Rev. Genet. 51, 265–285. https://doi.org/10.1146/annurev-genet-120215-035449

Stanzione, M., Baumann, M., Papanikos, F., Dereli, I., Lange, J., Ramlal, A., Tränkner, D., Shibuya, H., de Massy, B., Watanabe, Y., Jasin, M., Keeney, S., Tóth, A., 2016. Meiotic DNA break formation requires the unsynapsed chromosome axis-binding

protein IHO1 (CCDC36) in mice. Nat. Cell Biol. 18, 1208–1220. https://doi.org/10.1038/ncb3417

Stocco, C., Telleria, C., Gibori, G., 2007. The Molecular Control of Corpus Luteum Formation, Function, and Regression. Endocr. Rev. 28 (1), 117–149. https://doi.org/10.1210/er.2006-0022

Stracker, T., Usui, T., Petrini, J., 2009. Taking the time to make important decisions: the checkpoint effector kinases Chk1 and Chk2 and the DNA damage response. DNA Repair 8 (9), 1047–1054. https://doi.org/10.1016/j.dnarep.2009.04.012

Stracker, T.H., Petrini, J.H.J., 2011. The MRE11 complex: starting from the ends. Nat. Rev. Mol. Cell Biol. 12, 90–103. https://doi.org/10.1038/nrm3047

Stracker, T.H., Roig, I., Knobel, P. A, Marjanović, M., 2013. The ATM signaling network in development and disease. Front. Genet. 4, 37. https://doi.org/10.3389/fgene.2013.00037

Subramanian, V. V., MacQueen, A.J., Vader, G., Shinohara, M., Sanchez, A., Borde, V., Shinohara, A., Hochwagen, A., 2016. Chromosome Synapsis Alleviates Mek1-Dependent Suppression of Meiotic DNA Repair. PLOS Biol. 14, e1002369. https://doi.org/10.1371/journal.pbio.1002369

Subramanian, V. V, Hochwagen, A., 2014. The Meiotic Checkpoint Network: Step-by-Step through Meiotic Prophase. Cold Spring Harb. Perspect. Biol. 6, a016675–a016675. https://doi.org/10.1101/cshperspect.a016675

Suh, E.K., Yang, A., Kettenbach, A., Bamberger, C., Michaelis, A.H., Zhu, Z., Elvin, J.A., Bronson, R.T., Crum, C.P., McKeon, F., 2006. P63 Protects the Female Germ Line During Meiotic Arrest. Nature 444, 624–628. https://doi.org/10.1038/nature05337

Sun, Y.-C., Cheng, S.-F., Sun, R., Zhao, Y., Shen, W., 2014. Reconstitution of Gametogenesis *In Vitro*: Meiosis Is the Biggest Obstacle. J. Genet. Genomics 41 (3), 87–95. https://doi.org/10.1016/J.JGG.2013.12.008

Sym, M., Engebrecht, J.A., Roeder, G.S., 1993. ZIP1 is a synaptonemal complex protein required for meiotic chromosome synapsis. Cell 72 (3), 365–378. https://doi.org/10.1016/0092-8674(93)90114-6

Tajima, K., Orisaka, M., Mori, T., Kotsuji, F., 2007. Ovarian theca cells in follicular function. Reprod. Biomed. Online 15 (5), 591–609. https://doi.org/10.1016/S1472-6483(10)60392-6

Takahashi, T.A., Johnson, K.M., 2015. Menopause. Med. Clin. North Am. 99 (3), 521–534. https://doi.org/10.1016/j.mcna.2015.01.006

Takai, H., Naka, K., Okada, Y., Watanabe, M., Harada, N., Saito, S., Anderson, C.W., Appella, E., Nakanishi, M., Suzuki, H., Nagashima, K., Sawa, H., Ikeda, K., Motoyama, N., 2002. Chk2-deficient mice exhibit radioresistance and defective p53-mediated transcription. EMBO J. 21, 5195–5205. https://doi.org/10.1093/emboj/cdf506

Tam, P.P., Snow, M.H., 1981. Proliferation and migration of primordial germ cells during compensatory growth in mouse embryos. J. Embryol. Exp. Morphol. 64, 133–147.

Tao, Z.-F., Lin, N.-H., 2006. Chk1 Inhibitors for Novel Cancer Treatment. Anticancer. Agents Med. Chem. 6 (4), 377–388. https://doi.org/10.2174/187152006777698132

Taylor, W.R., Stark, G.R., 2001. Regulation of the G2/M transition by p53. Oncogene 20 (15), 1803–1815.

Tease, C., Hultén, M.A., 2004. Inter-sex variation in synaptonemal complex lengths

largely determine the different recombination rates in male and female germ cells. Cytogenet. Genome Res. 107, 208–215. https://doi.org/10.1159/000080599

Tilly, J.L., 2003. Ovarian follicle counts - not as simple as 1, 2, 3. Reprod. Biol. Endocrinol. 1, 11. https://doi.org/10.1186/1477-7827-1-11

Tilly, J.L., 2001. Commuting the death sentence: How oocytes strive to survive. Nat. Rev. Mol. Cell Biol. 2, 838–848. https://doi.org/10.1038/35099086

Tingen, C., Kim, A., Woodruff, T.K., 2009. The primordial pool of follicles and nest breakdown in mammalian ovaries. Mol. Hum. Reprod. 15 (12), 795–803. https://doi.org/10.1093/molehr/gap073

Trombly, D.J., Woodruff, T.K., Mayo, K.E., 2009. Suppression of Notch Signaling in the Neonatal Mouse Ovary Decreases Primordial Follicle Formation. Endocrinology 150 (2), 1014–1024. https://doi.org/10.1210/en.2008-0213

Turner, J.M.A., 2007. Meiotic sex chromosome inactivation. Development 134 (10), 1823–1831. https://doi.org/10.1242/dev.000018

Turner, J.M.A., Aprelikova, O., Xu, X., Wang, R., Kim, S., Chandramouli, G.V.R., Barrett, J.C., Burgoyne, P.S., Deng, C.-X., 2004. BRCA1, Histone H2AX Phosphorylation, and Male Meiotic Sex Chromosome Inactivation. Curr. Biol. 14 (23), 2135–2142. https://doi.org/10.1016/J.CUB.2004.11.032

Turner, J.M.A., Mahadevaiah, S.K., Fernandez-Capetillo, O., Nussenzweig, A., Xu, X., Deng, C.-X., Burgoyne, P.S., 2005. Silencing of unsynapsed meiotic chromosomes in the mouse. Nat. Genet. 37, 41–47. https://doi.org/10.1038/ng1484

van den Hurk, R., Zhao, J., 2005. Formation of mammalian oocytes and their growth, differentiation and maturation within ovarian follicles. Theriogenology 63 (6), 1717–1751. https://doi.org/10.1016/J.THERIOGENOLOGY.2004.08.005

Vogelstein, B., Lane, D., Levine, A.J., 2000. Surfing the p53 network. Nature 408, 307–310. https://doi.org/10.1038/35042675

Vries, S.S. De, Baart, E.B., Dekker, M., Siezen, A., Rooij, D.G. De, Boer, P. De, Riele, H., 1999. Mouse MutS-like protein Msh5 is required for proper chromosome synapsis in male and female meiosis. Genes Dev. 13 (5) 523–531.

Wallace, N.A., Belancio, V.P., Deininger, P.L., 2008. L1 mobile element expression causes multiple types of toxicity. Gene 419 (1-2), 75–81. https://doi.org/10.1016/j.gene.2008.04.013

Wang, X.Q., Redpath, J.L., Fan, S.T., Stanbridge, E.J., 2006. ATR dependent activation of Chk2. J. Cell. Physiol. 208 (3), 613–619. https://doi.org/10.1002/jcp.20700

White, Y. a R., Woods, D.C., Takai, Y., Ishihara, O., Seki, H., Tilly, J.L., 2012. Oocyte formation by mitotically active germ cells purified from ovaries of reproductive-age women. Nat. Med. 18, 413–421. https://doi.org/10.1038/nm.2669

Wickramasinghe, D., Ebert, K.M., Albertini, D.F., 1991. Meiotic competence acquisition is associated with the appearance of M-phase characteristics in growing mouse oocytes. Dev. Biol. 143 (1), 162–172. https://doi.org/10.1016/0012-1606(91)90063-9

Widger, A., Mahadevaiah, S.K., Lange, J., Ellnati, E., Zohren, J., Hirota, T., Pacheco, S., Maldonado-Linares, A., Stanzione, M., Ojarikre, O., Maciulyte, V., de Rooij, D.G., Tóth, A., Roig, I., Keeney, S., Turner, J.M.A., 2018. ATR is a multifunctional regulator of male mouse meiosis. Nat. Commun. 9, 2621. https://doi.org/10.1038/s41467-018-04850-0

Wojtasz, L., Cloutier, J.M., Baumann, M., Daniel, K., Varga, J., Fu, J., Anastassiadis, K.,

Francis Stewart, A., Reményi, A., Turner, J.M.A., Tóth, A., 2012. Meiotic DNA double-strand breaks and chromosome asynapsis in mice are monitored by distinct HORMAD2-independent and -dependent mechanisms. Genes Dev. 26, 958–973. https://doi.org/10.1101/gad.187559.112

Wojtasz, L., Daniel, K., Roig, I., Bolcun-Filas, E., Xu, H., Boonsanay, V., Eckmann, C.R., Cooke, H.J., Jasin, M., Keeney, S., McKay, M.J., Toth, A., 2009a. Mouse HORMAD1 and HORMAD2, Two Conserved Meiotic Chromosomal Proteins, Are Depleted from Synapsed Chromosome Axes with the Help of TRIP13 AAA-ATPase. PLoS Genet. 5 (10), e1000702. https://doi.org/10.1371/journal.pgen.1000702

Wojtasz, L., Daniel, K., Toth, A., 2009b. Fluorescence activated cell sorting of live female germ cells and somatic cells of the mouse fetal gonad based on forward and side scattering. Cytom. Part A 75A (6), 547–553. https://doi.org/10.1002/cyto.a.20729

Woltering, D., Baumgartner, B., Bagchi, S., Larkin, B., Loidl, J., de los Santos, T., Hollingsworth, N.M., 2000. Meiotic Segregation, Synapsis, and Recombination Checkpoint Functions Require Physical Interaction between the chromosomal proteins Red1p and Hop1p. Mol. Cell. Biol. 20, 6646–6658.

Wu, H.-Y., Burgess, S.M., 2006. Two Distinct Surveillance Mechanisms Monitor Meiotic Chromosome Metabolism in Budding Yeast. Curr. Biol. 16 (24), 2473–2479. https://doi.org/10.1016/J.CUB.2006.10.069

Wu, H.-Y., Ho, H.-C., Burgess, S.M., 2010. Mek1 Kinase Governs Outcomes of Meiotic Recombination and the Checkpoint Response. Curr. Biol. 20 (19), 1707–1716. https://doi.org/10.1016/J.CUB.2010.09.016

Xu, J., Gridley, T., 2013. Notch2 is required in somatic cells for breakdown of ovarian germ-cell nests and formation of primordial follicles. BMC Biol. 11, 13. https://doi.org/10.1186/1741-7007-11-13

Xu, Y., Ashley, T., Brainerd, E.E., 1996. Targeted disruption of ATM leads to growth retardation, chromosomal fragmentation during meiosis, immune defects, and thymic lymphoma. Genes Dev. 10, 2411–2422. https://doi.org/10.1101/gad.10.19.2411

Yang, F., Wang, P.J., 2009. The Mammalian Synaptonemal Complex: A Scaffold and Beyond. Genome Dyn. 5, 69–80. https://doi.org/10.1159/000166620

Ye, Q., Rosenberg, S.C., Moeller, A., Speir, J.A., Su, T.Y., Corbett, K.D., 2015. TRIP13 is a protein-remodeling AAA+ ATPase that catalyzes MAD2 conformation switching. Elife 4. https://doi.org/10.7554/eLife.07367

Yoshida, K., Kondoh, G., Matsuda, Y., Habu, T., Nishimune, Y., Morita, T., 1998. The Mouse *RecA*-like Gene *Dmc1* Is Required for Homologous Chromosome Synapsis during Meiosis. Mol. Cell 1 (5), 707–718. https://doi.org/10.1016/S1097-2765(00)80070-2

Zhang, C.-P., Yang, J.-L., Zhang, J., Li, L., Huang, L., Ji, S.-Y., Hu, Z.-Y., Gao, F., Liu, Y.-X., 2011. Notch Signaling Is Involved in Ovarian Follicle Development by Regulating Granulosa Cell Proliferation. Endocrinology 152 (6), 2437–2447. https://doi.org/10.1210/en.2010-1182

Zhang, X., Li, Y., Xu, H., Zhang, Y.-W., 2014. The γ-secretase complex: from structure to function. Front. Cell. Neurosci. 8, 427. https://doi.org/10.3389/fncel.2014.00427

Zhou, B.S., Elledge, S.J., 2000. The DNA damage response: putting checkpoints in perspective. Nature 408, 433–439. https://doi.org/10.1038/35044005

Zielinska, A.P., Schuh, M., 2018. A microscopy-based approach for studying meiosis in live and fixed human oocytes. Methods in Cell Biology. 145, 315-333. https://doi.org/10.1016/bs.mcb.2018.03.039